공학박사학위논문

A Study on the Design and Operation of LNG-FSRU Topside Processes using Dynamic Simulation

동적 시뮬레이션을 활용한 LNG-FSRU 탑사이드 공정의 설계 및 운전에 대한 연구

2015년 2월

서울대학교 대학원

화학생물공학부

이 상 호

Abstract

A Study on the Design and Operation of LNG-FSRU Topside Processes using Dynamic Simulation

Sangho Lee

School of Chemical & Biological Engineering

The Graduate School of Seoul National University

Recently, the necessity of liquefied natural gas(LNG) supplying facility such as LNG terminal is increasing due to the emerging demand of LNG. Among the LNG supplying facilities, floating storage and regasification unit(FSRU), which has advantages on the construction period and cost than onshore LNG terminal attracts attention in these days. Designing LNG-FSRU is similar to onshore LNG terminal or LNG carrier but unlike the traditional process design procedure, the topside process of LNG-FSRU should be designed considering the offshore features. Moreover, to develop the topside process and proper operating procedure with safety, plenty of sensors as well as an exact dynamic simulation model are required.

This thesis addresses a study on the design and operation of LNG-FSRU topside process using dynamic simulation. The effects of offshore features to LNG-FSRU topside process are analyzed and an exact dynamic simulation model for LNG-FSRU is developed in this thesis. In addition, an automatic variable estimation method for any points that the operators want to know is proposed.

This thesis has three main parts. First, the effects of three main offshore features, including ship motion effect, limitation on topside footprint, and weight, are analyzed by using process simulation. Based on the result of the effects, a topside process of LNG-FSRU is designed. Second, an exact dynamic simulation model of LNG-FSRU topside process is developed. Especially the boil-off gas recondenser, which is the most difficult to build an exact dynamic simulation model is simulated with higher accuracy than previous research. Finally, a methodology to estimate process variables at any points on the pipeline of LNG-FSRU is proposed. The proposed methodology reduces the variable estimation time by 1/10.

Keywords: LNG-FSRU, Topside design, Dynamic Simulation, BOG recondenser, Automatic soft sensor generation

Student ID: 2007-21208

Contents

List of Figures

LIST OF TABLES

CHAPTER 1 : INTRODUCTION

1.1. Research motivation

Because of the rapid industrialization of undeveloped countries, the demand of energy is increasing. Liquefied natural gas (LNG) is the most attractive energy source because of low price and relative eco-friendliness so that the demand of LNG is exploded in these days.[1–3] To supply LNG to its demands, various facilities are necessary as figure 1-1 and among these, LNG storage terminal, which serves natural gas to individual users takes the most important part in LNG value chain. The increasing tendency of LNG terminal projects in figure 1-2 proves the importance of LNG terminals.[4], [5]

However, the construction of an LNG terminal accompanies a huge interruption, that is, the protest by local residents. Though the problem is solved, another problem remains, the large land cost. Because the LNG terminal contains dangerous facilities that deals with flammable and explosive component, the enough separation distance between the process equipment must be secured.[6], [7] Because of these situation, LNG-FSRU is focused as a reasonable alternative for onshore LNG terminal. Focusing on the number of offshore terminals in figure 1-2, it is certain that the LNG-FSRU market is expanding. (Figure 1-2)[1]

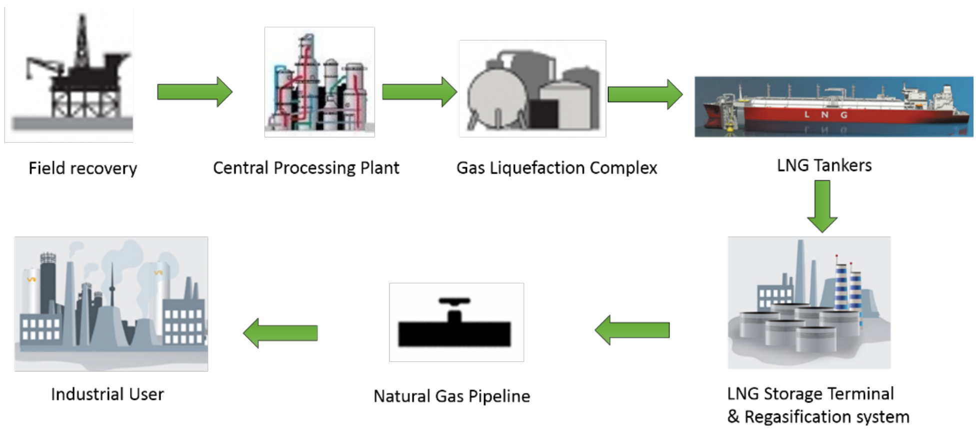

Figure 1-1. LNG value chain diagram

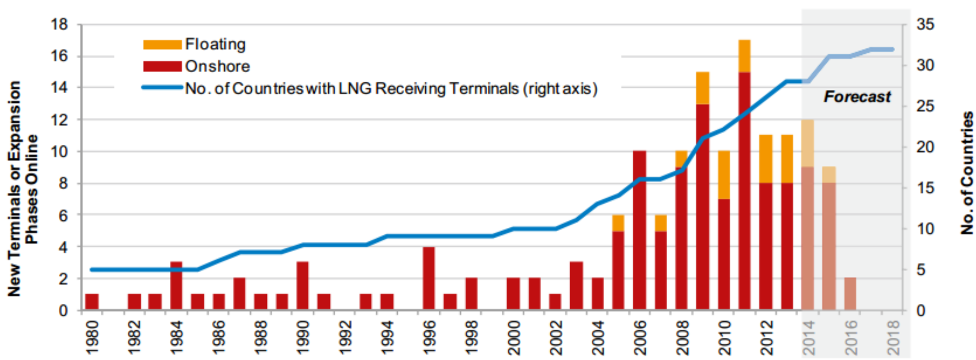

Figure 1-2. Start-Ups of LNG Receiving Terminals, 1980-2018[1]

LNG-FSRU is similar to onshore LNG terminal or LNG carrier that many Korean shipbuilding companies which already leading the LNG carrier market have a huge potential to dominate the FSRU industry. Despite the advantage, the topside process design for the LNG-FSRU makes a technical barrier to the shipbuilders so that the economic feasibility of project is decreased for them.[8], [9]

The topside process design for an offshore process is basically the same as general chemical process design technique, but some serious features are omitted and these features will bring many design change from the onshore process. Thus, in the designing procedure of topside process in LNG-FSRU, the offshore features must be considered. [8], [10–15]

After the process flowsheeting is finished, making the dynamic simulation model will follow to make piping and instrument diagram(P&ID), analyzing the hazard and operability(HAZOP) of the target design, and finishing the front-end engineering design(FEED) package. On building the dynamic simulation model of LNG-FSRU, the most important and difficult problem is to model the reliquefaction system. There are several researches about the boil-off gas (BOG) recondenser but most of the researches are focusing on the control logic or proposing novel structure for recondensing system and inattentive to exact simulation which is significant for the management of terminal operation.[16–20]

When the HAZOP study is completed, compensating actions are followed to solve serious problem of the process and most of the actions are about adding sensors to the plant. This is also applied in LNG-FSRU. Moreover, LNG-FSRU is a facility that manages a high pressure and cryogenic fluid which is explosive and flammable compound, the property of the fluid at every position needs to be monitored thoroughly. This issue is soluble by lots of sensor installation cost but it deteriorates economic feasibility of overall project. So that a soft sensor technique that does not need any additional sensor installation cost might be helpful.[21–23]

1.2. Research objectives

The objective of this thesis is to design a process for the topside of an LNG-FSRU regarding the offshore issue, to develop a dynamic simulation model which can represent exact process status especially for BOG reliquefaction system, and to make a sensing technique to estimate every position of LNG-FSRU by using the process simulation software. The achievements in each chapter will result meaningful progress on the design of LNG-FSRU topside process.

1.3. Outline of the thesis

Each chapter of this thesis considers the issues about the design of topside process on a LNG-FSRU. Chapter 2 addresses a design of topside process for an LNG-FSRU by regarding the offshore feature. In chapter 3, a dynamic simulation model of LNG-FSRU is built with higher precision than before. Chapter 4 deals with the methodology to build an automatic simulation-based soft sensor for any position of pipeline which will help FSRU’s sensor problem. Lastly, in Chapter 5, the thesis conclusion and recommendation for future works will be presented.

CHAPTER 2 : TOPSIDE PROCESS DESIGN OF LNG-FSRU

2.1. Introduction

In these days, many offshore plants for mining energy resources such as natural gas and petroleum in deep-sea fields are under construction. Most of these offshore plants are held in Korean shipbuilding companies but these shipbuilding companies have tough time on these offshore projects because of lack of basic design ability. [24] The basic design of offshore plant is divided to two different areas - topside/hull area - and for Korean shipbuilders, the topside design is the very problem. Designing the topside area needs plenty of knowledge about the process system and equipment but it is a strange area to the traditional shipbuilding companies. Nevertheless the topside design itself does not take large portion in overall project, this designing technique must be secured that it determines feasibility and period of the project. [25–28]

Especially for LNG-FSRU, unlike the other offshore plants, the topside design on each of different cases is similar and that means when the standard topside design is well-developed, the design will be applied in many other projects without big changes. Thus, it is necessary to build a certain LNG-FSRU topside design.

In the topside design problem, the key point is to design the process flow and equipment. Basically, to design topside process is not far from designing an onshore chemical processes but some additional issues which are only for offshore plant must be considered. The following three issues are the most important things which are not mentioned in traditional process design;

1) Limitation on the plant size : When the size of an offshore plant increases, the cost of offshore plant increases further. The reason of the further increase cost is because the construction cost is sensitive to the structure's size. Moreover the offshore platform must be constructed in a shipbuilding dock and the size of dock limits the platform's size. To solve the problem by limitation of size, more consideration on process safety should be followed in the process design.

2) Ship motion : For the floating plant like FSRU, the vessel usually moves on the ocean by tides, waves and even winds. This ship motion can affect many process units above the floating structure. For an example of three phase separator, when the motion of platform induced to the process unit, fluids inside the separator may be mixed or the interface of fluids faltered so that the separator efficiency will be decreased. In another example of packed bed column seen in **figure 2-1,** the contacting area will be changed by the column motion. This ship motion problem can be solved by prediction of efficiency changes for each process unit or selecting an insensitive process equipment for topside process.

3) Topside weight : As seen in many recent marine accidents, overloading can cause capsize of floating platform. In order to prevent these accidents the center of gravity must be located below the center of buoyancy. (**Figure 2-2**) By the way, when the weight of topside process is comparatively larger the platform's center of gravity rises and

dynamic stability of floating object will be decreased. This is the first reason to enlighten weight of process equipment. Secondly the static load which means the weight of a single stationary body or the combined weights of all stationary bodies in a structure reflects on both the storage capacity of plant and equipment cost.[12], [29–37]

Without consideration about these issues, the design of offshore topside process will not be rigid and safe because these issues will affect each process equipment or overall process flow and give uncertainties or efficiency changes. Therefore in this research, LNG-FSRU topside process is designed with considering these three issues – plant size, ship motion, and topside weight.

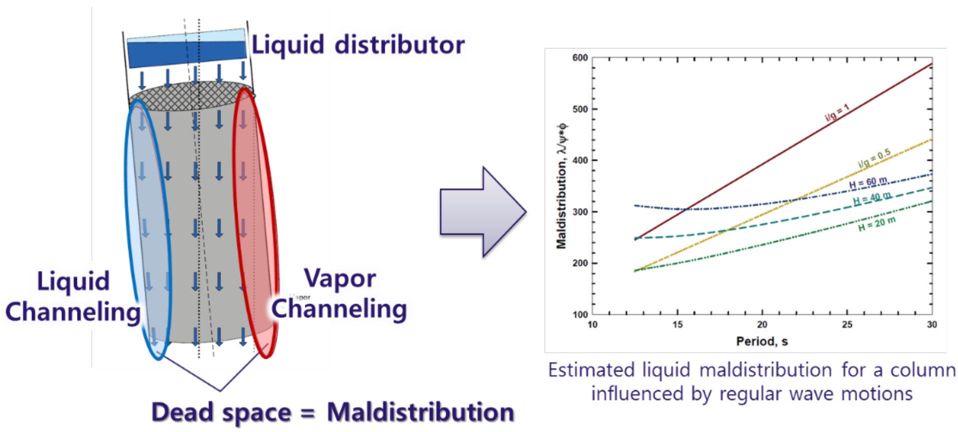

Figure 2-1. Efficiency loss due to equipment motion on floating platform[38]

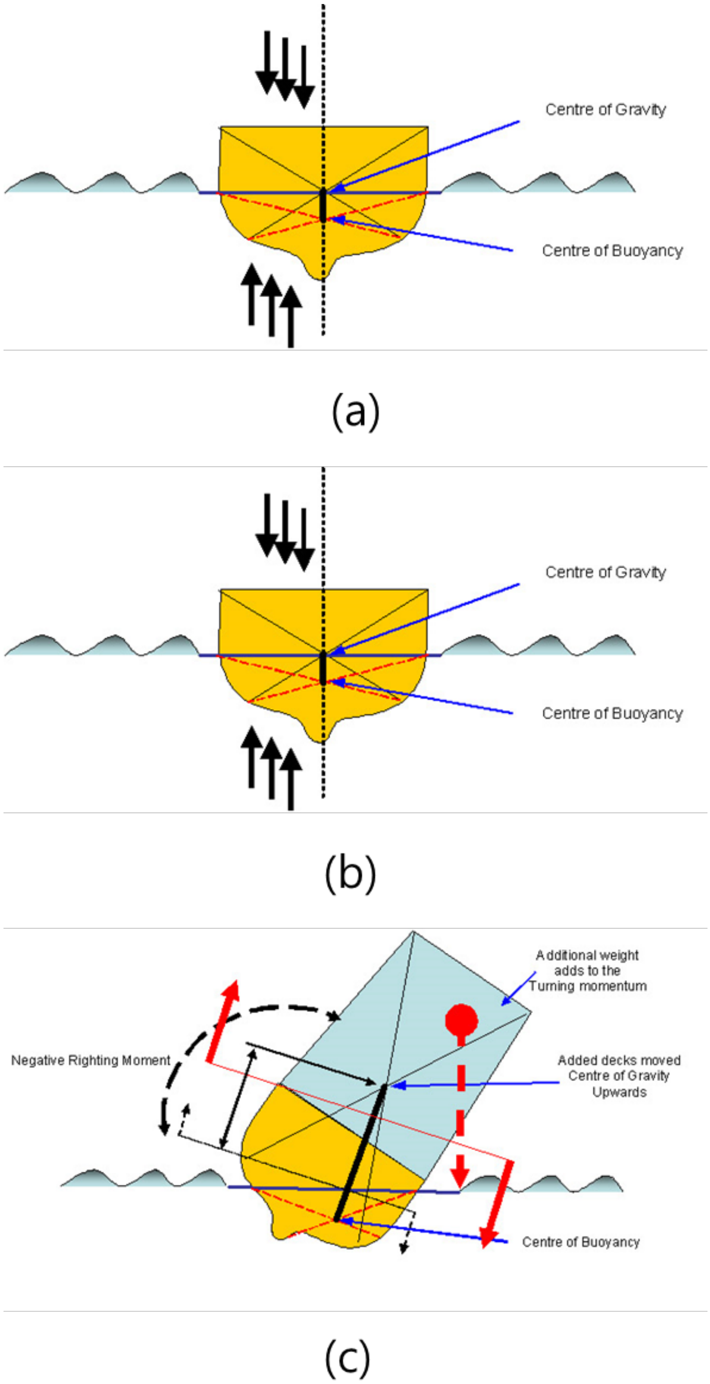

Figure 2-2. Dynamic stability of floating object with topside weight increase

2.2. Theoretical backgrounds

2.2.1. LNG-FSRU

LNG-FSRU is a new concept to supply a natural gas from offshore regasification plant to onshore consumer. It has been proposed as alternatives to traditional onshore re-gasification plants. Recently some of FSRUs are already on operation and many other FSRU are under construction as seen in the **table 2-1**. As the price of LNG is decreased a lot in these days, the LNG-FSRU will receive more attention for energy suppliers.

Before designing the topside process of LNG-FSRU, the basic process scheme should be specified for better process design. While FSRU has basically the same structure with an LNG receiving terminal, it is necessary to focus on the LNG onshore terminal process scheme. Following features are the essential features for LNG terminal;

- Unloading
- Storage
- BOG recovery and pressurization
- Vaporization
- Send-out gas quality adjustment

These features must be included in the LNG terminal process flowsheet so that the process flowsheet seen in **figure 2-3** is generated as a basic standard. Nowadays, lots of LNG onshore terminal are constructed based on this process and the LNG-FSRU also follows same process scheme.

Table 2-1. A list of world's LNG-FSRU[39]

Owner	**Name**	**Storage volume (m3)**	**Gas throughput (bcm/yr)**	**Regas capacity (MMscfd)**	**Length overall (m)**	**Molded Breadth (m)**	**Draft (m)**	**Notes**
Hoegh	Hull No. 2548	170,000	2.5	240	290	46	12.6	under construction
Hoegh	Hull No. 2549	170,000	4.1	400	290	46	12.6	under construction
Hoegh	Hull No. 2550	170,000	3.9	375	290	46	12.6	under construction
Hoegh	Hull No. 2551	170,000	5.1	500	294	46	12.6	under construction
Hoegh	Independence	170,000	4.1	400	294	46	12.6	
Hoegh	Lampung	170,000	4.1	400	294	46	12.6	
Golar	Freeze	125,000	4.9	475	288	43	11.5	conversion
Golar	Spirit	129,000	2.5	240	290	45	12.5	conversion
Golar	Winter	138,000	5.1	500	277	43	11.4	conversion
Golar	Satu	125,000	5	490	293	42	11.7	conversion
Golar	Igloo	170,000	7.5	725				Delivery `14
Golar	Eskimo	160,000	7.5	725				Delivery `14
EON Ruhrgas	Toscana (was Golar Frost)	137,000	3.75	360	306	48	12.3	permanently moored
Excelerate	Excelsior	138,000	4.1	400	277	43	12.2	LNGC w/Regas Capability
Excelerate	Excelerate	138,000	4.1	400	277	43	12.2	LNGC w/Regas Capability
Excelerate	Excellence	138,000	4.1	400	277	43	12.2	LNGC w/Regas Capability
Excelerate	Exemplar	150,900	5.1	500	290	43	12.4	LNGC w/Regas Capability
Excelerate	Explorer	150,900	5.1	500	290	43	12.4	LNGC w/Regas Capability
Excelerate	Express	150,900	5.1	500	290	43	12.4	LNGC w/Regas Capability
Excelerate	Exquisite	150,900	5.1	500	290	43	12.4	LNGC w/Regas Capability

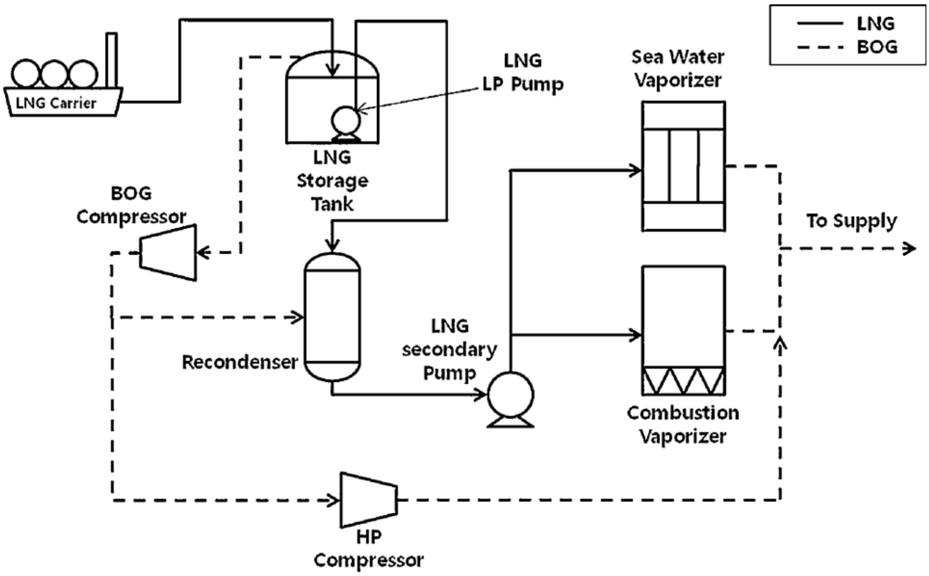

Figure 2-3. Typical LNG receiving terminal process flow

Brief explanation of the **figure 2-3** is as follows;

A LNG carrier delivers LNG to a receiving terminal. Following berthing, the carrier pumps LNG ashore through unloading arms to a cryogenic pipeline to the storage tanks. The LNG will be stored at atmospheric pressure in specially designed cryogenic LNG storage tanks. The storage tanks will prevent heat input not to boil the LNG by its insulated surface. The LNG boil-off gas that is formed during transfer and storage is returned from the storage tanks to the ship by a blower or compressor so that ship pump load and BOG due to displacement in storage tanks can be handled. When the amount of BOG exceeds the amount to fill the empty volume in LNG tanker, the excess BOG is recovered by boil-off gas compressors and recondenser. The stored LNG is pumped at pipeline pressure by high pressure multistage cryogenic pumps and re-gasified by heating it with seawater using heat exchangers. The type of heat exchanger is changed by the circumstance of the terminal's site and for LNG-FSRU, the selection of heat exchanger will be important.[40], [41]

One more thing to discuss about LNG-FSRU design is to define the construction type of LNG-FSRU. There are two different type of LNG-FSRU, "new-building" and "conversion" from LNG carrier and "New-building" means, literally, to design an entire LNG-FSRU at the beginning, while "conversion" means adding the topside modules such as regasification module on existing LNG carrier. Nowadays, mostly the new-building LNG-FSRU come up for new LNG-FSRU projects than conversion because of its short lead time. **Table 2-2** shows the typical lead time of each LNG terminal projects and the building time of new-building FSRU is shorter than of conversion. For this reason, only the new-building LNG-FSRU will be discussed in this research.

Table 2-2. Typical lead time of LNG-FSRU

Construction basis	Typical lead time
FSRU-conversion of existing carrier	3-4 years
FSRU-new building	1-2 years
Construction time for onshore facility	3-4 years
Permitting process (Typically)	2 years

2.2.2. Traditional process design procedures

In order to design a LNG-FSRU topside process, it is necessary to examine the general process design methodology. There were many researches about chemical process design procedures and the hierarchical methodologies aligned by Douglas or Seider are the dominant techniques for chemical process design in these days.[42–44] As seen in **figure 2-4,** the process design methodology suggested by Seider covers overall area for chemical process design procedures and by the end of the method, Front-End Engineering Design (FEED) package can be delivered. However, this methodology is not perfect for offshore plants especially for the topside processes because the topside design of offshore plant should contain offshore problems those are not included in the traditional process design methodology.

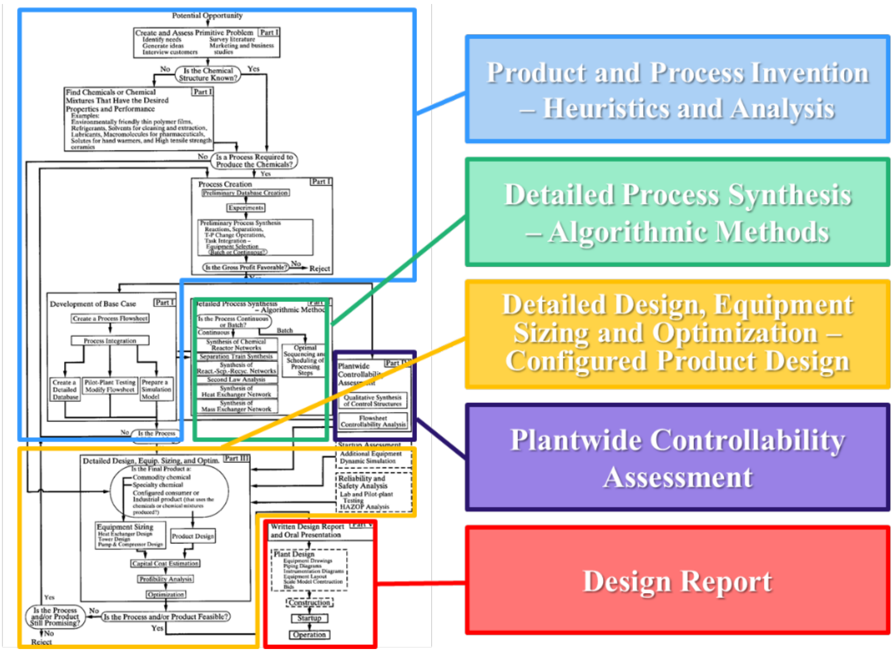

Figure 2-4. A flowchart of general chemical process design procedure

2.2.3. Process design for offshore plant topside

While the offshore plant industry has been developed for several decades, some researchers have studied about the methodology for designing the topside process of offshore plant. Hwang proposed an optimized methodology for building an integrate solution to offshore topside process engineering. In the early stage of offshore industry, there were some design cases for designing offshore production facilities by following the traditional process design methodology with larger design margin.[45] The offshore topside design methodology has been progressed and an integrated solution (**Figure 2-5**) to offshore topside process engineering was developed recently. However, there is no consideration of topside process design for offshore condition but focus on application of basic process engineering procedure to offshore plant.[36]

The most influential design methodology for LNG-FSRU topside process was suggested by Han.[46] This research insists that design of LNG-FSRU should be based on the experiences from the onshore LNG terminal, FPSOs and LNG carriers. This insistence is materialized and accepted by many other researches and classification materials. [47–49] Though these researches brought an improvement of topside design, the offshore condition was not reflected to the topside process system well.

In this research, LNG-FSRU topside design which is suitable for offshore condition is developed. The developed design will be more economically feasible, have lighter equipment, and include consideration on topside layout.

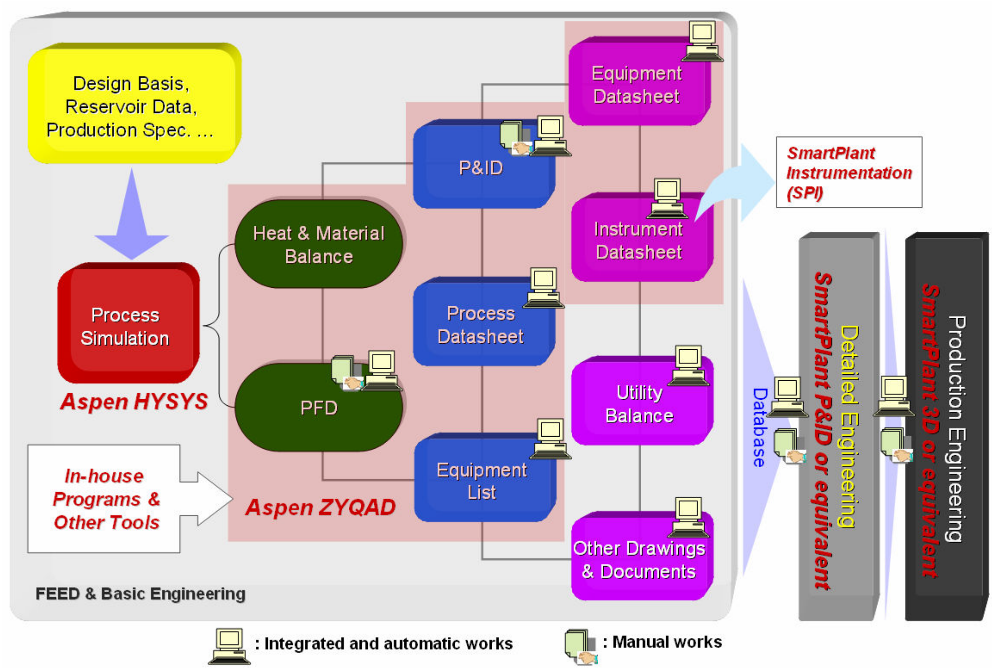

Figure 2-5. Integrated procedure for offshore process engineering[36]

2.3. Basis of design for LNG-FSRU

Design of LNG-FSRU topside process should be based on the design specification and circumstance of target site. Therefore these specifications must be defined first.

2.3.1. Design specification

The design basis of LNG-FSRU is as follows;

Terminal Sendout[8], [50] :	Max. 5.2 mtpa
	= 593.6 ton/hr (115% load)
	Min. 0.45 mtpa
	= 51.27 ton/hr
	100 bar (ANSI 600 pressure class)
Turn down ratio(TDR) :	10 : 1
Offloading System[51], [52] :	Ship 125,000 m3 ~ 210,000 m3
	Offloading Rate 12,000 m3/h
LNG Cargo Tank[8], [16], [53] :	Capacity 45,000 m3 * 6
	Design pressure 250 mbarg
	Operating pressure 200 mbarg
	BOR = 0.15 wt%/day
Seawater Temperature Difference :	8°C
Design lifetime :	20 years

LNG Composition :	Methane	0.9133
	Ethane	0.0536
	Propane	0.0214
	i-butane	0.0046
	n-butane	0.0047
	i-pentane	0.0001
	n-pentane	0.0001
	Nitrogen	0.0022

The specifications above are referred from the LNG-FSRU and onshore terminal design studies by Sohn, Lee and Lee.[8], [9], [53]

2.3.2. Target specification

General offshore plants have various specifications with their location, purpose and characteristics of the field. However in LNG-FSRU, there are not huge differences between the vessels. Especially on the topside process, the basic features are not changed by project sites so that the topside process of LNG-FSRU can be standardized. To develop a standard LNG-FSRU topside process flowsheet, it is essential to define the environmental condition of target sites such as seawater temperature.

Following contents are the most influential environmental factors for designing topside process of LNG-FSRU, which are also specified in the basis of design(BOD) for each LNG-FSRU project.

1) Location data : **Figure 2-6** shows current states of LNG-FSRU projects over the world. As seen in the figure, many planned projects are concentrated on the region between -30 to 30 degree in latitude.

   One more thing to consider target location is about the demanding countries. The most attractive strength of LNG-FSRU for energy suppliers is shorter leading time. Moreover, LNG-FSRU does not need to secure large land area and civil construction work as onshore LNG terminal that it is an optimal type of supplying LNG for the developing countries. As many developing countries such as India, Indonesia, Malaysia and Mexico are in the equatorial region that the target location is specified to the region between -30 to 30 degree in latitude.

2) Metocean data – seawater temperature : After the target location is defined, seawater condition of the target should be specified because the seawater condition is the most effective thing in determining the topside process of LNG-FSRU such as vaporization method. Seawater temperature over global ocean is displayed in the **figure 2-7** and the raw data of the sea surface temperature (SST) is available at a webpage of National Climatic Data Center at National Oceanic and Atmospheric Administration (NOAA).[54] As it is seen in the figure and the raw data, the average temperature at the target area in winter is 26 ^{o}C, which value will be a standard for designing vaporization method and equipment.

3) Metocean data – air temperature : Air temperature as well as seawater temperature is an important variable for designing topside process of

LNG-FSRU. As a promising vaporization method for LNG-FSRU is the ambient air vaporizer(AAV) and air temperature can define the amount of heat flux from the atmosphere so that air temperature should be specified before designing the topside process. According to the anomaly data of the target area from NOAA at **figure 2-8** and average temperature data from Jones as **figure 2-9,** the air temperature at the target region is set to -13 ^{o}C.[55], [56]

4) Motion analysis : Ship motion is, as mentioned above, the most influential factor on offshore processes that consideration about the motional effect on the topside process must be included in the process design work. When the ship motion is induced to process units over topside, sometimes efficiency can change or possibility of failure can increase. Therefore we need to consider how the process unit will be affected by ship motion.

   To estimate ship motion effect, how much the ship will be shaken is determined at first. There are many researches of rolling or pitching phenomena for floating plant and several design cases of LNG-FSRU contain the wave analysis report. [57–61] According to these research, the most frequently remarked standards are, 2 degrees of roll for design and 6 degrees for maximum amount. For the quantitative result, the most probably maximum(MPM) amount of roll amplitude is suggested for 100-year environment as below.

   100 years design environment

   H_s (maximum wave height) = 12.2 m

T_p (wave period)	= 14.2 s
V_w (wind speed)	= 36.5 m/s (at 30 degrees)
V_c (current speed)	= 1.75 m/s (at 45 degrees)

MPM roll amplitude for 100 years = 5.8 degree

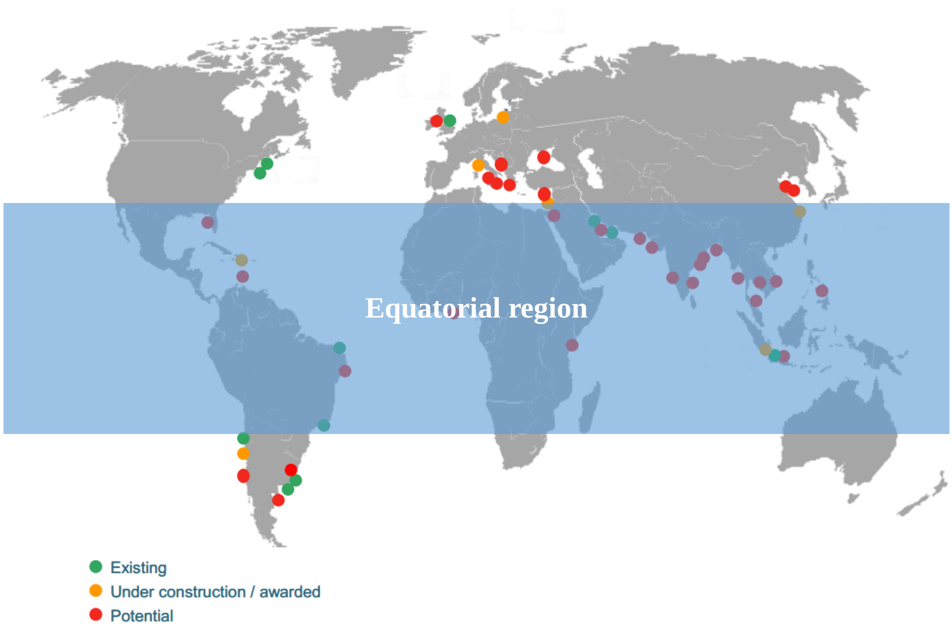

Figure 2-6. Current status of world’s LNG-FSRU projects[62]

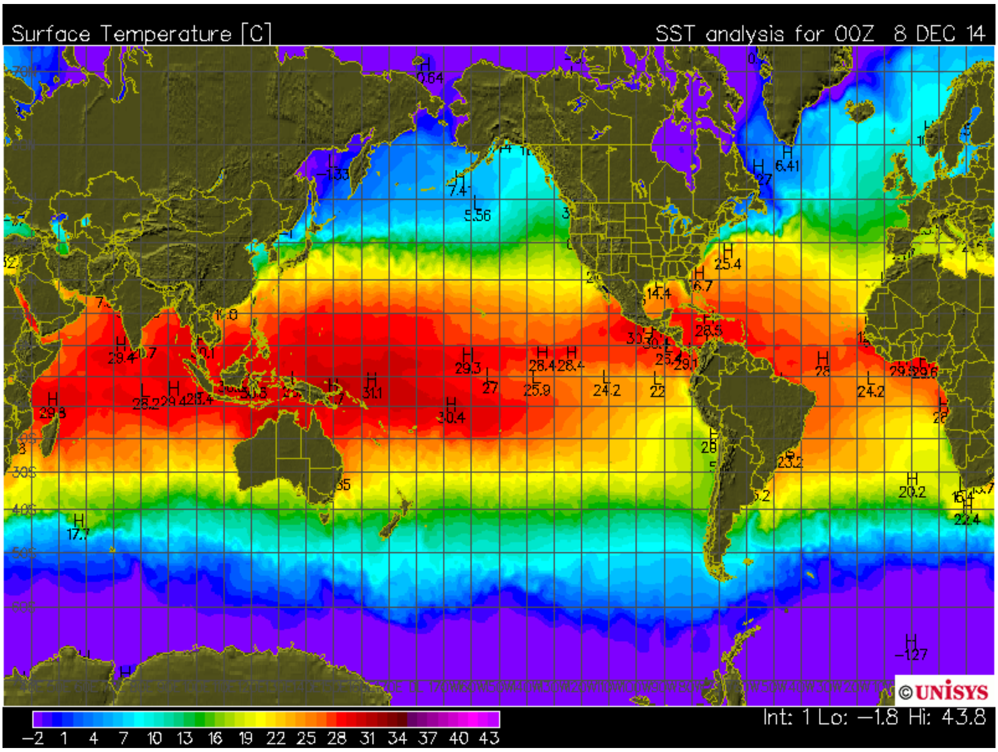

Figure 2-7. Sea surface temperature distribution

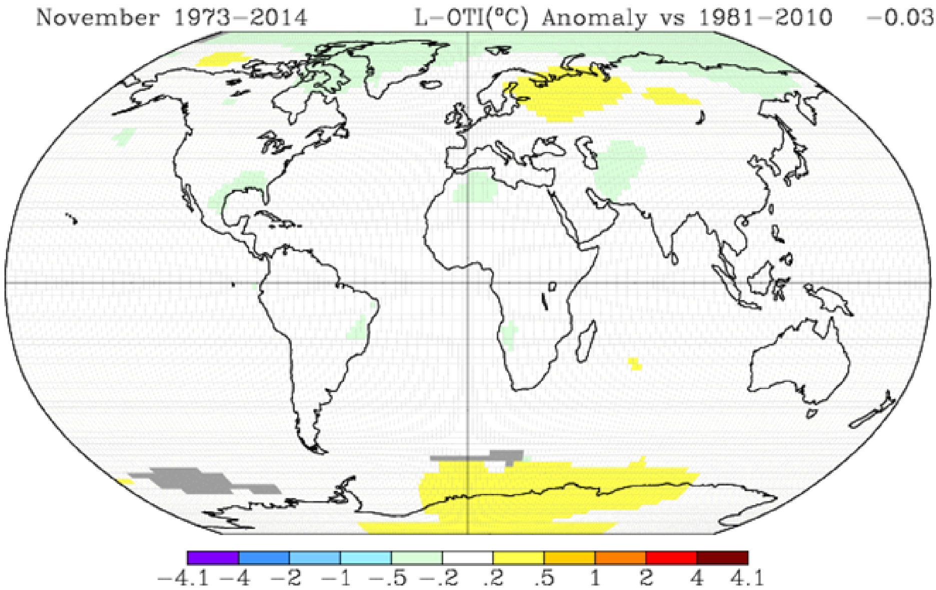

(a)

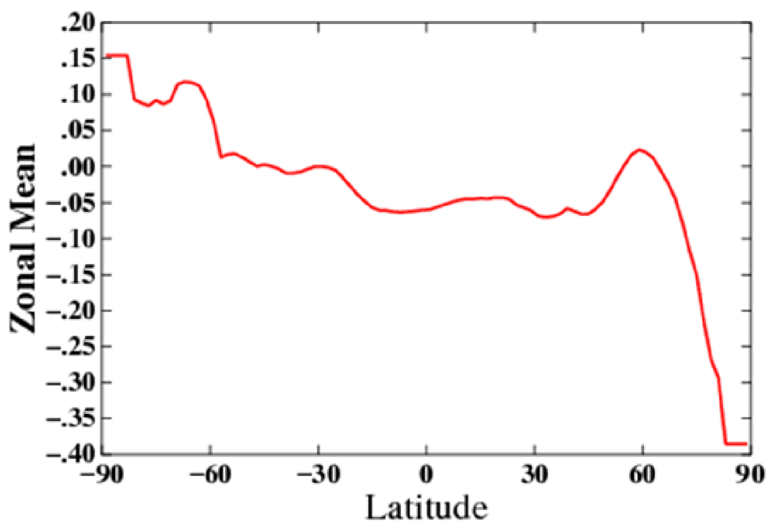

(b)

Figure 2-8. Anomaly data of air surface temperature; (a) over the world, (b) by latitude

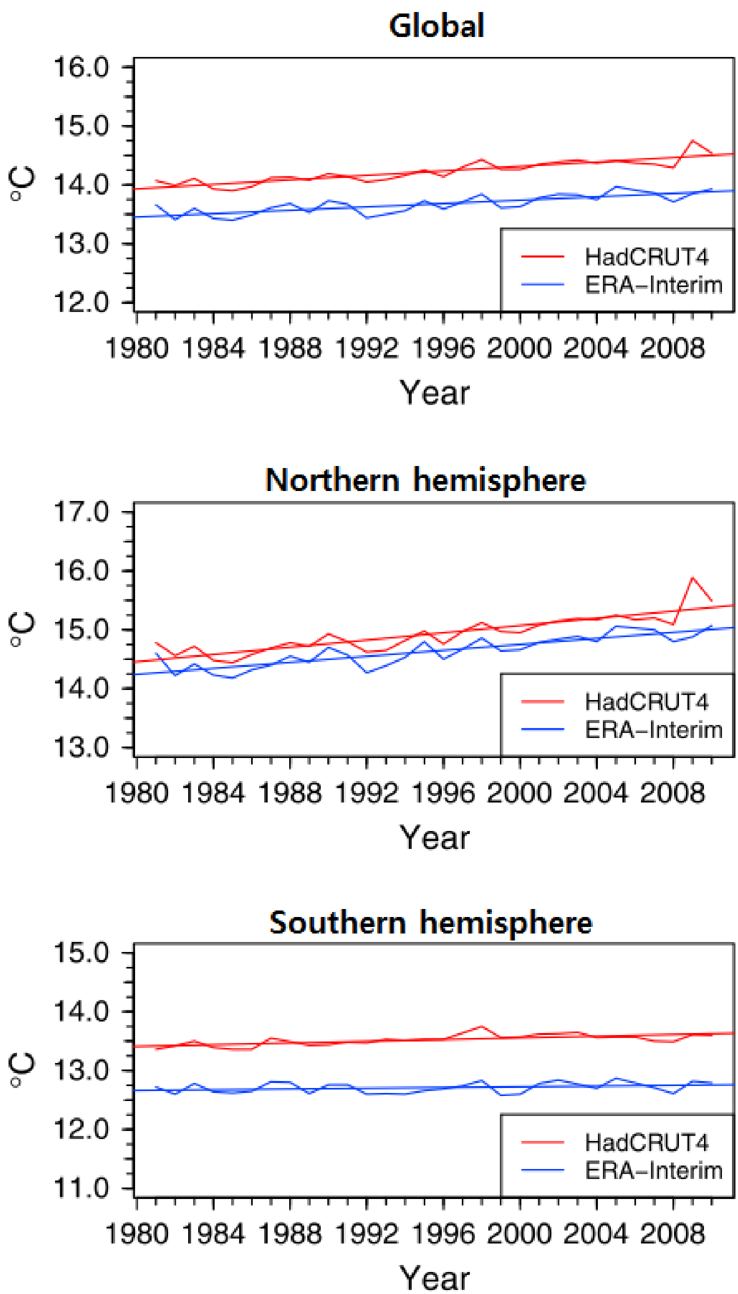

Figure 2-9. Global average temperature data from 1981 to 2011[55]

2.4. LNG-FSRU Topside process design

Based on the design specification and target information, the topside process of LNG-FSRU is designed. To make a topside design of LNG-FSRU, the basic process scheme is derived from the basic process of onshore LNG terminal and alternative designs from other researches. Detailed process variables are updated with using the design specification and offshore restrictions after the basic scheme is fixed and finally the topside design of LNG-FSRU is determined.

2.4.1. Basic process scheme

The first thing to do for designing topside process is to build a basic process scheme. As Douglas suggested, every process design work will be meaningful after the base block flow is determined.

The basic process scheme of LNG-FSRU refers the onshore LNG terminal. **Figure 2-9** illustrates the basic scheme which is displayed by the process simulation model and **table 2-3** shows the list of major systems and components. Because the onshore LNG terminal has the same purpose with similar specifications that it is rational to use the terminal's process scheme.

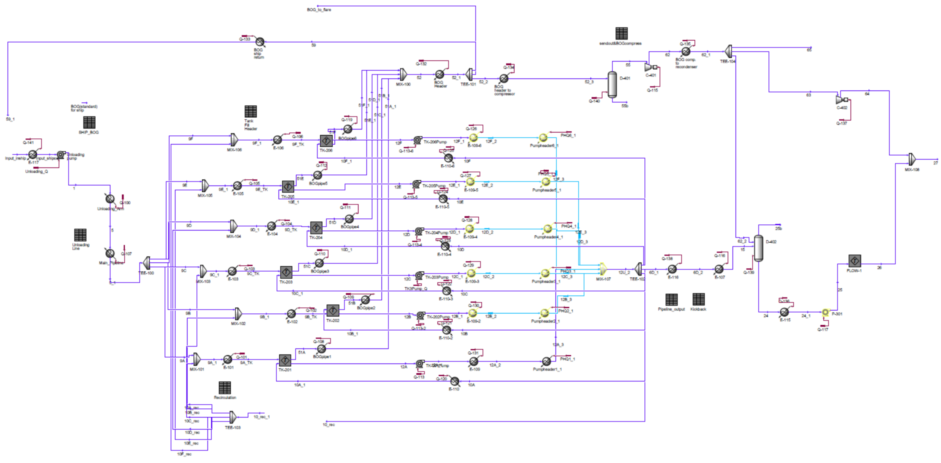

Figure 2-10. LNG-FSRU basic process scheme

Table 2-3. Major systems and components of LNG-FSRU topside

Major system	Components
LNG Unloading and Transfer System	LNG unloading arm
LNG Storage System	LNG storage tank
	LP pump
Vapor Handling System	BOG compressor
	BOG recondenser
	Flare
Vaporization and Sendout System	HP pump
	Vaporizer
Utility system	Utilities

When the basic scheme of the process is built, declaration of operation scenario comes after. The reason to declare the operation scenario is that the process condition changes with each scenario. There are two major differences between the scenarios those are unloading status and sendout rate. According to these differences the base scenarios are established as 4 cases;

1) LNG unloading / maximum sendout
2) No ship connection / maximum sendout
3) LNG unloading / minimum sendout
4) No ship connection / minimum sendout

2.4.2. Detailed design of topside process

After the basic process scheme is decided, detailed design variables need to be specified to complete the topside process design. The detailed information such as equipment type and size and process variable will be determined in this step with satisfying the design specifications.

In addition, offshore features will be applied to topside design in this step. Because the offshore features can affect the selection of equipment and performance, the topside design will compromise with the features. **Table 2-4** shows the consideration points of offshore feature for each process component.

Table 2-4. Offshore effects on process components

Process components	Offshore features		
	Ship motion effect on equipment	Compactness	Equipment weight
Loading pipe	○	Do not exceed the plant size	Weight of component must be under 2000 ton
Storage tank	○		
Flare	×		
BOG compressor	×		
Precooler	×		
Recondenser	○		
LP Pump	×		
HP pump	×		
Vaporizer	○		
ORV	○		
STV	×		
IFV	×		
AAV	×		
SCV	○		

(Where ○ means "need to consider" and × means "neglectable")

As presented in **table 2-4**, many process components are affected by the ship motion and they should follow the limitation of area and weight. With consideration on these additional factors, the following provides the detail information and standard of the process flow:

- LNG unloading pipeline

The purpose of LNG unloading line is transferring LNG from carrier to storage tank. To prevent heat input from outside, insulation material is installed over all pipelines. The overall heat transfer coefficient is calculated with using the following condition;

Insulation material :	urethane foam (thermal conductivity : 0.0232 W/mK)
Insulation thickness :	20 cm

Due to the effect of ship motion, the flow inside the loading pipe also fluctuated. This phenomenon will cause unstable LNG flow rate or even evaporation at a worst case. Therefore, to avoid the risk of ship motion, the length of unloading arm should be limited according to the ship discharge pressure. In addition, the fluid inside the pipeline should be subcooled not to vaporize. These features will be considered during the simulation.

Additionally, one thing to consider remains what is about the offshore problem. Due to the ship motion, the flow rate of LNG can be affected and fluctuated. To assure stable flow of LNG inside the unloading line, the pressure drop by inclined situation is calculated by process simulation software as below.

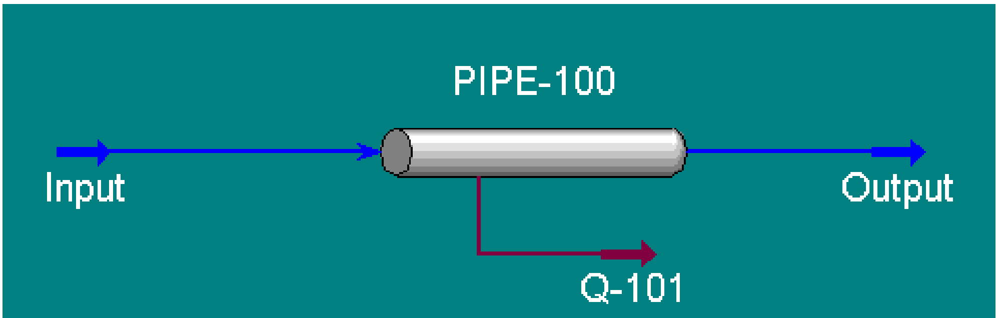

PIPE-100		
Inside Diameter(1)	818.8	mm
Outside Diameter(1)	828.0	mm
Pipe Length(1)	300.0	m
Elevation(1)	30.00	m
Feed Temperature	-158.0	C
Product Temperature	-158.0	C
Feed Pressure	5.500	kg/cm2
Product Pressure	4.107	kg/cm2
Pressure Drop	1.366	bar

Figure 2-11. Simulation result of unloading pipeline for tilted situation

Simulation input condition :

Length of maximum loading line :	300m
Tilting angle :	6^o
Flow rate :	1 e 6 kg/h
Inlet pressure :	5.5 bar
Pipe diameter :	828 mm

Simulation result :

Pressure drop :	1.095 bar

Usually many LNG carrier send LNG at 4~5 bar that the pressure drop for inclined case will not be a huge problem for unloading process.

- LNG storage tank

Usual onshore LNG terminals use 0.1 wt%/day for BOR, however in LNG-FSRU, the standard of BOR value refers to LNG carrier.

Number of storage tanks :	6
Storage tank capacity :	45,000 m3
Boil off rate(BOR) :	0.15 wt%/day

- LP pump

As the maximum sendout rate is nearly 600 ton/h that each LP pump, the pump capacity is designed to satisfy the sendout rate. There are 6 storage tanks in FSRU and when all pumps are in operation, the capacity will fulfill the sendout rate specification. One more thing to consider is that the LP pumps should be installed inside the LNG storage tank that it is too complicate to maintenance during operation. Therefore the pumps will be installed redundantly.

Features :	In-tank type pump
	2 * 100% pumps installed
Pump capacity :	130 ton/h per single LP pump (130% of design load)
Number of LP Pumps :	12

- BOG compressor

BOG compressor gathers boil-off gas from LNG storage tank and sends pressurized gas to BOG recondenser. The most important variable about BOG compressor is discharge pressure and the value is determined for maximum efficiency. Zolfkhani presented a research about optimum pressure for BOG compressor and recondenser which is from 7 to 8 barg like **figure 2-11**.[63] Besides there are many researches and patents of the condition of BOG recondenser and usually 8 barg is used.

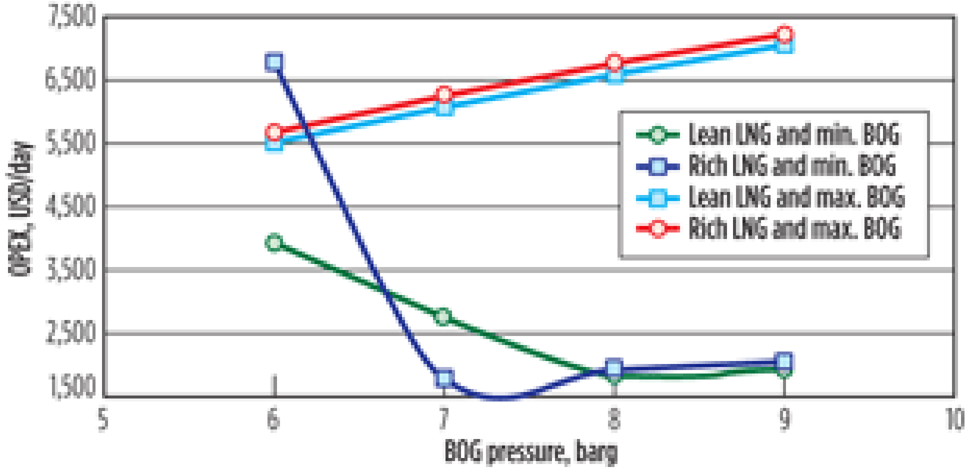

Figure 2-12. Operation costs by various BOG pressure at BOG compressor

The capacity of BOG compressor is specified from the calculation result of the BOG production rate in LNG-FSRU. However the BOG production rate is different by the scenario and it will be confirmed at the end of the design procedure that the capacity will be decided at last. Other design specifications refers to many researches and actual LNG terminals in operation.[16], [20], [64]

Compressor type :	Centrifugal type
Discharge pressure :	8 barg
Compressor efficiency :	75 %

- BOG recondenser

The BOG recondenser takes a part of recovering and liquefying BOG. Besides, the recondenser is used as a knock-out drum for HP pump as displayed in the process flowsheet. That means, the recondenser must keep its liquid level during the HP pump operation and when the recondenser level decreases, the HP pump should be turned off in order to prevent failure of HP pump. This is the primary issue to design size of the recondenser. Assume that the LNG input to the recondenser suddenly stopped, the BOG will push the filling LNG. HP pumps must be shut down until the recondenser is empty. Therefore the size of BOG recondenser will be determined with the information about the pump shut down time and BOG volume flow rate.[65]

$$V = f \cdot t_r \quad (1)$$

V : recondenser unit size

f : BOG volumetric flow rate

t_r : minimum shutdown time for HP pump

- Flare

Flare system disposes the excess boil-off gas which is not able to be recovered in vapor handling system by burning it over the flare stack. There is a limitation to the pressure of disposed BOG on API standard 521, which is over 5 bar.[66] This standard will be applied to the design result.

- HP pump

According to the design specification for sendout gas pressure, the product, vaporized LNG must be pressurized over 100 bar. Because it is more feasible to pressurize LNG at first, HP pumps are prior to the vaporizer. The pressure of HP pump is decided with consideration of sendout pressure and the pressure drop from the vaporizer. Usually the pressure drop of LNG vaporizer is suggested to 2 bar that the result of HP pump pressure is as follows;

HP pump pressure : 102 bar

Another necessary specification of HP pumps is capacity and number of units. Usually the capacity of pump is getting larger, the overall capital cost is decreased but at the minimum send out situation, the excess amount of pressurized LNG will be returned to BOG recondenser. Because of the pump efficiency, the returned LNG BOG will evaporate and increase excess BOG. So it will be determined in process simulation model for minimum sendout/unloading case to minimize excess BOG.

- Vaporizer

There are many options to vaporize LNG as displayed in **figure 2-13**, and the following 5 types are the most widespread vaporizer for LNG regasification terminal.

  - Open Rack Vaporizers (ORV)
  - Submerged Combustion Vaporizers (SCV)
  - Ambient Air Vaporizers (AAV)
  - Intermediate Fluid Vaporizers (IFV)
  - Shell and Tube Vaporizers(STV)

To develop a topside process of LNG-FSRU, an appropriate type of vaporization method will be selected during the design procedure.

ORV is the one of the most popular type of vaporizer in existing regasification terminals especially in Korea, Japan and Europe because of its easy operation and maintenance. As seen in the **figure 2-14**, ORV uses the seawater as heating material and when the relatively hot seawater is distributed above, input LNG is evaporated absorbing the heat from the hot water.

SCV is another widespread vaporizer for the LNG terminal in the sub-equatorial region. If the seawater is not relatively hot enough and when there is a harsh regulation for seawater temperature difference, SCV is preferred to ORV. The schematic diagram for SCV is displayed in **figure 2-15**.

AAV uses ambient air as heat source as seen in the **figure 2-16**. To use this type of vaporization method, the temperature of target location must be high enough.

IFV has somewhat complex structure than other vaporization methods above but it has an advantage on safety so that this method attracts attention of LNG industry. The simplified structure is seen in **figure 2-17** and propane and water-glycol mixtures are utilized for the heating media.

STV is to use a simple shell and tube heat exchanger as vaporizer. The basic concept of STV is similar to ORV, what is to use seawater as a heat source and the seawater directly heat the LNG. The difference between these vaporizers is the structure of vaporizer unit. STV has strengths on various aspects, fast and easy operation, simple system, compact design, and offshore compatibility. [67–70]

The selection of an appropriate vaporization method will be handled in the next section.

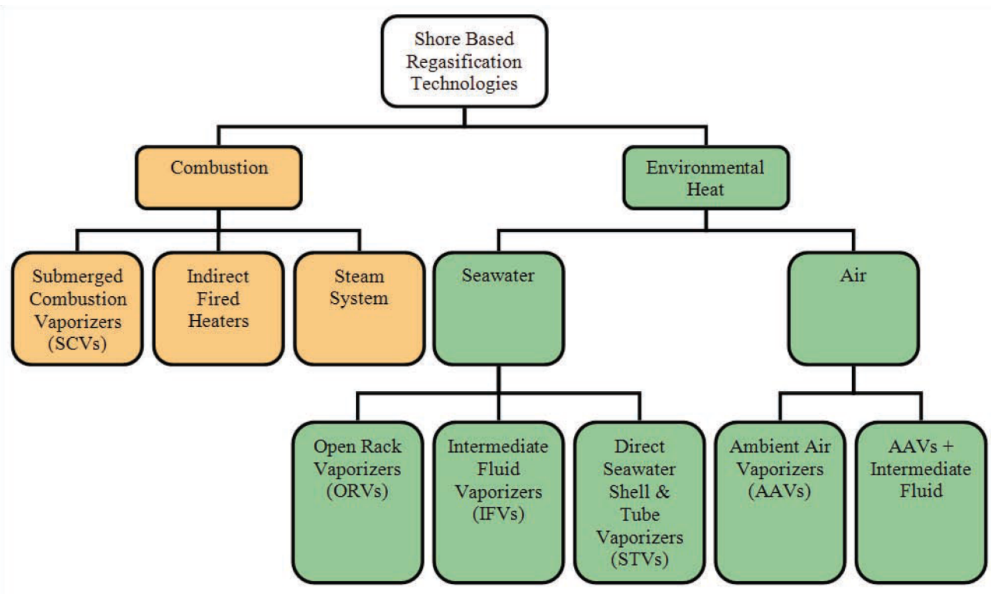

Figure 2-13. A classification for LNG regasification processes[71]

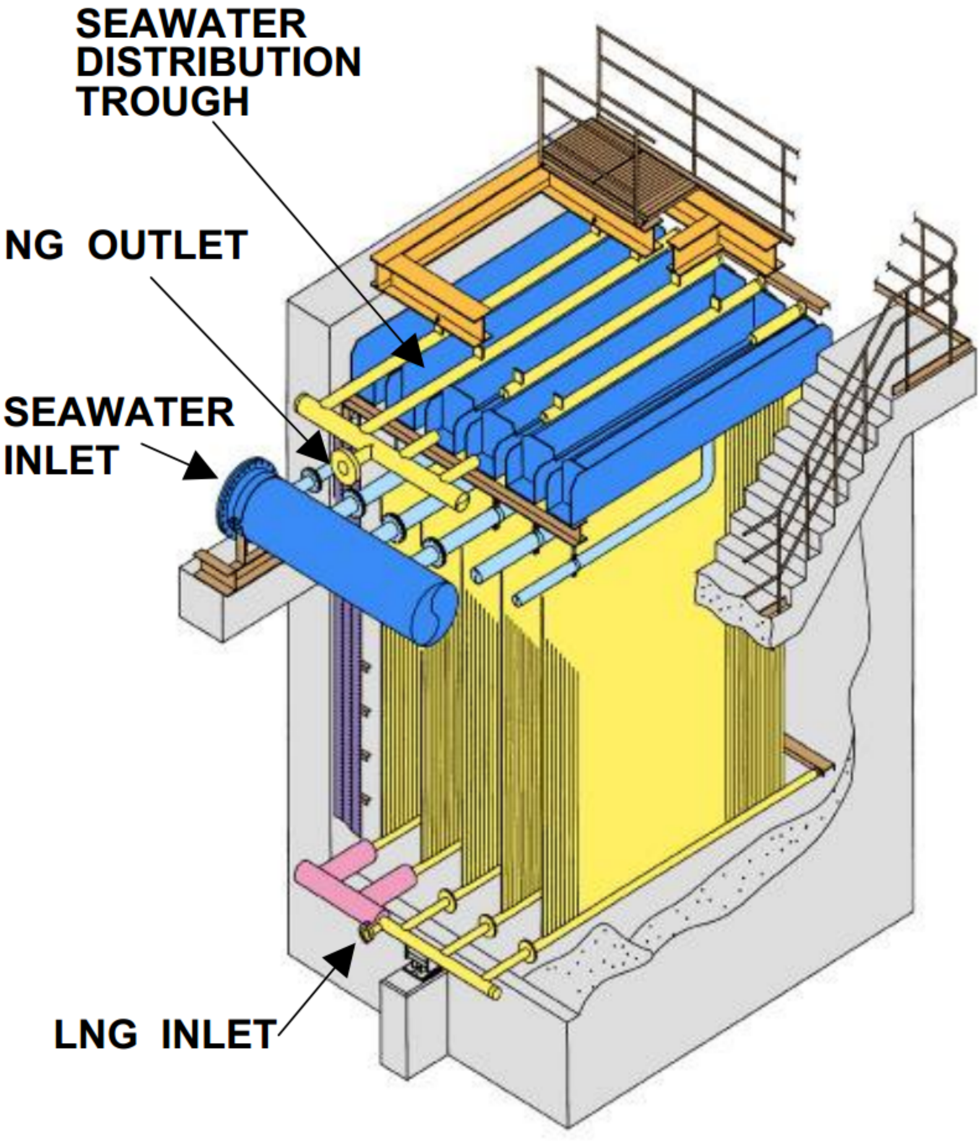

Figure 2-14. A bird view of open rack vaporizer(ORV)

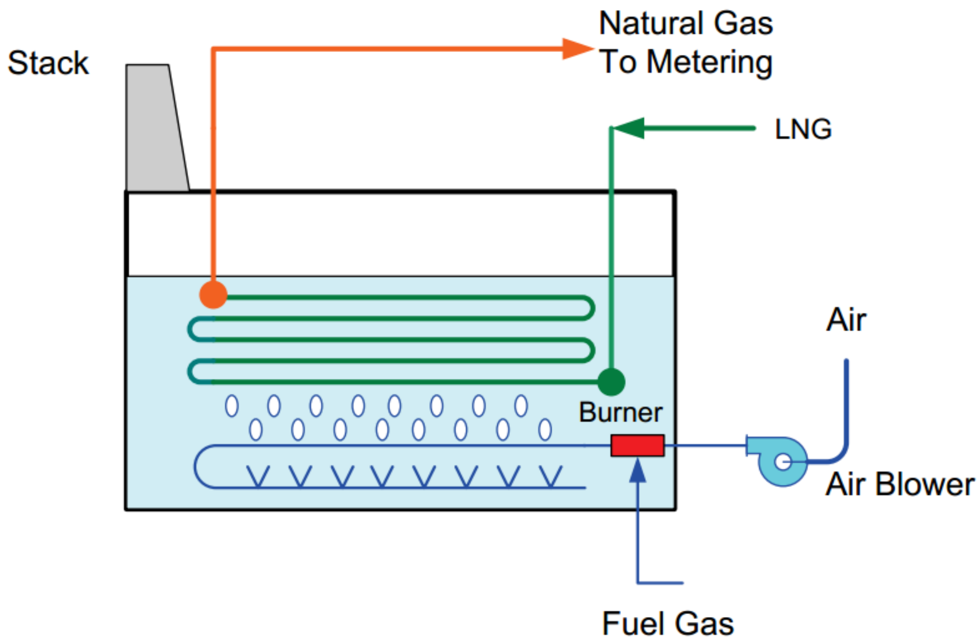

Figure 2-15. A schematic diagram of submerged combustion vaporizer(SCV)

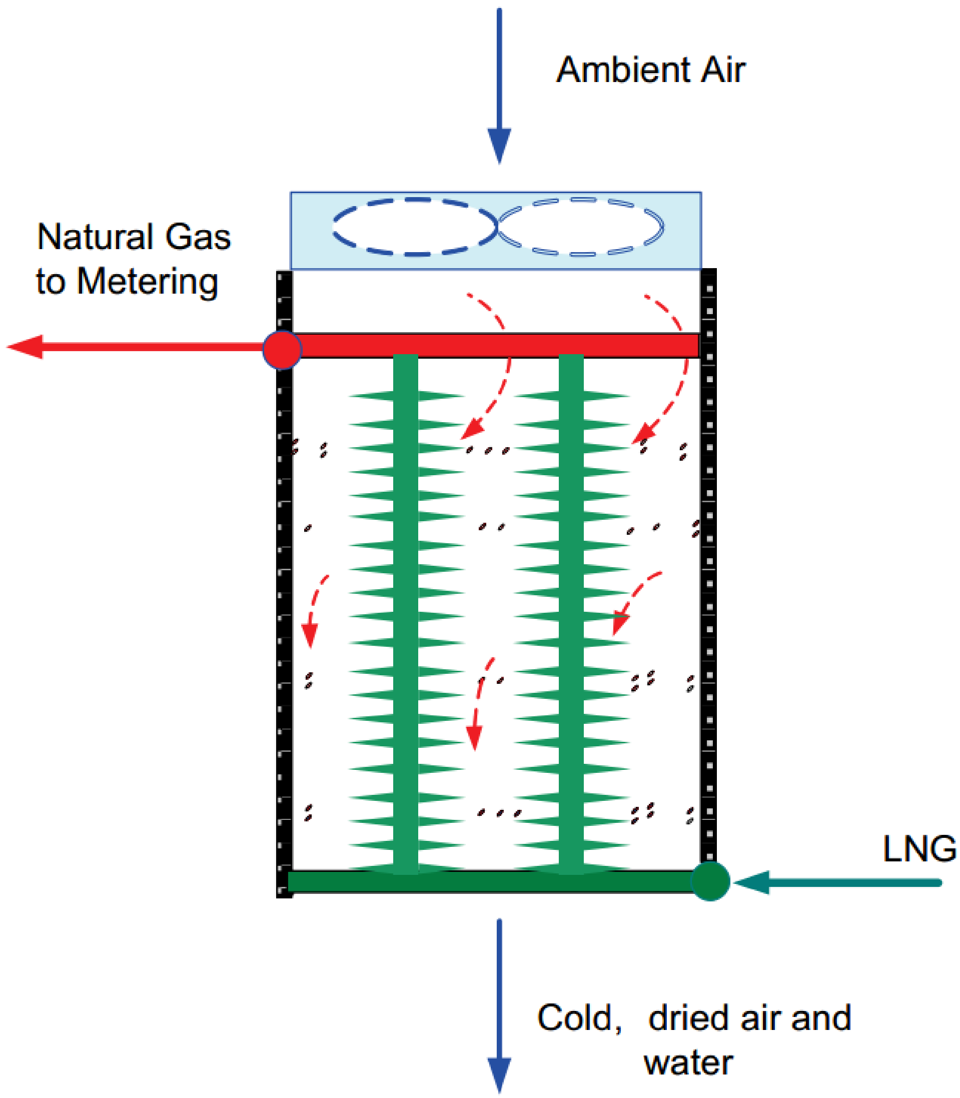

Figure 2-16. A schematic diagram of ambient air vaporizer(AAV)

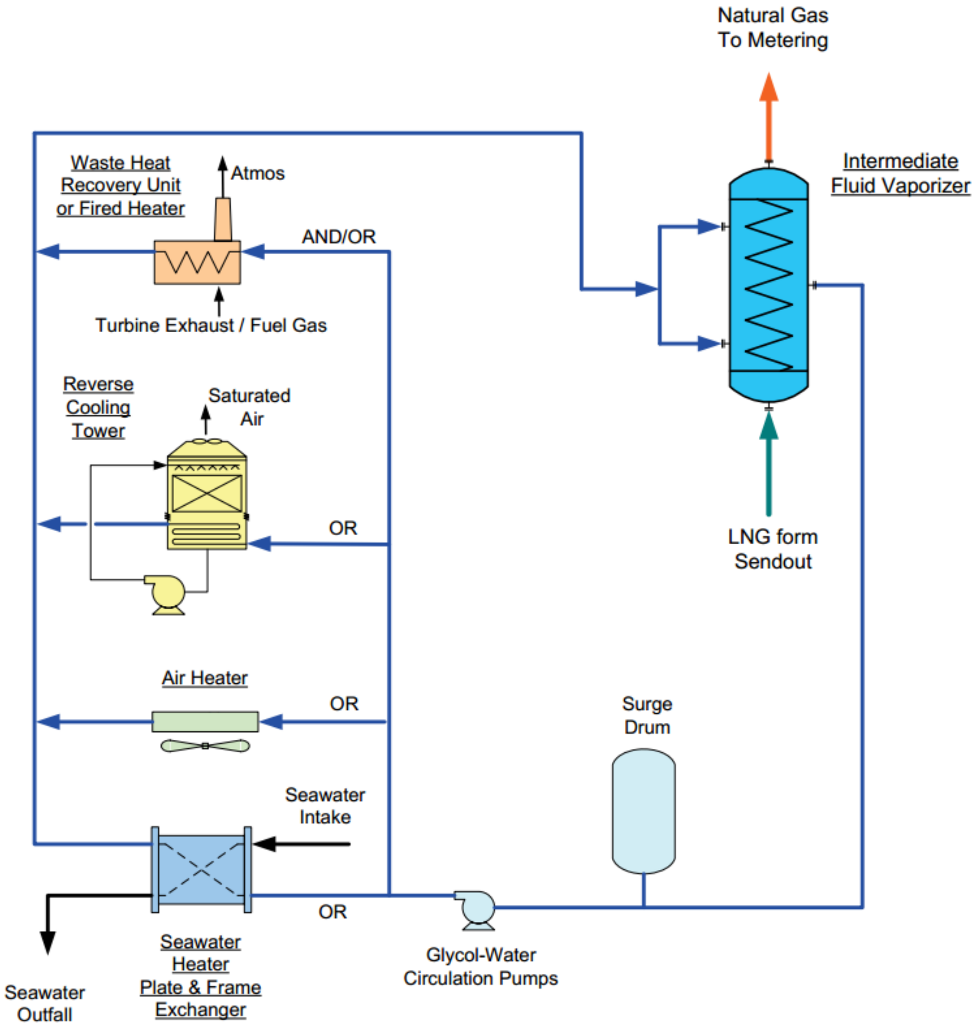

Figure 2-17. Examples of intermediate fluid vaporizers (IFV)

2.4.3. Vaporizator selection

In this section, each vaporization methods are designed to satisfy the design specification and finally the best option is selected for LNG-FSRU topside process.

At first, the target design specifications are following;

Send-out gas temperature :	5 ^oC
Allowable pressure loss :	5 bar
Seawater temperature difference :	7 ^oC
Seawater input temperature :	26 ^oC

In this research, ASPEN Exchanger Design & Rating V7.3(EDR) is applied to design the vaporizers more precisely.

- Open Rack Vaporizers (ORV)

The open rack vaporizer uses seawater as heating material and it uses gravitational force to flow heating media. Table 2-5 and 2-6 shows the design specification of ORV example. Unfortunately ASPEN EDR does not have an exact model for ORV, the size and weight is calculated by manual calculations.

Table 2-5. A data sheet of sample ORV

DATA SHEET

OPEN RACK VAPORIZER		
MANUFACTURER	KOBE STEEL, LTD.	
ITEM NO.	-	
NO. OF UNITS	2	
	PERFORMANCE OF ONE UNIT	
NO. OF PANELS	5 (5 PANELS × 1 BLOCKS) (*)	
NO. OF TUBES PER PANEL	90 (*)	
LENGTH OF HEAT TRANSFER TUBE	6000mm(*)	
TYPE OF HEAT TRANSFER TUBE		
FLUID NAME	LNG	SEA WATER
MOL. WEIGHT	-	-
FLOW-RATE TOTAL (Ton/hr)	110	2,840 (*)(**)
NOR. INLET OPERATING PRESS. (barg)	55	0.5
TEMP. WARM END (℃)	4.4	25.6
COLD END (℃)	-153.9	18.3 (*)
HEAT LOAD (MW)	22.96 (*)	
ALLOWABLE /CAL.P.D. (bar)	1.8 / 2.0 (*)	- / 0.5 (*)
FOULING FACTOR (m2K/W)	0	0.00017
DESIGN PRESSURE (barg)	99	6 (*)
DESIGN TEMPERATURE (℃)	−170∼65 (*)	0∼60 (*)
CORROSION ALLOWANCE (mm)	0 (*)	0 (*)
	MATERIAL	
HEAT TRANSFER TUBES	ASTM B221M 6063(*)	
HEADERS	ASTM B241M 5083(*)	FRP (*)
FLANGES	ASTM B247M 5083(*)	FRP (*)
MANIFOLD PIPES	ASTM B241M 5083(*)	FRP (*)
LNG/NG END COVER	ASTM B247M 5083(*)	

Table 2-6. A geometric data sheet of sample ORV

Name	Material	Height (ft)	Width (ft)	Length (ft)	Total weight(ton)	
					Dry	Oper.
LNG open rack vaporizer	AL-6XN	29	15	23	42.2	99.8

For the calculation of ORV, the design result from Dendy and Nanda is referred as a standard.[72] According to their result in **table 2-7**, the cost and geometric data of ORV will be available when the result of another option, STV is calculated.

One more thing to consider in designing ORV is when the ORV is shaken by ship motion, its vaporization efficiency is changed by the contacting area ratio(CAR). This concept is well applied by PFR which is dealt with the first section of this chapter and the same concept is applied to the ORV design. In details of changing efficiency of ORV, we need to calculate the contacting area ratio. When the seawater falls gravitationally to the tilted area as seen in **figure 2-18(b)**, the contacting area S_1 is decided by θ which is a tilting angle. In this research, the tilting angle refers to the MPM roll amplitude that the value is 6 degrees.

The equation for contacting area ratio is determined as follows.

$$CAR = \frac{S_1}{S_1+S_2} = \frac{\frac{(x+(x-h\cdot\tan\theta))\cdot h}{2}}{x\cdot h} \quad (2)$$

When the CAR is applied to ORV, the height and width of ORV must be specified. If we assume the height and width as **table 2-6**, CAR value will be 0.92. However if we focus on each tube of ORV, CAR value is calculated as 0.0381, which means the size of ORV should be designed 26 times larger to operate in tough wave condition.

Therefore ORV is not recommended for LNG-FSRU except the LNG-FSRU is anchored to landside.

Table 2-7. Calculation result of vaporization methods

System		SCV	STV-Indirect	STV-Direct	SCV-hybrid	ORV-hybrid
Footprint		1	3.8	2.1	7.1	2.2
Total Installed Cost		1	1.4	1.3	1.4	1.4
Annual Operating Cost	Annual net (MMBTU)	1	0.28	0.4	0.34	0.3
	Annual (MW-hrs)	1	1.47	1.28	1.72	1.01

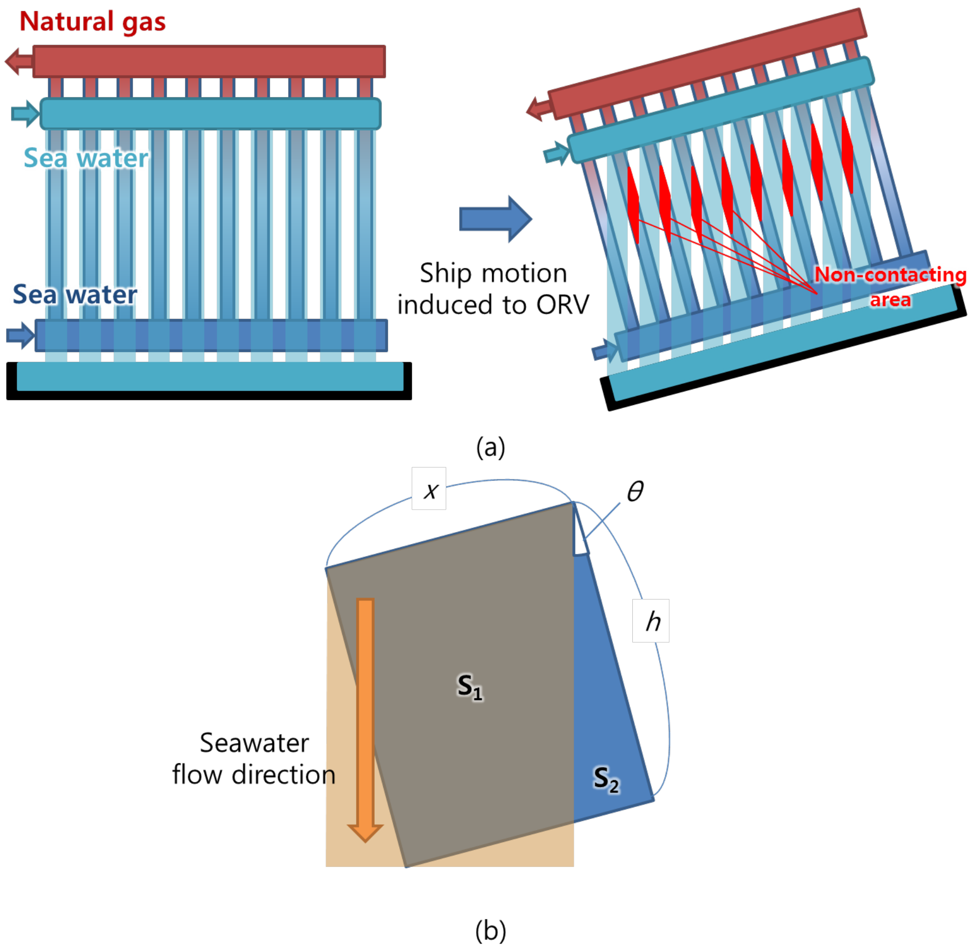

Figure 2-18. Efficiency loss of ORV due to ship motion; (a) a concept of efficiency loss, (b) calculation for efficiency change

- Submerged Combustion Vaporizers (SCV)

Before entering the detail design step, it is necessary to consider the economic feasibility of SCV because this type uses fuel to heat the LNG. If the heating cost is burden, this type does not need to be considered.

To check the economic feasibility, the amount of vaporization heat is calculated. The equation below depicts the LNG vaporization heat.

$$Q = m \cdot \Delta H_{vap} + \mathrm{m} \cdot C_{p,l} \cdot \Delta T_l + \mathrm{m} \cdot C_{p,v} \cdot \Delta T_v \quad (3)$$

Where Q is the overall heat amount, m is the mass flow rate of send-out LNG, $C_{p,l}$ and $C_{p,v}$ are the heat capacity of LNG at liquid state and vapor state. ΔH_{vap} is the heat of vaporization of LNG. ΔT_l is the temperature difference from the initial state to vaporization temperature and ΔT_v is the temperature difference between final state and bubble point temperature.

The amount of heat of vaporization can be calculated easily by process simulation software and the result for maximum send-out case is about 3.88 e 8 kJ/h and while the heat value of natural gas is 52.2 MJ/kg, the required amount of natural gas is 7.66 ton/h.[73] As the maximum send out gas flow rate is about 600 ton/h, over 1 % of LNG must be burnt to produce natural gas that this method is not applicable for the LNG-FSRU compared to other vaporization method.

- Ambient Air Vaporizers (AAV)

Aspen EDR supports the ambient air vaporizer but there is a limitation on the temperature range. The additional assumptions are below;

Ambient air temperature :	13 ^oC
Input LNG temperature :	-100 ^oC
Estimated pressure drop :	5 bar

The result is seen in the **table 2-8**. To cover the temperature difference between the LNG input to AAV and general LNG properties from HP pumps, a simple shell and tube heat exchanger is applied before the AAV. The shell and tube heat exchanger will use seawater as a heat source. To design a simple heat exchanger, the following information applied.

Input LNG temperature :	26 ^oC
Output LNG temperature :	18 ^oC

The design of STV is available at **table 2-9**.

Table 2-8. A specification sheet of AAV

Size & Type	20.6286 / 24.0192	m	Type	Forced		Number of Bays	4	
Surf/Unit-Finned Tube	97023.4	m2	Bare area/bundle	516.3	m2	Area ratio	23.49	
Heat exchanged	100171195	kcal/h		MTD, Eff		36.18	C	
Transfer Rate-Finned	28.6	Bare, Service		670.4	Clean	673	kcal/(h*m2*C)	

PERFORMANCE DATA - TUBE SIDE

Fluid Circulated							In/Out		
Total Fluid Entering	kg/h	600000			Density, Liq	kg/m3	331.56	/	463.19
			In/Out		Density, Vap	kg/m3	140.35	/	78.97
Temperature	C	-100	/	8.7	Specific Heat, Liq	kcal/(kg*C)	1.0855	/	0.715
Liquid	kg/h	600000	/	0	Specific Heat, Vap	kcal/(kg*C)	0.8613	/	0.6511
Vapor	kg/h	0	/	600000	Therm. Cond, Liq	kcal/(h*m*C)	0.103	/	0.092
Noncondensable	lb/h		/		Therm. Cond, Vap	kcal/(h*m*C)	0.04	/	0.036
Steam	lb/h		/		Freeze Point	C			
Water	lb/h		/		Bubble / Dew point	C	-49.98	/	-6.4
Molecular wt, Vap		16.1	/	16.1	Latent heat	BTU/lb			
Molecular wt, NC					Inlet pressure (abs)	kgf/cm2	91.775		
Viscosity, Liq	cp	0.0912	/	0.1031	Pres Drop, Allow/Calc		5	/	3.128
Viscosity, Vap		0.0144	/	0.0133	Fouling resistance	m2*h*C/kcal	0		

PERFORMANCE DATA - AIR SIDE

Air Quantity, Total	6000008	kg/h			Altitude	0	m
Air Quantity/Fan	117.278	m3/s			Temperature In	25	C
Static Pressure	186	Pa			Temperature Out	-44.51	C
Face Velocity	3.13	m/s	Bundle velocity	3.71 kg/s/m2	Design Ambient	13	C

DESIGN-MATERIALS-CONSTRUCTION

Design pressure	115.228	kgf/cm2	Test Pressure	Design temperature	0 C

TUBE BUNDLE			Header			Tube				
Size	m	20.6286	Type	Box		Material			Carbon Steel	
Number/bay	2		Material	Carbon Steel		Specifications				
Tube Rows	7		Passes	6		OD	25.4	Min Thk.	1.65	mm
Arrangement			Plug Mat.			No./Bur	329	Lng	20	m
Bundles	2	par	Gasket Mat.			Pitch	60 / 51.96		30	deg
Bays	4	par	Corr. Allow.		mm	**Fin**				
Bundle frame			Inlet Nozzle	1	146.33 mm	Type			G-finned	
MISCELLANEOUS			Outlet nozzle	1	193.68 mm	Material			Aluminum 1060	
Struct. Mount.			Special Nozzles			OD	57.15	Tks	0.28	mm
Surf.Prep			Rating			No.	433 #/m	DesTemp		C
Louvers			TI	PI		Code				
Vibration Switches			Chem Cleaning			Stamp		Specs		

MECHANICAL EQUIPMENT

Fan,Mfr., Model			Driver, Type		Speed Reducer, Type	
No./Bay	3		RPM	Mfr.	Mfr.&Model	
Dia.	4.572	m	Blade(s)	No./Bay	No./Bay	
Pitch			Angle	RPM	Rating	
Blade(s)			Hub	Enclosure	Ratio	
hp/Fan	36.736	kW	MinAmb	V/Phase/Hz	Support	
Control Action on Air Failure-					Louvers	
Degree Control of Outlet Process Temperature						
Recirculation					Steam Coil	No
Plot Area		m2	Drawing No.	Wt.Bundle 17832.2	Wt. Unit	142657.2 kg
Notes:						

Table 2-9. A TEMA sheet of preheater for AAV

Heat Exchanger Specification Sheet

Company:								
Location:								
Service of Unit:		Our Reference:						
Item No.:		Your Reference:						
Date:	Rev No.:	Job No.:						
Size 1574.8 /	3657.6 mm	Type BEM	Hor	Connected in	1	parallel	1	series
Surf/unit(eff.)	608.3 m2	Shells/unit 1		Surf/shell (eff.)		608.3		m2
PERFORMANCE OF ONE UNIT								
Fluid allocation			**Shell Side**		**Tube Side**			
Fluid name			BOG		LNG			
Fluid quantity, Total		kg/h	3377483		600000			
Vapor (In/Out)		kg/h	0	0	0	0		
Liquid		kg/h	3377483	3377483	600000	600000		
Noncondensable		kg/h	0		0			
Temperature (In/Out)		C	25	18	-150	-100		
Dew / Bubble point		C						
Density (Vap / Liq)		kg/m3	/ 997.24	/ 998.81	/ 446.93	/ 363.8		
Viscosity		cp	/ 0.8904	/ 1.053	/ 0.1145	/ 0.0441		
Molecular wt, Vap								
Molecular wt, NC								
Specific heat		kcal/(kg*C)	/ 0.999	/ 0.999	/ 0.7422	/ 0.8567		
Thermal conductivity		kcal/(h*m*C)	/ 0.522	/ 0.512	/ 0.152	/ 0.093		
Latent heat		kcal/kg						
Pressure (abs)		kgf/cm2	3	1.044	102	101.975		
Velocity		m/s	5.18		0.83			
Pressure drop, allow./calc.		kgf/cm2	2	1.956	1.122	0.025		
Fouling resist. (min)		m2*h*C/kcal	0		0	0	Ao based	
Heat exchanged	2362818	kcal/h			MTD corrected	144.86	C	
Transfer rate, Service	268.1		Dirty	1278.6	Clean	1278.6	kcal/(h*m2*C)	
CONSTRUCTION OF ONE SHELL					**Sketch**			
		Shell Side		**Tube Side**				
Design/vac/test pressure:	kgf/cm2	3.515 / /		112.491 / /	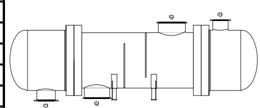			
Design temperature	C	60		37.78				
Number passes per shell		1		1				
Corrosion allowance	mm	3.18		3.18				
Connections	In mm	1	812.8 / -	1	558.8 / -			
Size/rating	Out	1	762 / -	1	457.2 / -			
Nominal	Intermediate		/ -		/ -			
Tube No. 3195	OD 19.05	Tks- Avg 2.11	mm	Length 3657.6 mm	Pitch 23.81	mm		
Tube type	Plain		Material	Carbon Steel	Tube pattern	30		
Shell	Carbon Steel	ID 1574.8	OD 1600.2	mm	Shell cover	-		
Channel or bonnet		Carbon Steel			Channel cover	-		
Tubesheet-stationary		Carbon Steel			Tubesheet-floating	-		
Floating head cover		-			Impingement protection	None		
Baffle-crossing	Carbon Steel	Type	Single segme	Cut(%d) 19.88 H	Spacing: c/c	641.35	mm	
Baffle-long	-		Seal type		Inlet	1270	mm	
Supports-tube			U-bend		Type			
Bypass seal			Tube-tubesheet joint		Exp.			
Expansion joint	-		Type					
RhoV2-Inlet nozzle	3605	Bundle entrance		7807	Bundle exit	9200	kg/(m*s2	
Gaskets - Shell side	-		Tube Side		Flat Metal Jacket Fibe			
Floating head	-							
Code requirements	ASME Code Sec VIII Div 1			TEMA class	R - refinery service			
Weight/Shell	48916.2		Filled with water	58801.7	Bundle	20065.8	kg	
Remarks								

- Intermediate Fluid Vaporizers (IFV)

IFV is divided to two different types which use propane as a heating media or ethylene glycol-water (EG/water). In this research, EG/water is utilized as a heating material because that solution is not explosible and safer than propane.

To design IFV, the first thing to do is setting up the boundary condition for heating material. **Table 2-10** shows the freezing point of EG/water solution. Usually the composition of EG in solution is given as 50 volume% to maintain the freezing point under -30 ^oC. If the lowest temperature of intermediate fluid is determined, another important factor of designing IFV is the highest temperature of intermediate fluid. When these parameters are determined, the intermediate fluid flow rate, heat transfer equipment and pump size will be defined as **Table 2-11.** As the lowest temperature of intermediate fluid is fixed to -30 ^oC, T_{out} of intermediate fluid is the key issue. **Figure 2-19** shows the trends of heat transfer area and flow rate that is determined by the lowest temperature. These y values in the **figure 2-19** can be converted to capital cost and operating cost and it is displayed in **figure 2-20**. Through the figure 2-20, the temperature is decided to 15 ^oC.

Table 2-10. Freezing points of Ethylene glycol solution

Ethylene Glycol Solution (*% by volume*)		**0**	**10**	**20**	**30**	**40**	**50**	**60**
Temperature	(^{o}F)	32	25.9	17.8	7.3	-10.3	-34.2	-63
	(^{o}C)	0	-3.4	-7.9	-13.7	-23.5	-36.8	-52.8

Table 2-11. A simple calculation for IFV boundary condition

Stream	**LNG**	**Intermediate Fluid**	**Sea water**
T_{out} (^{o}C)	10	-30	18
T_{in} (^{o}C)	-154	15	26
Δ T (^{o}C)	164	45	8
Flow rate (kg/h)	600000	1938496	8919778
Heat capacity (kJ/kg·^{o}C)	2.937	3.313	4.05
Heat flow (kJ/h)		3.13 e 8	
LMTD	46.7		19.0
U (kJ/kg·m_2·^{o}C)	8547		6201
A	785		2656

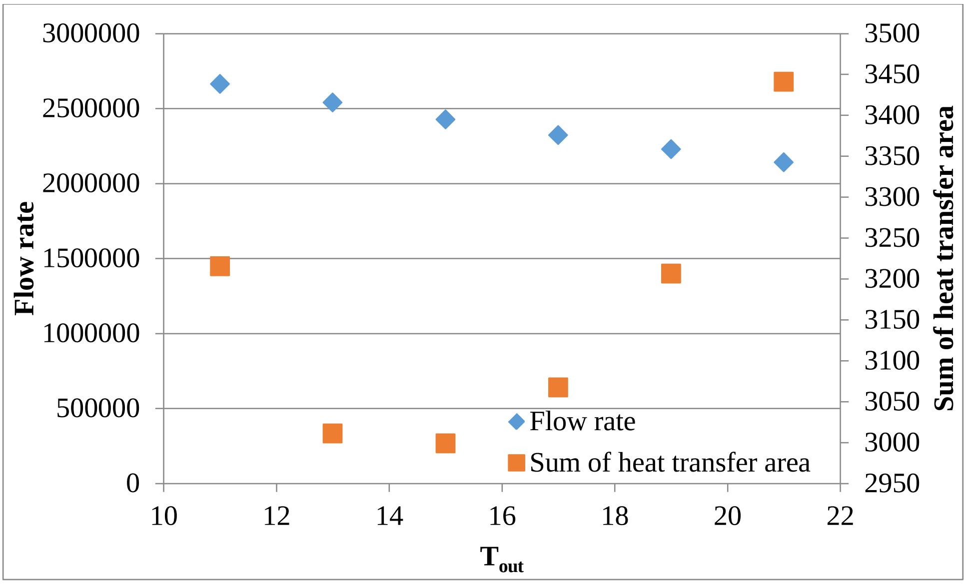

Figure 2-19. Heat transfer area and flow rate vs. T_{out} at intermediate fluid

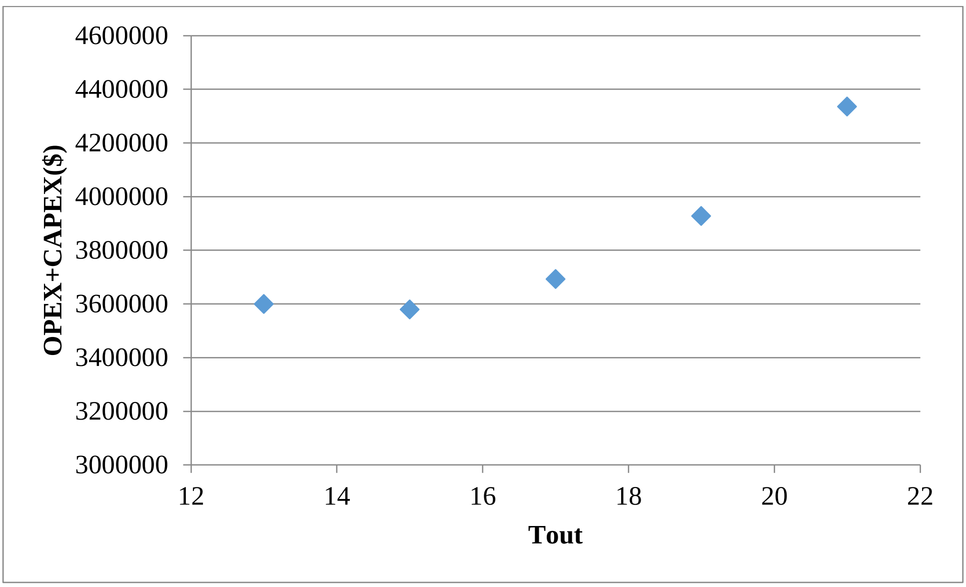

Figure 2-20. Total cost vs. T_{out} at intermediate fluid

Figure 2-20 and **table 2-12** describes a heat and material balance of intermediate fluid type vaporizer. The suggested system contains two heat exchangers and a pump. Additionally a steam heater can be included in the intermediate fluid cycle but in this research, it is not considered because of preventing CO2 emission.

The detailed design specification of equipment in IFV system is described in **Table 2-5** and this information will be input values for Aspen Capital Cost Estimator.

In the design of seawater heat exchanger, the rule for seawater temperature difference (-5 °C) is applied because there are many countries that have environmental regulation for sea water.[8]

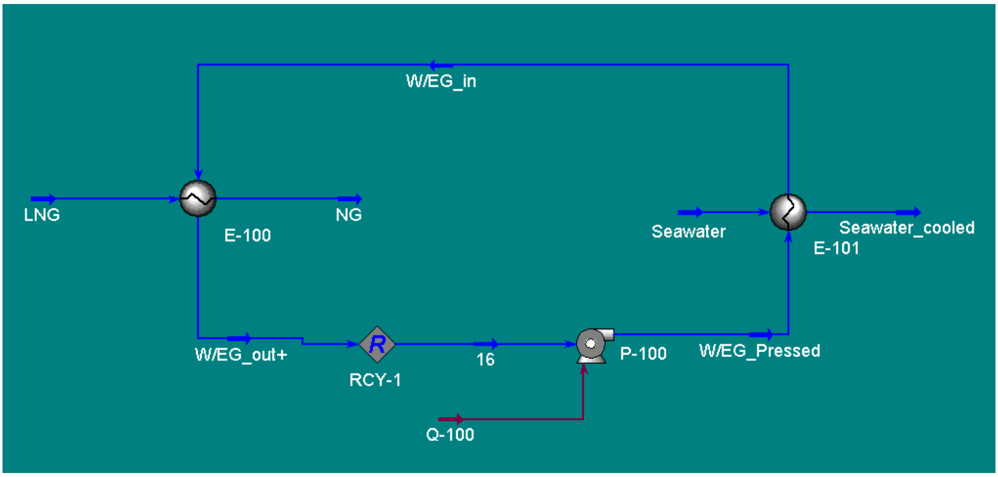

Figure 2-21. A simulation model for IFV

Table 2-12. A stream result of IFV

Name	**W/EG_out+**	**W/EG_in**	**NG**	**Seawater_cooled**
Vapor fraction	0	0	1	0
Temperature (°C)	-30.00	15.00	10.00	18.00
Pressure (kg/cm²)	2.00	4.59	103.90	1.13
Molar flow rate (kgmole/h)	7.992.E+04	7.992.E+04	3.303.E+04	6.778.E+05
Mass flow rate (kg/h)	3.200.E+06	3.200.E+06	6.000.E+05	1.251.E+07
Heat flow (kCal/h)	-7.189.E+09	-7.091.E+09	-6.312.E+08	-4.651.E+10
Name	**Seawater**	**LNG**	**W/EG_Pressed**	**16**
Vapor fraction	0	0	0	0
Temperature (°C)	26.00	-158.00	-29.86	-30.00
Pressure (kg/cm²)	2.66	104.00	6.12	2.00
Molar flow rate (kgmole/h)	6.778.E+05	3.303.E+04	7.992.E+04	7.992.E+04
Mass flow rate (kg/h)	1.251.E+07	6.000.E+05	3.200.E+06	3.200.E+06
Heat flow (kCal/h)	-4.641.E+10	-7.289.E+08	-7.189.E+09	-7.189.E+09

Table 2-13. A TEMA sheet of LNG-IF heat exchanger

Heat Exchanger Specification Sheet

Company:							
Location:							
Service of Unit:	Our Reference:						
Item No.:	Your Reference:						
Date:	Rev No.:	Job No.:					
Size	990.6 / 17995.9 mm	Type	BEM	Ver	Connected in	7 parallel	1 series
Surf/unit(eff.)	10492.3 m2	Shells/unit	7		Surf/shell (eff.)	1498.9	m2
PERFORMANCE OF ONE UNIT							
Fluid allocation			**Shell Side**		**Tube Side**		
Fluid name							
Fluid quantity, Total	kg/h		3366287		600000		
Vapor (In/Out)	kg/h		0	0	0	600000	
Liquid	kg/h		3366287	3366287	600000	0	
Noncondensable	kg/h		0		0		
Temperature (In/Out)	C		15	-30	-153	10.79	
Dew / Bubble point	C				-57.18	-63.84	
Density (Vap / Liq)	kg/m3		/ 1096.44	/ 1124.53	/ 451.1	109.49 /	
Viscosity	cp		/ 5.5041	/ 44.5658	/ 0.122	0.0148 /	
Molecular wt, Vap						18.16	
Molecular wt, NC							
Specific heat	kcal/(kg*C)		/ 0.6495	/ 0.6252	/ 0.7386	0.8113 /	
Thermal conductivity	kcal/(h*m*C)		/ 0.24	/ 0.229	/ 0.156	0.026 /	
Latent heat	kcal/kg				4.99	4.99	
Pressure (abs)	kgf/cm2		4.079	2.333	104.011	103.988	
Velocity	m/s		0.96		0.89		
Pressure drop, allow./calc.	kgf/cm2		2	1.746	2	0.023	
Fouling resist. (min)	m2*h*C/kcal		0		0	0	Ao based
Heat exchanged	9640567	kcal/h		MTD corrected	35.42	C	
Transfer rate, Service	259.4	Dirty	273.5	Clean	273.5	kcal/(h*m2*C)	
CONSTRUCTION OF ONE SHELL					**Sketch**		
		Shell Side		**Tube Side**			
Design/vac/test pressure:	kgf/cm2	4.921 / /		114.6 / /	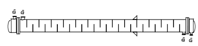		
Design temperature	C	54.44		-200			
Number passes per shell		1		1			
Corrosion allowance	mm	3.18		3.18			
Connections	In mm	1	355.6 / -	1	203.2 / -		
Size/rating	Out	1	254 / -	1	254 / -		
Nominal	Intermediate		/ -		/ -		
Tube No. 1418	OD 19.05	Tks- Avg 2.11	mm	Length 17995.9 mm	Pitch 23.81	mm	
Tube type	Plain	Material		Carbon Steel	Tube pattern	30	
Shell	Carbon Steel	ID 1000.1	OD 1022.35 mm	Shell cover	-		
Channel or bonnet	Carbon Steel			Channel cover	-		
Tubesheet-stationary	Carbon Steel			Tubesheet-floating	-		
Floating head cover	-			Impingement protection	None		
Baffle-crossing	Carbon Steel	Type	Single segme	Cut(%d) 39.69 H	Spacing: c/c	654.05	mm
Baffle-long	-	Seal type			Inlet	655.64	mm
Supports-tube		U-bend		Type			
Bypass seal		Tube-tubesheet joint		Exp.			
Expansion joint	-	Type					
RhoV2-Inlet nozzle	2057	Bundle entrance	1840	Bundle exit	2483	kg/(m*s2)	
Gaskets - Shell side	-	Tube Side		Flat Metal Jacket Fibe			
Floating head	-						
Code requirements	ASME Code Sec VIII Div 1			TEMA class	R - refinery service		
Weight/Shell	38787.8	Filled with water	50580.8	Bundle	26412.5	kg	
Remarks							

Table 2-14. A TEMA sheet of IF-Seawater heat exchanger

Heat Exchanger Specification Sheet

Company:											
Location:											
Service of Unit:			Our Reference:								
Item No.:			Your Reference:								
Date:	Rev No.:		Job No.:								
Size	1549.4 /	7493	mm	Type	BIM	Ver	Connected in	4	parallel	2	series
Surf/unit(eff.)	6680.8	m2	Shells/unit	8		Surf/shell (eff.)		835.1		m2	

PERFORMANCE OF ONE UNIT

Fluid allocation		Shell Side		Tube Side	
Fluid name					
Fluid quantity, Total	kg/h	13269510		3500000	
Vapor (In/Out)	kg/h	0	0	0	0
Liquid	kg/h	13269510	13269510	3500000	3500000
Noncondensable	kg/h	0		0	
Temperature (In/Out)	C	26	18	-30	15
Dew / Bubble point	C				
Density (Vap / Liq)	kg/m3	/ 1007.65	/ 1009.82	/ 1127.18	/ 1096.44
Viscosity	cp	/ 0.9738	/ 1.1733	/ 29.3569	/ 5.5048
Molecular wt, Vap					
Molecular wt, NC					
Specific heat	kcal/(kg*C)	/ 0.9545	/ 0.9548	/ 0.6205	/ 0.6495
Thermal conductivity	kcal/(h*m*C)	/ 0.434	/ 0.428	/ 0.231	/ 0.24
Latent heat	kcal/kg				
Pressure (abs)	kgf/cm2	4.079	2.234	6.118	4.224
Velocity	m/s	2.41		1.76	
Pressure drop, allow./calc.	kgf/cm2	2	1.845	2	1.895
Fouling resist. (min)	m2*h*C/kcal	0		0	0 Ao based
Heat exchanged	1018634 kcal/h		MTD corrected	24.19	C
Transfer rate, Service	630.3	Dirty 663.1	Clean	663.1	kcal/(h*m2*C)

CONSTRUCTION OF ONE SHELL

		Shell Side	Tube Side	Sketch
Design/vac/test pressure:	kgf/cm2	4.921 / /	7.031 / /	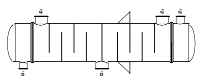
Design temperature	C	65.56	-200	
Number passes per shell		1	5	
Corrosion allowance	mm	3.18	3.18	
Connections	In mm	2 660.4 / -	1 457.2 / -	
Size/rating	Out	2 508 / -	1 406.4 / -	
Nominal	Intermediate	1 660.4 / -	1 406.4 / -	

Tube No.	1205	OD	30	Tks- Avg	2.11	mm	Lengt 7493	mm	Pitch	37.5	mm
Tube type	Plain			Material		Carbon Steel		Tube pattern		30	
Shell	Carbon Steel	ID	1550.9	OD 1576.39		mm	Shell cover		-		
Channel or bonnet		Carbon Steel					Channel cover		-		
Tubesheet-stationary		Carbon Steel					Tubesheet-floating		-		
Floating head cover		-					Impingement protection		None		
Baffle-crossing	Carbon Steel		Type	Single segme	Cut(%d)	24.42 H	Spacing: c/c		666.75		mm
Baffle-long	-			Seal type				Inlet	838.2		mm
Supports-tube				U-bend			Type				
Bypass seal				Tube-tubesheet joint			Exp.				
Expansion joint	-			Type							
RhoV2-Inlet nozzle	2019		Bundle entrance		6542		Bundle exit		5799	kg/(m*s2	
Gaskets - Shell side	-			Tube Side			Flat Metal Jacket Fibe				
Floating head	-										
Code requirements	ASME Code Sec VIII Div 1					TEMA class		R - refinery service			
Weight/Shell	19121.3			Filled with water		22720		Bundle	15797		kg
Remarks											

Table 2-15. Design data of IF-Pump

Parameter	Value	Units
Item type	CENTRIF	
Number of identical items	1	
EQUIPMENT DESIGN DATA		
Casing material	CS	
Design temperature	15	DEG C
Design gauge pressure	5	KPAG
Fluid head	34	M
ASA rating	150	CLASS
Driver power	420.7	KW
Speed	1800	RPM
Driver type	MOTOR	
Motor type	TEFC	
Pump efficiency	75	PERCENT
Seal type	SNGL	
PROCESS DESIGN DATA		
Liquid flow rate	777	L/S
Fluid specific gravity	1	
Fluid viscosity	1	MPA-S
Power per liquid flow rate	0.541441	KW/L/S
Liquid flow rate times head	26418	L/S -M
WEIGHT DATA		
Pump	1700	KG
Motor	1400	KG
Base plate	350	KG
Fittings and miscellaneous	300	KG
Total weight	3800	KG
VENDOR COST DATA		
Motor cost	51607	DOLLARS
Material cost	3509	DOLLARS
Shop labor cost	22151	DOLLARS
Shop overhead cost	22594	DOLLARS
Office overhead cost	16977	DOLLARS
Profit	18662	DOLLARS
Total cost	135500	DOLLARS

- Shell and Tube Vaporizers(STV)

Shell and tube vaporizer(STV) has the simplest structure of all vaporization method so that it is easiest problem to design it. There are two works to design STV, those are at first, setting up the boundary condition and next, detail design by ASPEN EDR.

The boundary condition of STV is similar to other vaporization methods as follows;

Input LNG temperature :	-154 °C
Send-out NG temperature :	10 °C
Seawater temperature :	26 °C
Seawater temperature difference :	8 °C

And the result of STV is seen at **table 2-16**.

Table 2-16. A TEMA sheet for shell and tube vaporizer

Heat Exchanger Specification Sheet

Company:							
Location:							
Service of Unit:		Our Reference:					
Item No.:		Your Reference:					
Date:	Rev No.:	Job No.:					
Size	1092.2 /	7023.1 mm	Type BIM	Ver	Connected in	4 parallel	1 series
Surf/unit(eff.)	2404.5 m2	Shells/unit	4	Surf/shell (eff.)	601.1 m2		
PERFORMANCE OF ONE UNIT							
Fluid allocation		**Shell Side**		**Tube Side**			
Fluid name							
Fluid quantity, Total	kg/h	12068248		600000			
Vapor (In/Out)	kg/h	0	0	0	600000		
Liquid	kg/h	12068248	12068248	600000	0		
Noncondensable	kg/h	0		0			
Temperature (In/Out)	C	26	18	-153	10.79		
Dew / Bubble point	C			-56.45	-58.54		
Density (Vap / Liq)	kg/m3	/ 1018.16	/ 1019.95	/ 476.41	110.12 /		
Viscosity	cp	/ 0.8705	/ 1.0531	/ 0.1424	0.0146 /		
Molecular wt, Vap					18.16		
Molecular wt, NC							
Specific heat	kcal/(kg*C)	/ 0.9785	/ 0.9786	/ 0.7684	0.8456 /		
Thermal conductivity	kcal/(h*m*C)	/ 0.524	/ 0.512	/ 0.16	0.036 /		
Latent heat	kcal/kg			4.99	4.99		
Pressure (abs)	kgf/cm2	4.079	2.376	104.011	103.984		
Velocity	m/s	3.64		1.45			
Pressure drop, allow./calc.	kgf/cm2	1.9	1.703	2	0.027		
Fouling resist. (min)	m2*h*C/kcal	0		0	0	Ao based	
Heat exchanged	9494797	kcal/h		MTD corrected	59.26	C	
Transfer rate, Service	666.4	Dirty	690.4	Clean	690.4	kcal/(h*m2*C)	
CONSTRUCTION OF ONE SHELL				**Sketch**			
		Shell Side	**Tube Side**				
Design/vac/test pressure:	kgf/cm2	4.921 / /	114.6 / /				
Design temperature	C	65.56	-200				
Number passes per shell		1	1				
Corrosion allowance	mm	3.18	3.18				
Connections	In mm	2 609.6 / -	1 254 / -				
Size/rating	Out	1 609.6 / -	1 304.8 / -				
Nominal	Intermediate	/ -	/ -				
Tube No.	1505	OD 19.05	Tks- Avg 2.11 mm	Length 7023.1 mm	Pitch 23.81 mm		
Tube type	Plain	Material	Carbon Steel	Tube pattern	30		
Shell	Carbon Steel	ID 1100.1	OD 1125.54 mm	Shell cover	-		
Channel or bonnet	Carbon Steel			Channel cover	-		
Tubesheet-stationary	Carbon Steel			Tubesheet-floating	-		
Floating head cover	-			Impingement protection	None		
Baffle-crossing	Carbon Steel	Type	Single segme	Cut(%d) 25.63 H	Spacing: c/c	552.45	mm
Baffle-long	-	Seal type			Inlet	839.79	mm
Supports-tube		U-bend		Type			
Bypass seal		Tube-tubesheet joint		Exp.			
Expansion joint	-	Type					
RhoV2-Inlet nozzle	2299	Bundle entrance	5586	Bundle exit	8712	kg/(m*s2	
Gaskets - Shell side	-	Tube Side		Flat Metal Jacket Fibe			
Floating head	-						
Code requirements	ASME Code Sec VIII Div 1			TEMA class	R - refinery service		
Weight/Shell	23978.8	Filled with water	24922.7	Bundle	13574.4	kg	
Remarks							

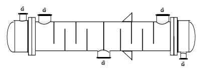

- Vaporizer selection

Using the result above, the vaporizer for LNG-FSRU is selected. The selected vaporization method will be economically feasible and safely operated even the offshore circumstances.

Before selecting the vaporization method, the result of vaporizer design is aligned in **table 2-17**. The design of SCV is excluded because of its carbon efficiency and the incomparably higher operating cost. The information of ORV is calculated from the relation at **table 2-7** and the simulation result of STV. ORV is designed based on the assumption that the LNG-FSRU is anchored at land side, not floating.

The footprint is calculated by ASPEN EDR and layouts in **figure 2-22, 23, 24**. There are significant differences between each method and regarding the size of FSRU fleet(300m * 50 m), all types can be installed but when the unloading/send-out pipeline of each tank is installed in center of the ship, IFV and AAV will not be applicable.

In conclusion, STV is the most feasible vaporization method for LNG-FSRU. ORV seems quite comparable but the assumption of FSRU's mooring position limits the compatibility.[74]

Table 2-17. Comparative analysis of vaporization methods

		ORV	SCV	AAV	IFV	STV
Weight (ton)	dry	113	-	192	427	96
	wet	117	-	227	540	100
Cost (million$)	Capital	0.946	-	1.44	2.90	0.806
	Operation (1year)	0.0399	11.0	0.0436	0.0675	0.0460
	Operation (20years)	0.799	221	0.871	1.35	0.920
OPEX +CAPEX (million$)		1.75	221	2.31	4.25	1.73
Footprint (m^2)		161	-	576	1035	154

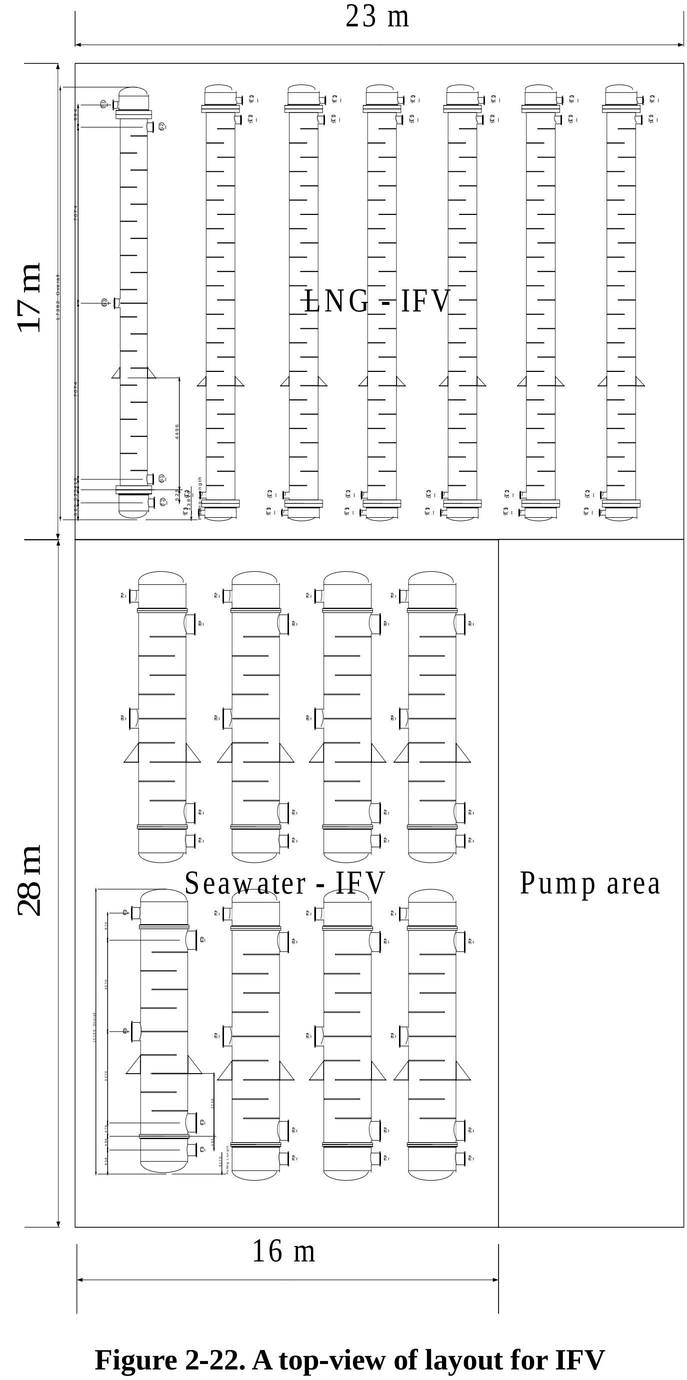

Figure 2-22. A top-view of layout for IFV

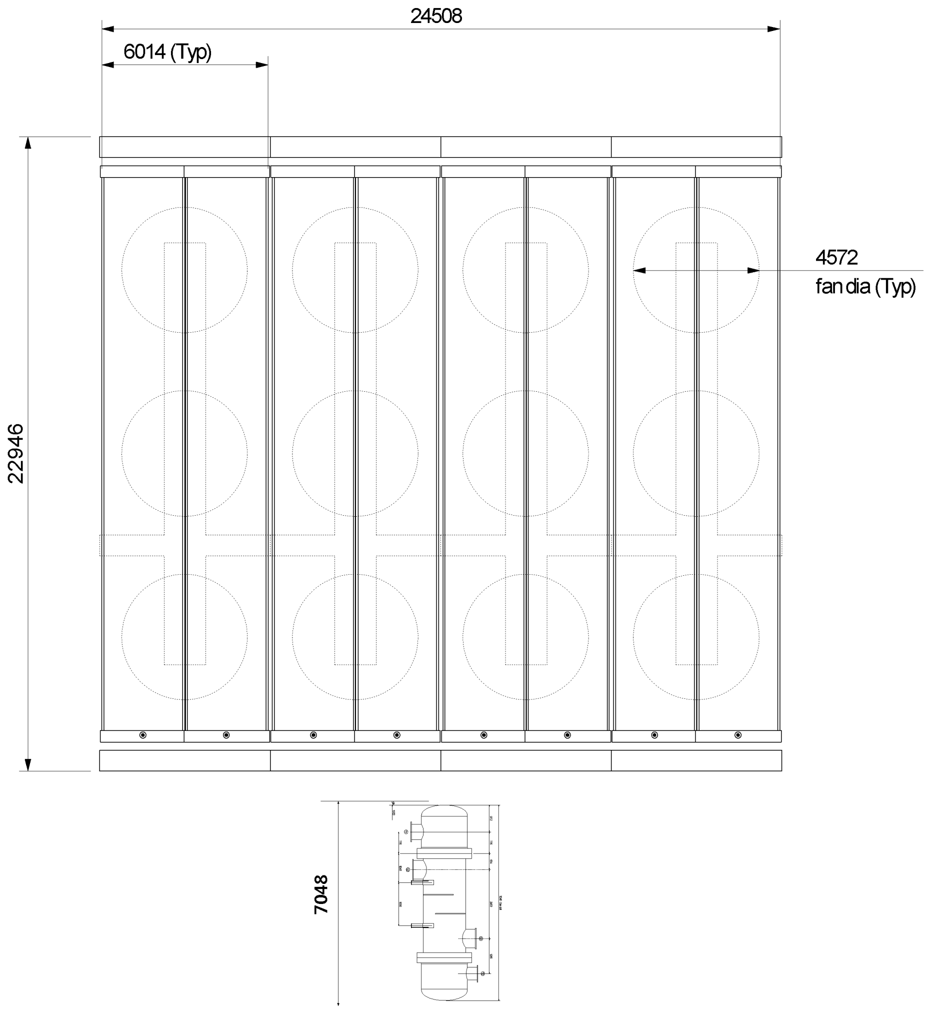

Figure 2-23. A top-view of layout for AAV

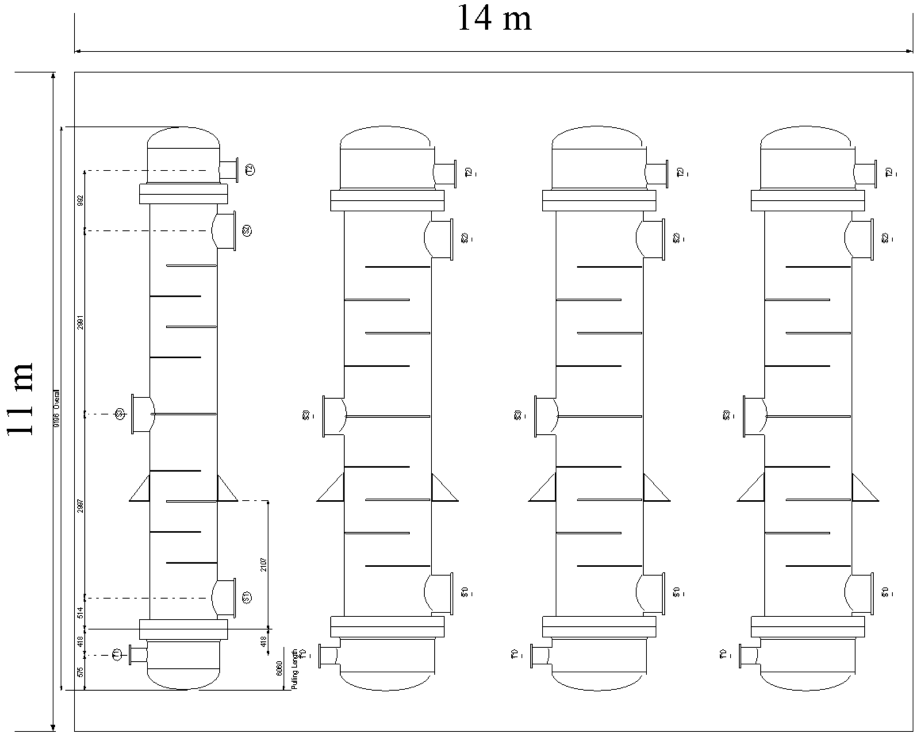

Figure 2-24. A top-view of layout for STV

2.4.4. Heat and material balance sheet

Gathering the information above, the final design of LNG-FSRU topside is determined for four different cases. The final design is embodied as a heat and material balance sheet(HMB). The calculation of HMB is performed by HYSYS V7.3 and the property package is selected as below;

Hydrocarbon : PRSV

Seawater : Electrolyte NRTL

The miscellaneous selections on design such as number of HP pumps are listed as follows;

Number of HP pumps :	100 ton /h * 6
	60 ton/h * 1
BOG compressor capacity :	27 ton/h * 2 (200%)
Pump operation status :	
	Case 1 : 5 pumps in operation
	Case 2 : 2 pumps in operation
	Case 3 : 5 pumps in operation
	Case 4 : 2 pumps in operation

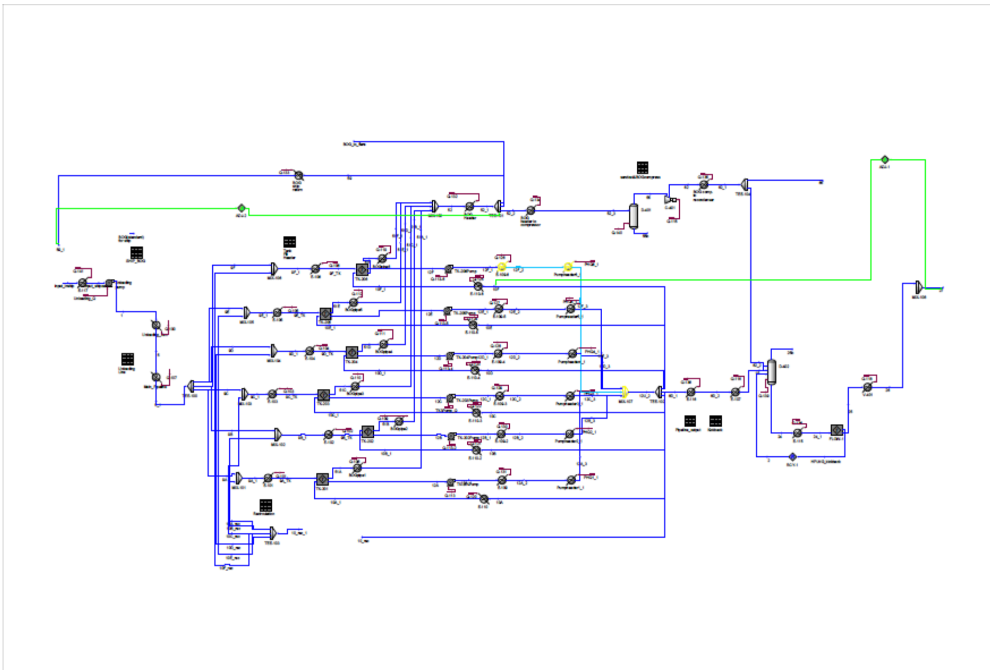

Figure 2-25. Process flowsheet of case 1 / Maximum sendout and unloading

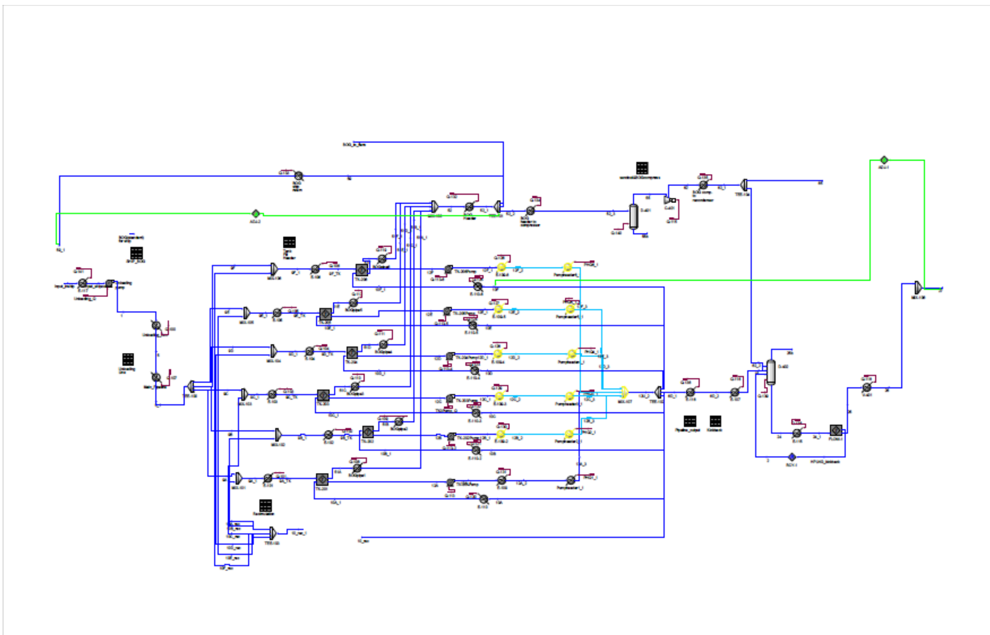

Figure 2-26. Process flowsheet of case 2 / Minimum sendout and unloading

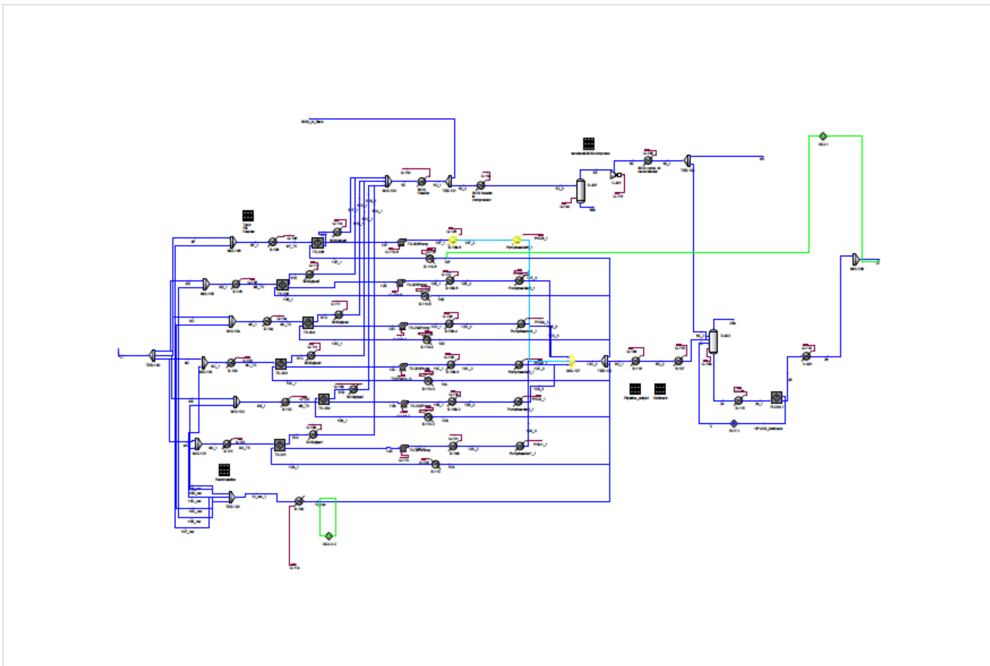

Figure 2-27. Process flowsheet of case 3 / Maximum sendout and no-ship

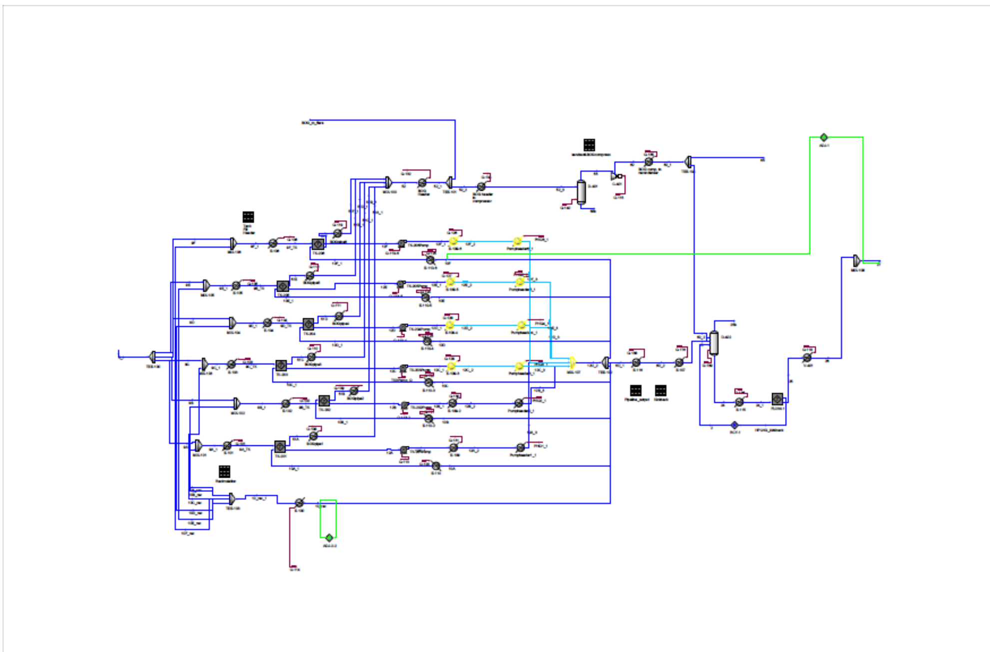

Figure 2-28. Process flowsheet of case 4 / Minimum sendout and no-ship

2.5. Result and discussion

The topside process of LNG-FSRU is designed with consideration of offshore features. And the vaporization method is also selected for LNG-FSRU. The selected vaporizer, STV is the cheapest method and its small footprint will help operators to do maintenance work. Even though ORV shows small difference between STV, it has weakness to secure safety in ship motion situation that ORV is not recommended as a vaporizer of FSRU. Thus if someone want to use ORV for a vaporizer, the fleet must be fixed to pier that no movement is induced to vaporizer unit. Otherwise, an improvement of ORV unit can be a solution to be utilized in LNG-FSRU. Kobelco suggested an advanced ORV that uses an overlapped column to prevent the effect of ship motion. [69] It will allow lower pressure for seawater than STV but the weight or price of the vaporizer unit can be higher that selecting ORV as a vaporizer must be considered cautiously.

IFV is safer than STV because of the existence of intermediate fluid. However, in this research, it is too expensive to use in LNG-FSRU and when the ship owner does not hesitate to invest on the safety, IFV will be another reasonable option. Actually in these days some other heating materials such as propane, butane, and even Freon are applied to IFV. Moreover, the new structure of vaporizer unit has been developed and the size of the unit is innovatively reduced that further studies on these vaporizers will be recommended.

In this research, AAV is designed with a lot of limit due to ASPEN EDR but it is still not a good choice for LNG-FSRU. Because of the sea condition, the humidity of LNG-FSRU is higher than that of land based terminal. This will make large amount of frost on vaporizer surface, which decreases the heat flux.

In actual operation, AAV should be shut down to eliminate frost and the operating time is shorter than others.

Including the comparative analysis of vaporization method, the LNG-FSRU topside process is designed. This developed design will improve safety and feasibility of LNG-FSRU.

CHAPTER 3 : DYNAMIC SIMULATION OF LNG-FSRU TOPSIDE PROCESS

3.1. Introduction

Development of a FEED package for a plant contains lots of information such as PFD, P&ID, heat and material balance table(HMB), HAZOP, equipment specification, and so on. This work is progressed with process simulation technique and nowadays the FEED package cannot stand without process simulation model. For an example on the chapter 2, a topside process design on flowsheeting level is completed using the steady state simulation model.

After the PFD is specified, works for further design level such as making P&ID follows. These works can lighten the burden by using the dynamic simulation model which can show the dynamic changes in chemical process. To build an exact dynamic model, it is necessary to secure enough information to model and to understand the target model precisely.

Among the many process units which are mentioned in chapter 2, we can say that the most important process unit is the BOG recondenser. In the LNG-FSRU and also in onshore receiving/regasification terminal, any chemical reaction does not exist. However, there are several units where phase changes occur and they are LNG storage tank, vaporizer, and BOG recondenser. Above these units, BOG recondenser is the only unit in LNG terminal where the vapor, BOG, is liquefied to LNG. Moreover, as the liquefaction is more delicate process than evaporation, lots of efforts to estimate and control the recondenser are delivered.

The importance of BOG recondenser is not just the complexity of operation but the process efficiency will also be determined by successive recondenser operation. When the BOG is not fully covered by recondenser, it should be flared in LNG-FSRU and seriously threaten economic feasibility.

Therefore, the accuracy of BOG recondenser modeling must be higher than any other facilities in LNG-FSRU. In this research, dynamic modeling of the BOG recondenser with a progress of accuracy is studied and the model is tested with the operation data from BOG recondenser in real LNG receiving terminal.

In this basic terminal design, the formation of boil-off gas (BOG) is an inevitable problem that can be a risk to the safety and economic feasibility of the terminal. When external heat permeates into the network, evaporating LNG will expand to 600 times its liquid volume. This BOG can increase the pressure inside the storage tank and damage process facilities. Moreover, if the evaporated gas is not recovered, it can be a significant economic loss. Therefore, a BOG treatment process is generally required in LNG receiving terminals.[75]

The BOG recovery process was developed a few decades ago, and its basic design is now standardized in previous research and patents.[76–79] In brief, the process involves the compression of BOG and its mixing with LNG in a sudden pressure vessel. Through this process, the wasted BOG is recovered and the problems caused by BOG formation are reduced. Furthermore, the pressure vessel, termed the BOG recondenser, can act as a buffer tank for the high-pressure pump used in many LNG receiving terminals.

As the BOG recondenser plays an important role in terminal operations, the performance of the recondenser should be analyzed precisely, and an accurate dynamic simulation model of the recondenser is therefore required. Such a model is more complex for a BOG recondenser, because, unlike other process units in an LNG terminal, a vapor-liquid phase change takes place within it. Some previous studies have been conducted employing a dynamic simulation of a BOG recondenser. However, insufficient accuracy was observed in these studies to allow their application to a real recondenser in an LNG terminal.[19] Thus, in this research, we propose a new dynamic modeling method to simulate a BOG recondenser with acceptable accuracy. The main feature of the proposed methodology is the use of variable flash ratio for modeling the BOG recondenser, which is in a non-equilibrium state. The proposed methodology is validated with the actual operating data from a BOG recondenser in a real LNG receiving terminal.

3.2. Theoretical backgrounds

3.2.1. BOG Recondenser

Before proposing the methodology, definition of the target must be specified. **Figure 3-1** shows the basic scheme of a BOG recondenser, which is the main target of this research. When the pressurized BOG from the BOG compressor enters the recondenser vessel, it is mixed with the input LNG from the low-pressure pump at the storage tank. The input BOG and LNG are both pressurized to about 9 bar, and when the BOG meets the surface of an LNG droplet or another cool material, it will be liquefied. After the BOG is liquefied and mixed with the LNG, it is transferred to secondary pump without any vapor remaining in the fluid. **Figure 3-2** provides a closer view of the recondenser, showing the separate area inside the pressure vessel in which the column is filled with steel packing. This provides an additional heat transfer area for contact with vapor. The size of this heat transfer area is determined by the liquid level of the recondenser, such that when the BOG/LNG ratio (BLR) is too high, the liquid level is lower and the heat transfer area increases. The larger available recondensation area drives an increase in the liquid level. Similarly, when the BLR is too low, the reduced heat transfer area will decrease liquid level.[16], [64]

In the first step of building a dynamic model for the BOG recondenser, a pressure vessel unit model is applied to represent the recondenser. The area inside the unit is regarded as a non-equilibrium region, since many changes in operation mode occur inside the recondenser and an assumption of equilibrium is not valid. There have been many previous studies featuring non-equilibrium calculations, and many dynamic process simulators, including HYSYS and DYNSIM, support them. However, based on such models, especially HYSYS dynamics does not show the sufficient accuracy on BOG recondenser in tracking abrupt changes and in estimation of liquid level inside the recondenser. When the accuracy of the model is insufficient, the operator-training simulator (OTS) for the LNG terminal will poorly represent actual situations and may be a serious problem for operator education. For example, if the model fails to estimate the liquid level in the BOG recondenser and an operator applies an inappropriate operating scenario, the system alarm cannot provide warning of the dangerous action. Therefore, building an exact model for the BOG recondenser is important for enhancing the safety of LNG-FSRU.

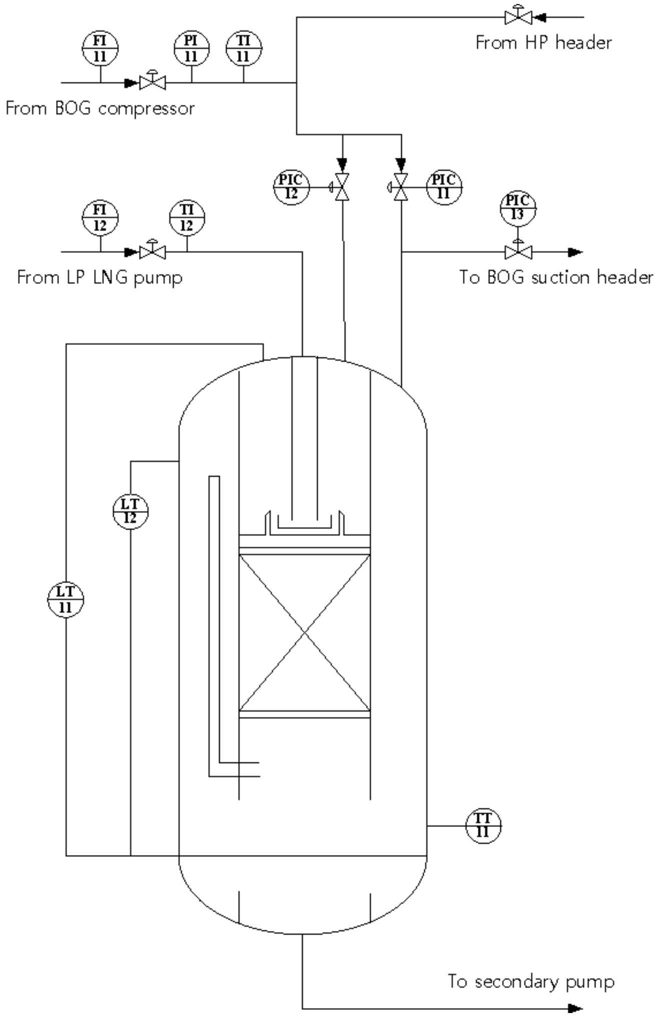

Figure 3-1. Process flow sheet of a BOG recondenser

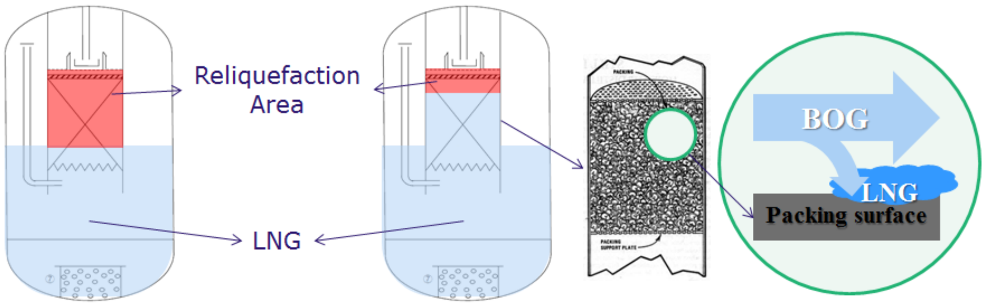

Figure 3-2. The phenomena inside BOG recondenser

3.2.2. Prior researches about recondenser modeling

As mentioned above, the accurate modeling for recondenser is important. Many researches about the recondenser support this importance.

Kim proposed a process with heat exchanger to improve recondensation performance and similar concept was tried by Park. Jung studied the design and operation of LNG terminals from the view of the operator's practices. Querol and Li also suggested advanced recondensation processes and these studies focused on the steady state analysis.[19], [80–82]

By the way the purpose of recondenser modeling is focused on the exact estimation about its operation so that it needs to be modeled in dynamic condition. There are also some researches about dynamic modeling cases for BOG recondenser. Li's work is a representative study about dynamic simulation for BOG recondenser with DYNSIM and a case study of an LNG terminal dynamic simulation by Jorge covered all area in LNG terminal and also the recondenser.

Moreover, in HYSYS, which is a widespread software in LNG industry, a feature to model the non-equilibrium vessel like the recondenser exist as flash ratio.[83] Despite the researches and commercial software improvement, the accuracy of HYSYS dynamics is still not reaching to real recondenser. This is because the studies above are regarding the recondenser as a simple pressure vessel and when someone uses this strategy to model a recondenser in HYSYS, it fails to precise estimation of level. As it is displayed in **figure 3-2**, the structure inside works for increasing recondenser's performance that the real recondenser cannot be expressed by simple vessel model.[19], [20]

In this study, we propose an advanced dynamic modeling method about BOG recondenser for HYSYS to overcome the accuracy problem. With using HYSYS, we will gather both high usability and acceptable accuracy.

3.3. Proposed modeling methodology

In this paper, we develop an advanced methodology to build a dynamic simulation model of a BOG recondenser with improved accuracy and reliability. Before describing the proposed methodology, the general dynamic simulation technique for a BOG recondenser should first be explained.

3.3.1. General dynamic simulation of a BOG recondenser

As the fluid inside the BOG recondenser is in a non-equilibrium state, it assumed that there are three different regions: vapor, liquid, and equilibrium areas. Each area has different fluid properties, and there is transfer of fluid between them. The rates of transfer are specified by a flash ratio value, which means a ratio of an amount sent to the equilibrium area over whole amount of such area's holdup. By controlling the flash ratio value, the model can calculate the properties and volume of each state. [84], [85]

Using the flash ratio concept, the model performance is greatly improved. However, when we use HYSYS with this flash ratio, insufficient accuracy in the predictions of liquid level remains a problem. **Figure 3-3** shows the relationship between the liquid level and the LNG input rate and BLR from actual operating data. Data from the simulation model with constant flash ratio is shown in **Figure 3-4**. The variation of liquid level with BLR predicted by the model seems quite similar to the real data, but for the relationship between liquid level and LNG input rate, the simulation model cannot estimate the tendency well. Moreover, the previous research with dynamic modeling of the BOG recondenser shows a problem with accuracy, especially in situation of changing liquid level. This is one of the most important variables in the BOG recondenser because it is directly connected with safety of the unit. Therefore, an advanced modeling technique for better accuracy is required.

The reason of this error is from the solving method of HYSYS. Material, energy, and composition balances in Dynamic mode are not considered at the same time. Material or pressure-flow balances are solved for at every time step. Energy and composition balances are defaulted to solve less frequently. Pressure and flow are calculated simultaneously in a pressure-flow matrix. Energy and composition balances are solved in a modular sequential fashion. This results, when input volume flow changes, the hold-up amount inside the vessel is changed in such time step and even flash ratio is applied to the model, the entire calculation for hold-up volume is also changed.

In this research, the enhancement in the accuracy of the predictions of liquid level in the BOG recondenser is realized by varying the flash ratio with changing operating conditions, in particular, the LNG input rate. **Figure 3-5(a)** demonstrates that the liquid level prediction of the simulation model depends on the flash ratio. When the flash ratio varies with the LNG input rate, the dynamic simulation model of BOG recondenser can estimate liquid level with enhanced accuracy. Therefore, in this research, the flash ratio is determined as a function of LNG input rate so that the flash ratio value is changed by the LNG input rate value.

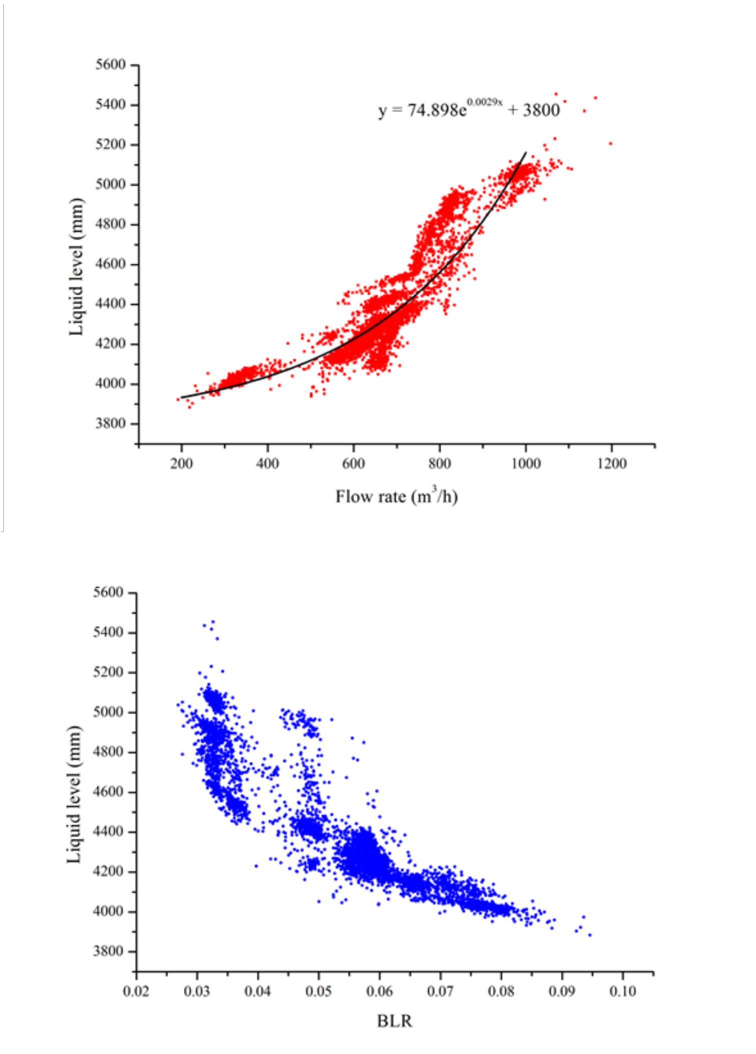

Figure 3-3. Relationship between the liquid level and the LNG input rate and BLR from the actual operation data

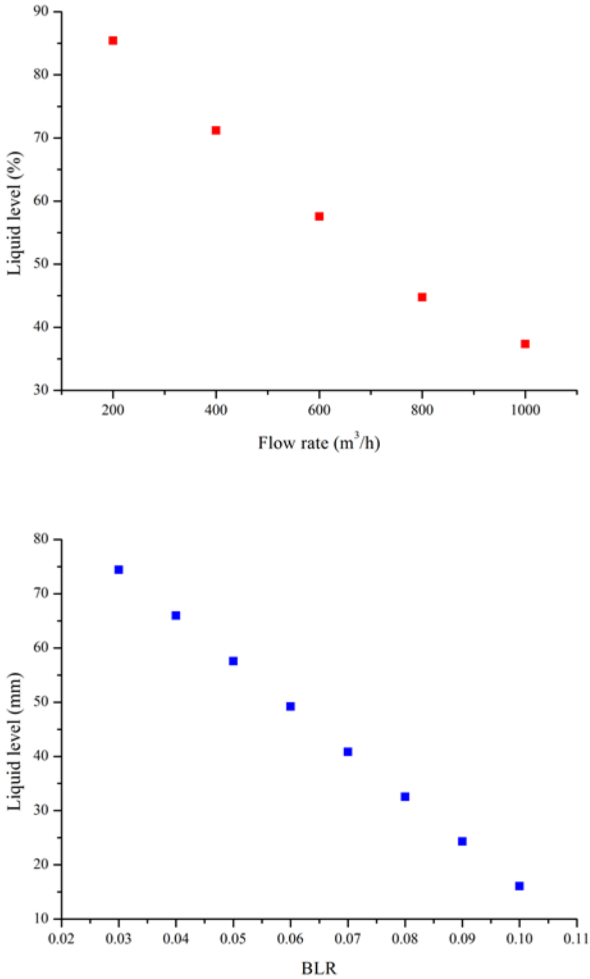

Figure 3-4. Relationship between the liquid level and the LNG input rate and BLR from a simulation model with constant flash ratio

3.3.2. Building the flash ratio function

The procedure for building the flash ratio function is as follows.

1) Perform dynamic simulations with varying flash ratio to create data sets for liquid level versus LNG input rate, as shown in **Figure 3-5(a).**
2) Compare the simulation data from step 1 with a fit of the actual operating data for liquid level versus LNG input rate in the BOG recondenser (the function given in **Figure 3-5(a)**) as seen in **Figure 3-5(b).**
3) Find the points of intersection between the simulation results and the actual data set, and extract the LNG input rate values at these points.
4) Fit an equation to the flash ratio versus LNG input rate at the intersection points, as shown in **Figure 3-5(c).**

With this procedure, the function relating flash ratio to LNG input rate is derived. Using this equation in the dynamic simulation model, we obtain accurate values for the liquid level in the BOG recondenser.

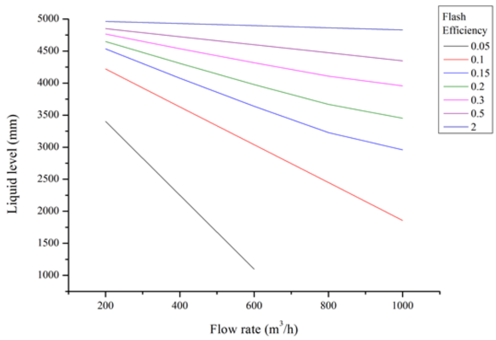

(a)

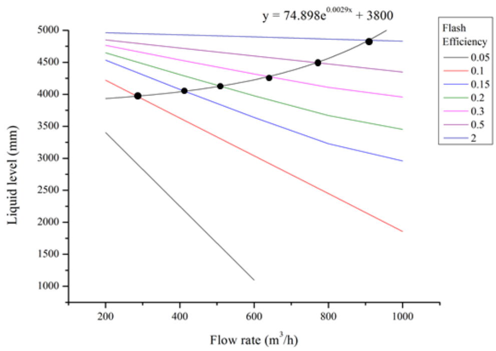

(b)

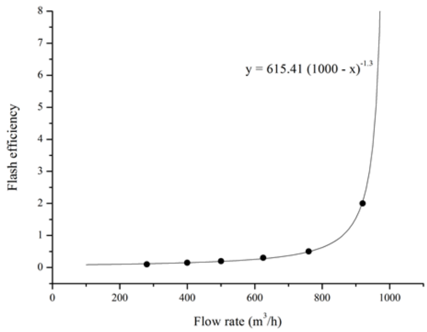

(c)

Figure 3-5. Flash ratio function modeling process. (a) Multiple simulation results for the relationship between the liquid level and the flow rate for various flash ratio; (b) intersections of the simulation result and the equation from the actual data; and (c) the flash ratio values that satisfy the actual data

3.4. Case study : Data preprocessing

The original operation data is gathered through the distributed control system of real onshore LNG terminal. Every data is captured at intervals of one minute and data during three days with multiple unloading and offloading operations.

3.4.1. Noise filtering

Before the objective data selection, the gathered data is filtered at first. The raw data has lots of noises even in a single operation mode as seen in the **Figure 3-6** so that these noises should be eliminated. According to the figure, temperature and BOG incoming rate data for 20 minutes show lots of noises despite the operation mode is not changed. When we use the data with noises in simulation, the stiffness of the data can threat convergence of simulation model.
The noise filtering method is selected to simple moving average because the size of raw data is too massive. The simple moving average method is efficient and speedy, thus, it is utilized in many industrial area.[86]

$$SMA = \frac{p_M + p_{M-1} + \cdots + p_{M-(n-1)}}{n}$$

SMA = *averaged value*

p_M = *measured value of specific time*

n = *number of data horizon*

The equation above represents the concept of simple moving average. The key issue of the methodology is how to define the number of data horizon. If the data horizon is large, the averaged value will not consider the rapid mode change and when the data horizon is too small, the random noise cannot be filtered sufficiently. In this case study, the number of data horizon is selected as 9, and the representative result for incoming BOG rate is seen in **Figure 3-7**. The figure shows more rigid line on the reconciled data (red dots) and catches dramatic mode change with satisfactory speed. These filtered data will be the base of precise simulation.

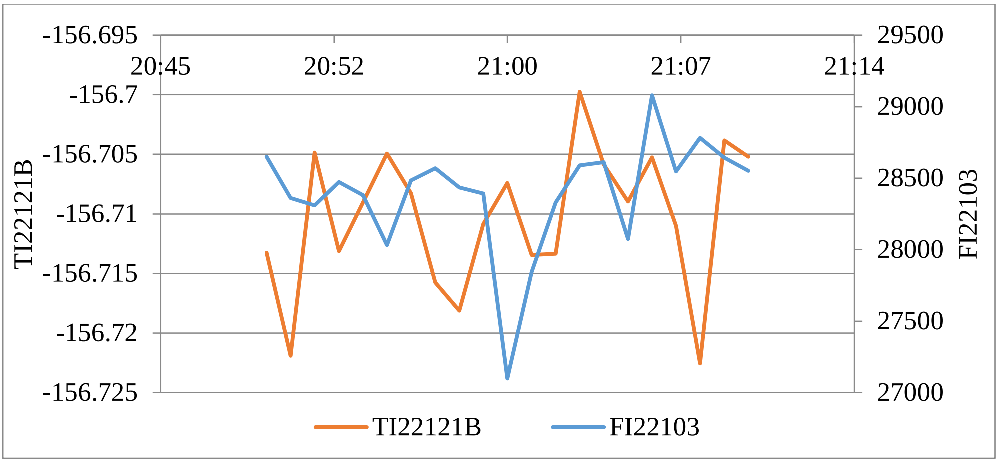

Figure 3-6. Temperature of the liquid in recondenser and flow rate of incoming BOG for 20 minutes

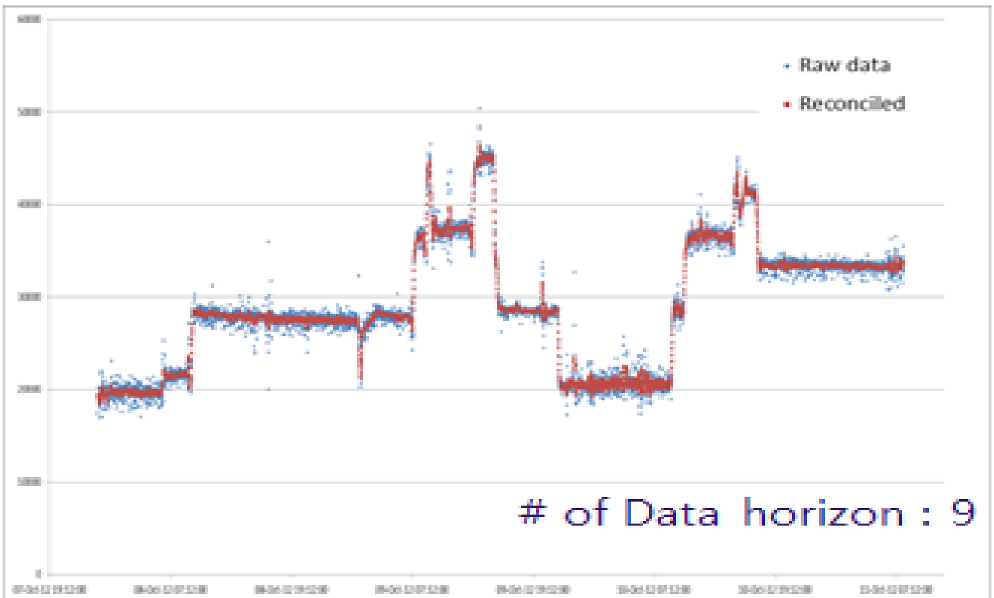

Figure 3-7. BOG incoming rate change for three days

3.4.2. Raw data selection

After the raw data is filtered and the noise of raw data is eliminated enough, the data which represents the individual operation mode will be selected. To make a precise dynamic simulation model, it should be based on steady state modes and trained with various operation modes, that providing good quantity and quality data sets is the key point in dynamic modeling procedure.

The objective data is classified to two cases those are steady state and transient state and the steady state data should satisfy the conditions below;

1) Small difference between the reconciled data and real data
2) The gradient of reconciled data is close to zero
3) The period when core data such as flow rate and pressure are stable

For the transient state, the periods when significant operation mode changes exist are selected with satisfying the condition above the mode change. Following these conditions, several periods are selected as **figure 3-8**.

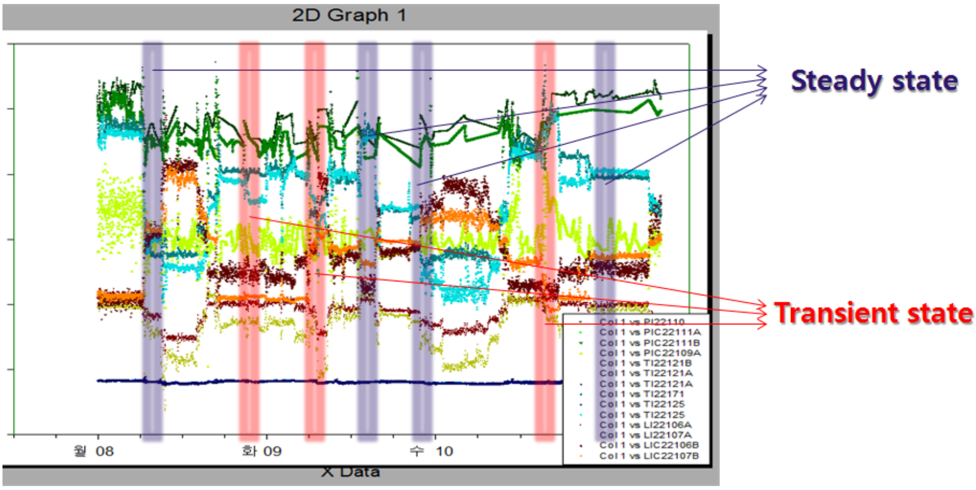

Figure 3-8. Selected regions in the overall data from the BOG recondenser

3.5. Case study : Advanced dynamic modeling for BOG recondenser

To validate the proposed technique, it was applied to the BOG recondenser in the South Korean LNG terminal. Using the actual operational data set from the BOG recondenser, the simulation model with the flash ratio function was built and the model was tested with real operating situation. In addition, a virtual scenario for an extreme level change was studied to emphasize the usefulness of this technique.

3.5.1. Model building

As the first step of the case study, a dynamic simulation model was built to describe the target BOG recondenser. For performing the dynamic simulation, Aspen HYSYS V7.3 was selected because it is verified for many cases in LNG industry. The Peng-Robinson-Stryjek-Vera (PRSV) equation of state was utilized as a property package, and the input composition of LNG given in **Table 3-1** was assumed.[87]

The target of the case study has two symmetrical recondenser units as seen in Figure 6, and this basic structure is reflected in the simulation model. In a detailed view of each recondenser model, the single recondenser unit must be composed of the two separate pressure vessel models. Inside the BOG recondenser shown in **Figure 3-1**, there are two different areas – the inner packing area and outer annulus section. These areas have different features, but they interact with each other so that it is necessary to model the target with separate pressure vessel models. By using the separated models, it can be observed that when the input BOG rate becomes larger, the liquid level in the packing area decreases and the level in the annulus area increases. The size information of each unit model is based on the real geometry data and design specifications such as the volume, height, and diameter, and therefore, we can build the dynamic simulation model realistically.

To take into account the variable flash ratio, which is the key feature of this research, a modeling procedure to generate an equation for this efficiency value variation is necessary. There are many different efficiency values for feed/recycle streams with vapor and liquid areas in the holdup model at HYSYS Dynamics as seen in the **table 3-2**, however to simplify the problem, the only changing value is the recycle efficiency. All the other values are fixed to zero for vapor feed/product and maximum value for each liquid areas because it is assumed that all input vapor goes to vapor holdup and the liquefaction is occurred only in the equilibrium area.

Applying the procedure described in section 3.2.2, the flash ratio function relating the LNG input rate in Figure 3-5(c). is generated.

$$FE = 615.41(1000 - x)^{-1.3} \quad (1)$$

where FE is the flash ratio value, and x is the LNG input rate (m3 h-1)

Table 3-1. Composition of feed LNG

Component	Composition
CH_4	0.8926
C_2H_6	0.0864
C_3H_8	0.0144
n-C_4H_{10}	0.0027
i-C_4H_{10}	0.0035
N_2	0.0004

Table 3-2. Efficiency values for HYSYS holdup model

Recycle efficiencies		**Feed Efficiencies**		**Product Efficiencies**	
Vapor	Variable	**Vapor**	0	**Vapor**	0
Liquid	100	**Liquid**	100	**Liquid**	100

3.5.2. Model validation

The model including the flash ratio function was tested firstly with an actual operational data set at the operating mode change situation, and secondly with a virtual scenario in which LNG input rate was abruptly decreased for the purpose described above.

For model validation, the manipulated variables in the operating data were entered into the dynamic simulation model, which was developed as described in section 3.4.1, and the result compared to the actual operating data. The manipulated variables include the controller operating data and the other dependent variables such as pressure, temperature, and input flow rate. The variation in the simulation result over time can be generated by changing the manipulated variables at specified time intervals. **Figure 3-9** displays the sensor information with the manipulated variables highlighted in red text.

The simulation is performed as follows. In addition to the basic simulation model in **Figure 3-9**, a spreadsheet for evaluating Eq. (1) to determine the efficiency values of the simulation model and changing the manipulated variables of the model was used. The manipulated variables were changed periodically using the actual time dependent data set. The simulation result is compared with data from the real recondenser or the simulation result from constant flash ratio model, and displayed in **Figures 3-10** and **3-11**. The constant flash ratio model is based on the same simulation model mentioned above but the flash ratio value is fixed at its initial value. The virtual scenario is based on the assumption that the LNG input flow rate is decreased abruptly at first, and subsequently raised, with the liquid level expected to vary in response to this operational mode change.

As displayed in **Figure 3-5**, the general process of dynamic modeling is constituted with (1) training with various steady state data, (2) time dependent variable change and (3) detail specification update. Other process is not far from other dynamic simulation cases but in this case, updating the detail specification needs to be clarified. In the theoretical background section, the hold-up efficiency is mentioned and it will be explained in detail.

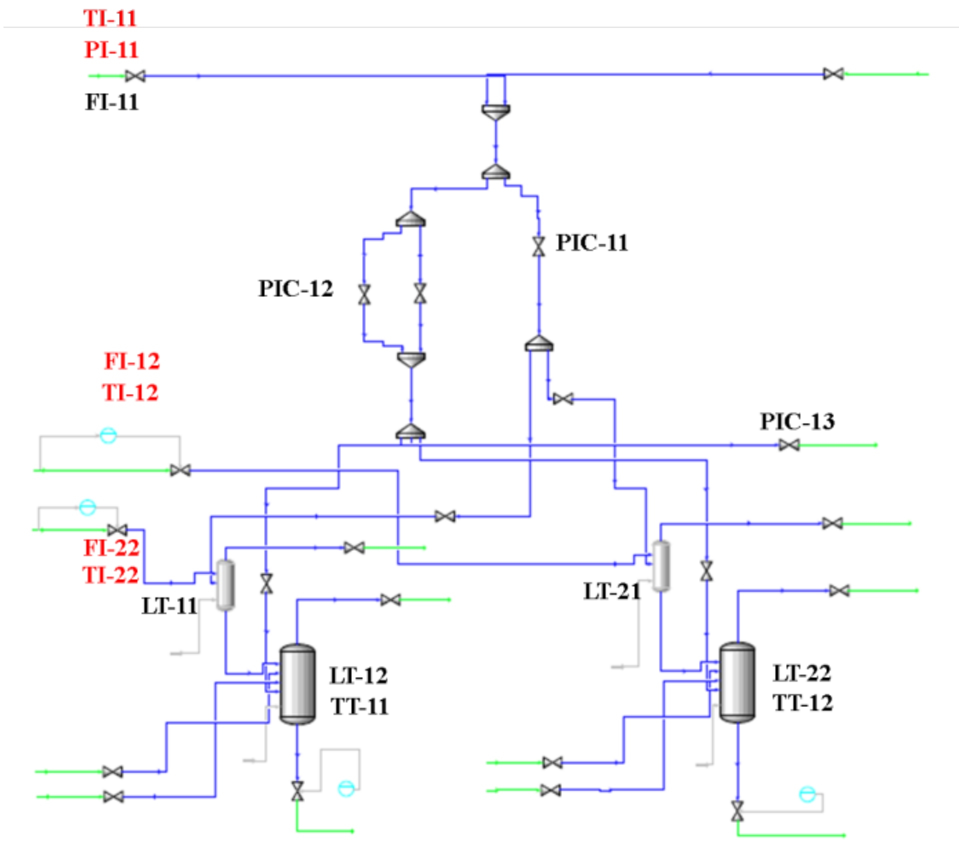

Figure 3-9. Simulation model for the target recondenser

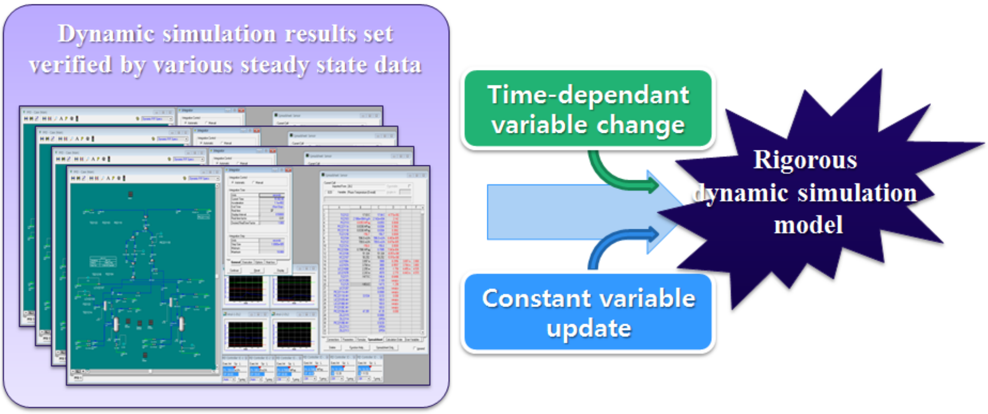

Figure 3-10. Dynamic simulation modeling procedure

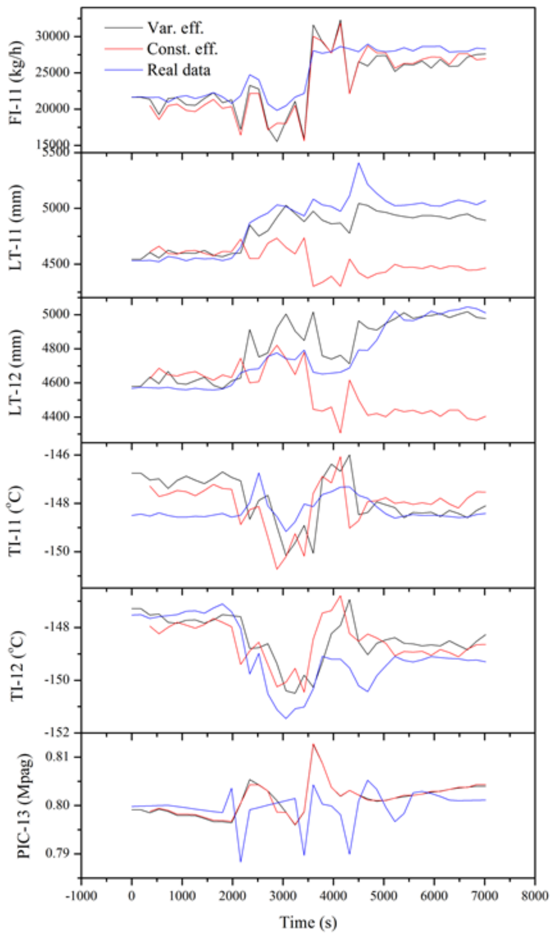

Figure 3-11. Simulation result of the virtual scenario

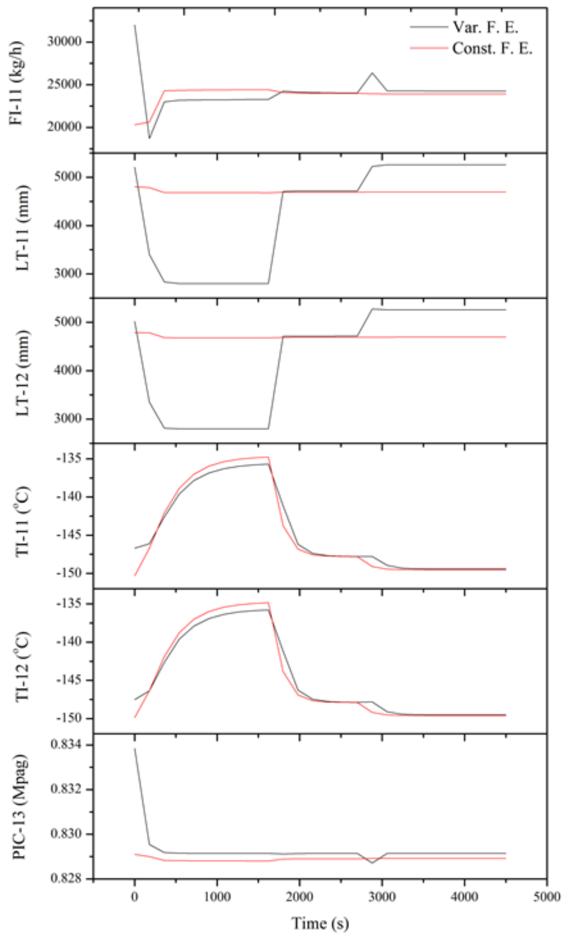

Figure 3-12. Holdup efficiency changes during the simulation of the transient case

3.5.3. HYSYS non-equilibrium solving method

HYSYS is widespread process simulation software especially in LNG industry. It contains lots of process unit model such as distillation column, pipe, separator, and so on. For simulating BOG recondenser, the most usual process model is simple separator and many researches are based on the very simple model. However, there is a problem to build an exact model, that is, the simple separator model assumed an equilibrium state inside the vessel. This makes a difference between the simulation and a real operation of BOG reliquefaction. The condition inside the BOG recondenser is frequently changing as the data from **Figure 3-5**, and the temperature distribution of BOG inside the vessel therefore the equilibrium assumption is not suitable for the BOG recondenser.[83]

In order to solve the problem, many process dynamic simulators like HYSYS are supporting the non-equilibrium state calculation. To consider the non-equilibrium state, the hold-up efficiency, mentioned above, is utilized. **Figure 3-11** represent the concept of hold-up efficiency. It assumed that in vapor-liquid phase, there are 3 different region; vapor/liquid/equilibrium area. Therefore if the fluid enters to the vessel, some amount will go to the vapor or liquid region, and then others will head to the equilibrium area. The ratio for the separation is defined as an efficiency and when we firstly enter some value on that efficiency, the efficiency will be reflected in every equilibrium calculation in the vessel. The hold-up efficiency for a vessel in an example of HYSYS is showed in **figure 3-12**.[78]

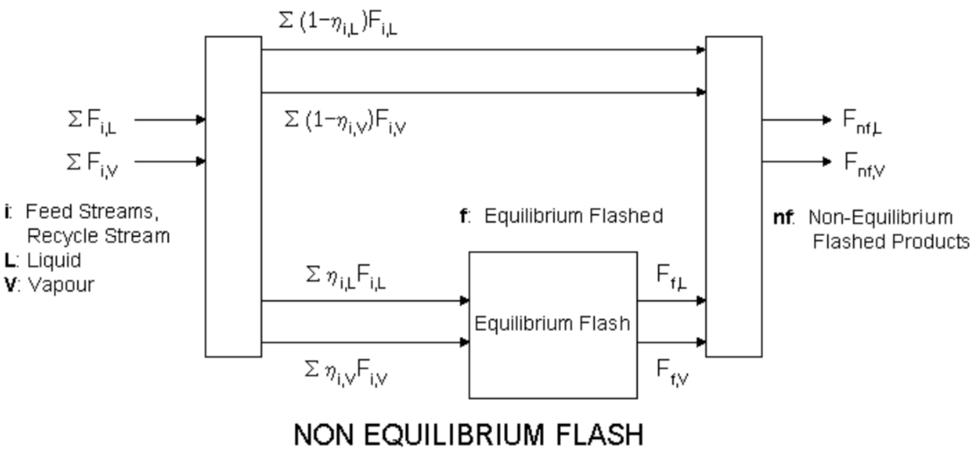

Figure 3-13. Concept of hold-up efficiency for non-equilibrium flash

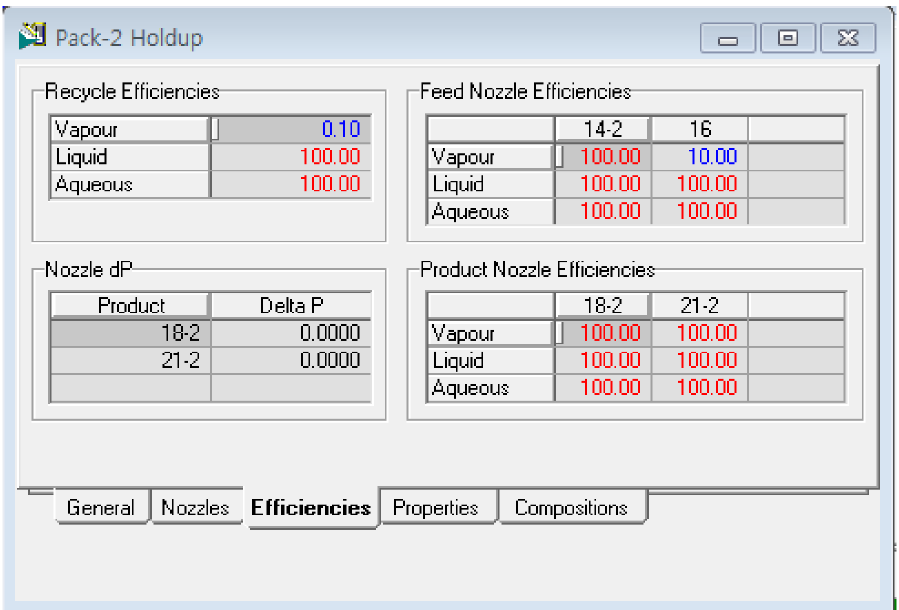

Figure 3-14. An example of hold up efficiency in HYSYS

Nevertheless, a problem still remains, that is, the efficiency can be changed in BOG recondenser. As described above, the rate of BOG reliquefacton is varied through the heat transfer area but when the hold-up efficiency is fixed, this change cannot be reflected. So in this research, we built a model that changes the hold-up efficiency depending on the liquid level of recondenser.

3.6. Result and discussion

In the first case study with the actual data set, the dynamic simulation model shows quite good performance in estimating the process variables in the BOG recondenser. As is evident in **Table 3-3**, the model shows an error of about 2% in the liquid level, which is somewhat smaller than the error of the constant flash ratio model. The performance of developed model in tracking the operational mode change is better than that of the constant flash ratio model, which cannot track the liquid level change at all.

Assessing the predictions in more detail, the output of the model showed good agreement with the actual data for the pressure, liquid level, and temperature inside the BOG recondenser. The error in the BOG flow rate (FT-11) prediction was about 7.22%, the largest for any of the variables. The reason for this relatively large error is the use in the model of design data instead of the actual data for specifications such as size of the valve. Similarly, the valve flow coefficient (Cv) of the valve and feed composition can be changed during operation; the Cv, in particular, is closely related to the BOG flow rate. Even the characteristic curve of the valve can be changed over time, and contribute to error in the estimation of BOG flow rate.

There is another variable for which the performance of simulation model predictions is of lower quality. The errors in the temperature predictions for each recondenser unit seem satisfactory (**Table 3-3**). However, predictions of the simulation model over time do not track the real data perfectly (**Figure 3-11**). Several factors may contribute to this difference. The most significant is that in the real BOG recondenser, the temperature of the upper part of liquid is higher than that of the bottom, so the level change caused by operational mode change can affect the liquid temperature. However, as mentioned in section 3.3.1 above, the liquid inside a vessel is modeled as a uniform fluid, so the prediction of temperature inside the recondenser may show some amount of error.

The second scenario shows the effectiveness of the model built with proposed methodology. If there is a radical operating change, such as in the LNG input rate in the second case study for example, the proposed simulation methodology successfully reflects the operational mode change in its results. However, in the model based on constant flash ratio, the prediction liquid level is not changed. Therefore, if an OTS is based on the constant flash ratio model, and an inexperienced operator is trained by that OTS, the trainee cannot observe the level change. Moreover, when the level alarm rings at 4000 mm of LT-11 or LT-12, the constant flash ratio model cannot alert the trainee, even in a more dangerous scenario.

Finally the dynamic simulation of LNG-FSRU is built using the developed simulation model of BOG recondenser as **figure 3-12**.

Table 3-3. Estimation error of variable and constant flash ratio method

	FI-11	PIC-13	LT-12	LT-11	TI-11	TI-12
Variable (%)	7.22	0.43	2.03	1.47	0.59	0.48
Constant (%)	7.68	0.44	8.22	5.55	0.59	0.56

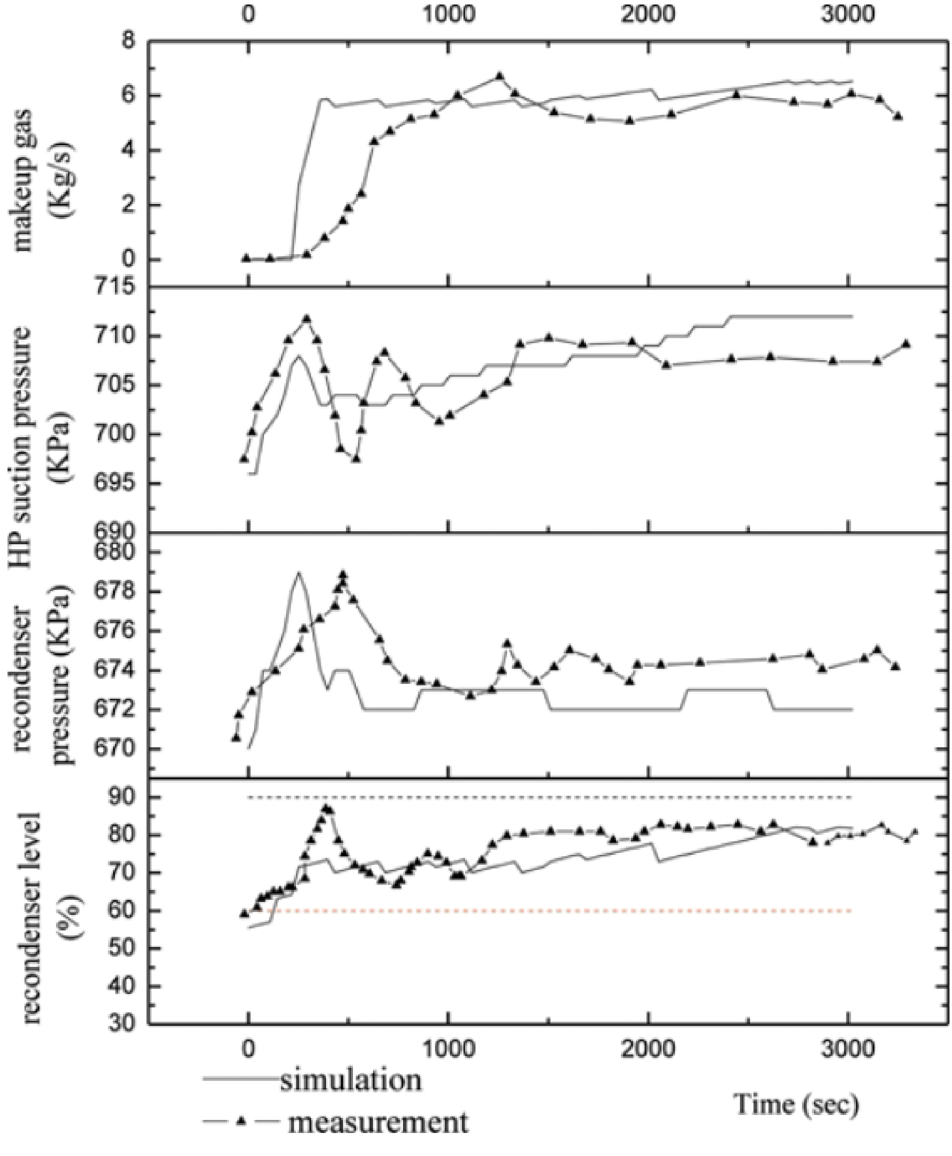

Figure 3-15. Simulation results from former dynamic simulation (Y. Li et al, 2012)

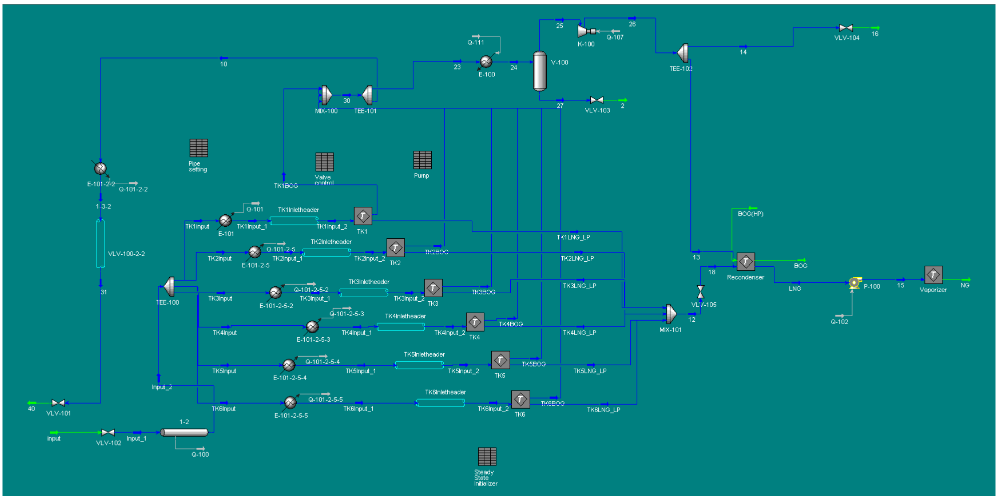

Figure 3-16. Dynamic simulation model for LNG-FSRU

CHAPTER 4 : AUTOMATIC SIMULATION-BASED SOFT SENSOR GENERATION FOR LNG-FSRU

4.1. Introduction

As we have discussed about the design of LNG-FSRU, HAZOP study is also included in FEED package. After the HAZOP study is finished, it is necessary to make design changes to react the problem mentioned in the study, if the preliminary design is well developed, the basic design is not changed too much but the supplement of control and monitoring area usually raised during the HAZOP study. This is also applied to LNG-FSRU and the sensor problem is an inevitable issue, especially for LNG pipes.

A normal LNG-FSRU has many pipes that carry LNG under cryogenic conditions (-160 °C and 1 atm). The temperature difference between the LNG and the ambient outside causes heat transfer, and if the insulation of the pipeline fails to maintain the cryogenic conditions, the LNG inside the pipeline will evaporate and expand to 600 times its original volume. Because this vaporized LNG, the so-called boil-off gas (BOG), may harm the terminal's safety with its abrupt expansion, it is necessary to monitor the exact status of the fluid at as many places as possible. For detailed and precise monitoring of the system, various types and large numbers of sensors are required, consequently resulting in a large sensor installment cost.

In typical LNG pipelines, the types of sensors are limited and only distributed temperature sensors are widely installed because they allow to estimate not only the temperature of fluids but also the leakage of the pipeline with a minimal investment. However, many operators without the requisite engineering background find it difficult to determine the status of the fluid in the pipeline at a particular point with such insufficient data. In the chemical engineering industry, the problem of scarce sensors is usually solved by employing a soft sensor technique. Soft sensors, which are the predictive models that use process observations when hardware sensors are unavailable, have been studied for several decades as a solution to the data insufficiency problem and are currently being applied in various industrial fields.[23], [79] There have been many reports on soft sensor techniques, and they are generally classified as data-based or model-based approaches.

At first, many studies have dealt with data-based methodology, and a meaningful progress has been made in the soft sensor approach based on the process data.[80] Principal component analysis (PCA) and partial least squares (PLS) are the most famous methodologies for soft sensors. Park estimated the composition of toluene using PCA and PLS, whose real-time instrumentation is complicated.[81] In addition to PCA and PLS, the artificial neural network (ANN) method is widely used to estimate process variables without sensors; Thompson and Fellner have reported some good examples of ANN.[82], [83]

Though many data-based methodologies have been developed and sometimes even combined with each other to solve data insufficiency problems, data-based methods are not suitable when the sensor target locations are randomly selected. Solving the problem using a data-based method must follow another modeling procedure for the location factor, which requires professional knowledge of data-based methods.

Model-based approaches were developed to compensate for the disadvantage of the data-based approach mentioned above. The model-based approach provides an answer for the location factor with the first-principles model, e.g., mass/energy balance and reaction kinetic equation sets. Furthermore, if the Kalman filter is included in the model-based approach, as was the case recently, the result is an effective solution for the unmeasured data problem and even real-time estimation. Pantelides has reviewed the overall model-based approach, and Papastratos showed state estimation cases using an online first-principles model with the Kalman filter.[84], [85]

Despite the effectiveness of model-based methods, the complexity of the modeling process prevented their widespread use. As Psichogios showed, the modeling procedure to build equation sets for model-based soft sensors is not easy for those who do not have mathematics and chemical engineering background.[86] To easily calculate more complicated and specific values, process simulation software has been developed and progressed for many years. Software packages such as ASPEN PLUS and gPROMS are composed of various first-principles models and equation sets, and they help to accurately simulate virtual chemical process and estimate nearly all the unmeasured variables in chemical processes.[87]

Although these process simulators are widely utilized to estimate unmeasured variables, the difficulty in using the simulation software remains for process operators without any computer programming and chemical engineering background. In order to enable such people in monitoring sensor-uninstalled areas or predicting dangerous process phenomena, without any complicated simulation or modeling, it is necessary to develop a methodology that minimizes the user's intervention on the variable estimation process and even their use of the process simulation software. There are several reports on simulation automation, but they did not focus on how the methodology will relate to the user.[88]–[90] Barth's other study also dealt with the automatic simulation model generation, and it was oriented toward the conversion of design information to the simulation model.[91]

Therefore, this research aims to build an efficient metho1dology for automatic model-based soft sensor (AMS) generation to help undereducated operators. The AMS methodology involves automatic modeling boundary selection, simulating the model and calculating the target variables with an error minimization approach. Through this methodology, an operator can automatically obtain the fluid data at the target location by simply selecting any location on the pipeline. Finally, this methodology is verified with the help of a case study for an unloading pipeline LNG-FSRU.

4.2. LNG terminal

The LNG terminal is a facility that stores LNG supply that is distributed to consumers. When LNG is shipped by an LNG carrier, the terminal receives the LNG through an unloading pipeline and stores it in insulated storage tanks at less than -150 °C and atmospheric pressure. For feeding gas through the pipeline network, the LNG is pressurized and vaporized to 0 °C at approximately 80 bar through high-pressure pumps and an LNG vaporizer. In addition to this basic structure, some facilities have equipment such as BOG recondenser and compressor installed to eliminate BOG (boil-off gas) from the terminal.

BOG formation is usually a serious problem in terminal operation because the economic feasibility of the terminal depends on how much BOG is recovered or flared. In addition, BOG formation is important with respect to safety as well as economy because it becomes 600 times larger in volume and can damage process units. In order to prevent BOG formation causing serious trouble, the status of the LNG should be monitored.

Monitoring of chemical or energy processes requires sufficient data; thus, there are some design guidelines for the LNG terminal regarding its equipment to ensure that there are enough sensors for monitoring. However, the guidelines are mainly focused on individual pieces of process equipment such as a storage tank or a compressor and not the pipeline, which is vulnerable to the damage caused by BOG.

Because of the loose regulations and high sensor cost, most of installed sensors in LNG terminal pipelines are distributed temperature sensors that can monitor both temperature and leakage. These sensors, however, are not able to estimate the exact state of the LNG inside the pipeline because even at the same temperature, variations in the pressure cause differences in the properties such as vapor fraction.

In addition, in real terminal pipelines, there are more sensors installed in the ship input line or the inlet line of the storage tanks; nonetheless, they cannot help monitor the exact status of all location in the pipeline without process simulation software. This is the reason why AMS must be applied to the LNG terminal pipeline industry. Through AMS, information on the fluid at all locations is available.

4.3. Methodology

The general procedure of the proposed AMS methodology is shown in **Figure 4-1** and stated in detail below.

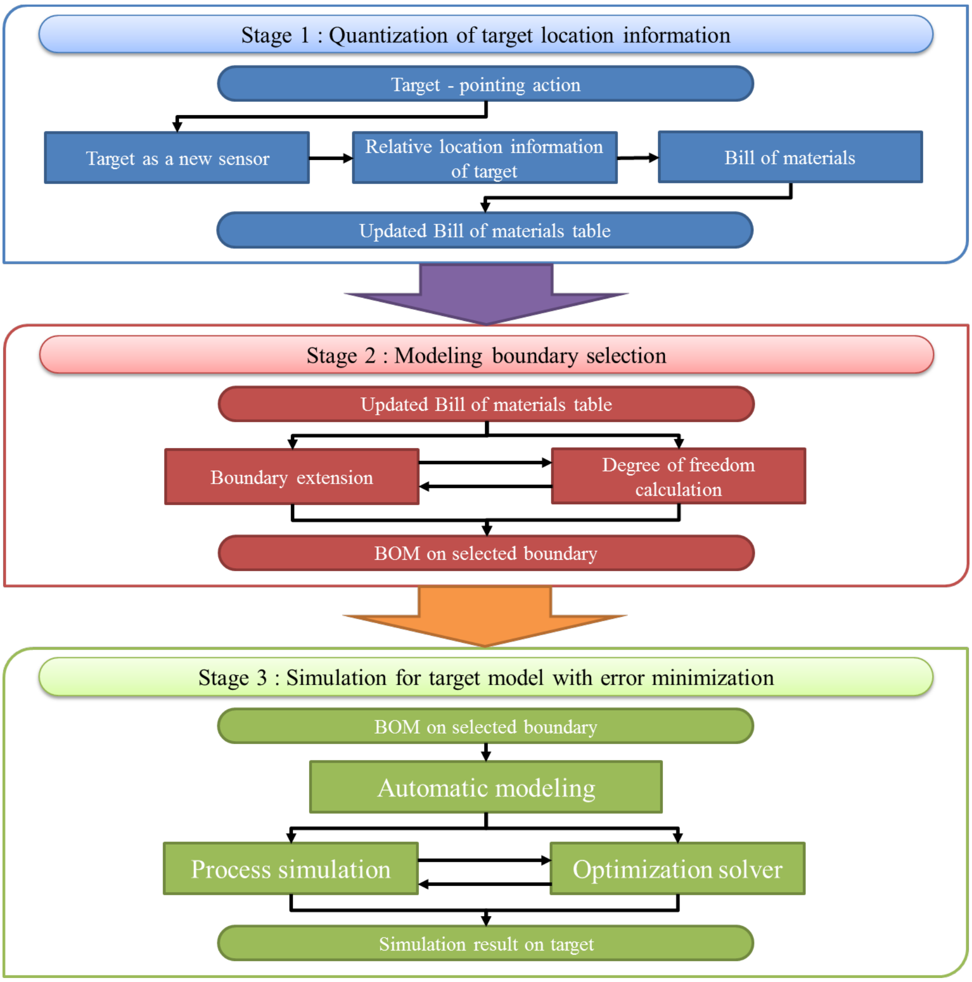

Figure 4-1. General procedure of automatic model-based soft sensor methodology

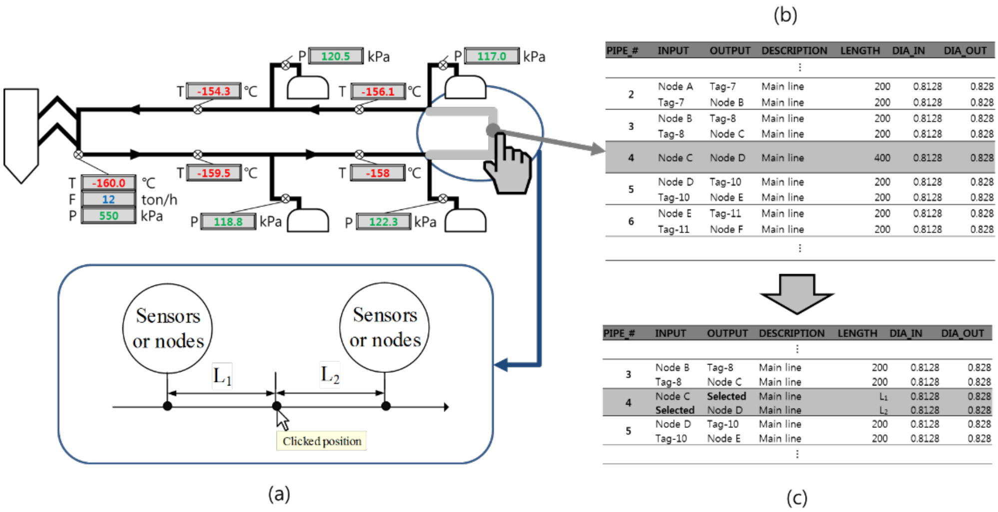

Figure 4-2. Overall scheme of Stage 1: Quantization of positional information. (a) Graphical example of the base GUI; (b) an example of the bill of materials (BOM); (c) updated BOM.

4.3.1. Quantization of target location information

First of all, AMS (automatic model-based soft sensor) methodology must contain a feature to turn the user's pointing action on the graphic user interface (GUI) into quantized information in order to build a simulation model. **Figure 4-2** shows the basic concept of this stage. The base GUI-like distributed control system displays several types of information about the target plant. There are many areas that no sensor is installed, so when a user clicks the desired position on the GUI, the position is regarded as a new sensor, and two types of information, the selected pipe unit and the relative distance between the neighbor sensor, i.e., the node and target position, are extracted. These data are transferred to bill of materials (BOM) table, which includes the length, elevation, material properties, and starting/end point information as seen in **Figure 2(b)**. The BOM table is available from digitalized plant design software such as Autocad and Cadworx, so obtaining the data about pipeline is not a complex problem. With the positional information extracted, the BOM table is reconstructed as seen in **Figure 2(c)**; the pipe that includes the selected point is divided into two new pipes, and this change is reflected in the BOM table.

4.3.2. Model boundary selection

After the location information is reorganized into spreadsheet form, the model boundaries for the target location simulation are specified automatically. The main purpose of this stage is to find the simplest boundary set for efficient process simulation with minimum calculation time. **Figure 4-3** demonstrates the boundary selection procedure. The algorithm includes the following steps: (1) checking the degrees of freedom (DOF) of the target stream only, (2) finding the nearest new data point, (3) expanding the modeling boundary to the nearest new data point, (4) eliminating any redundant data points, and (5) rechecking the DOF for a new model boundary. These steps are repeated until the DOF is reaches to zero with a minimum number of boundary data.

Specifically, Step 1 checks the availability of a simple model formulation. The “stream” refers to an area between the neighboring intersection nodes, and if there are a sufficient number of measured data with zero DOF of the target stream, the simulation for the target position is possible only with pipe models of a single target stream. The DOF calculation for a pipeline is easily derived from an example of a heated pipe in heat transfer textbooks, as explained in the next section.[92]–[94] The DOF calculation relies on the two assumptions below.

(1) The overall heat transfer coefficient is constant in the modeling boundaries.

(2) Other specifications such as roughness factor and LNG composition are fixed.

The first assumption comes from the fact that the heat transfer coefficient of insulated LNG pipe is not sensitive in the temperature range of terminal pipeline operation. **Figure 4-4** represents the difference of the overall heat transfer coefficient at various temperatures and the overall heat transfer coefficient remains unchanged within the typical LNG terminal operation temperature. The composition of the fluid inside the pipeline and the pipe specifications are predefined at the designing state of pipeline, and this is accounted for in the second assumption. This assumption will make the problem simpler. Under these conditions, the number of free variables in a single pipe is four, as presented in the next section, so that searching for the four nearest measured data points is performed in Step 1 of the algorithm.

If there are an insufficient number of data for the selected streams, then the procedure goes to the next step and finds the next nearest data point. This means the closest sensor in terms of distance so as to minimize differences between simulation and reality. By selecting the sensor and checking the distances recursively, the nearest sensor is added to the model boundary.

After the new measured data are added, the nodes between the newly added data are checked. Counting the number of intersecting nodes and measured data will help to calculate the degrees of freedom. Before calculating the degrees of freedom, the measured data should be filtered by eliminating redundant types of data to prevent insolubility of the simulation and increase its accuracy. The redundancy problem is solved by neglecting the measured data when there are more than three measured points with the same data type in a single stream. After the redundant data is neglected, the degrees of freedom are calculated as seen in the next section and the case studies below. The overall procedure is performed recursively until the degrees of freedom for the specified boundary is less than zero.

By the end of this stage, the BOM of the selected boundary is generated. This is performed by selecting all the pipe units connected to the sensors and nodes checked above.

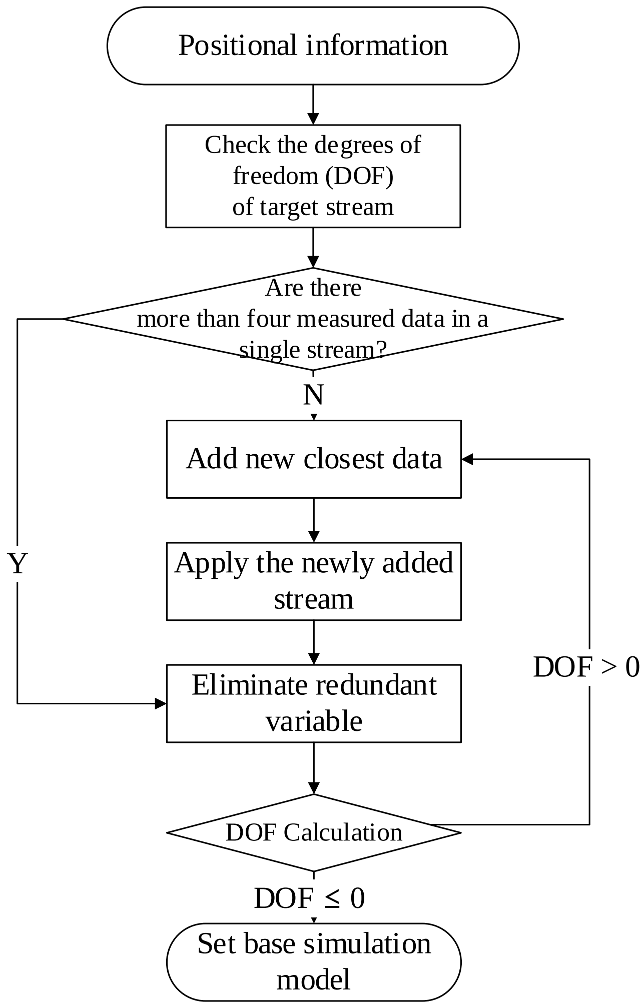

Figure 4-3. Model boundary-selection algorithm.

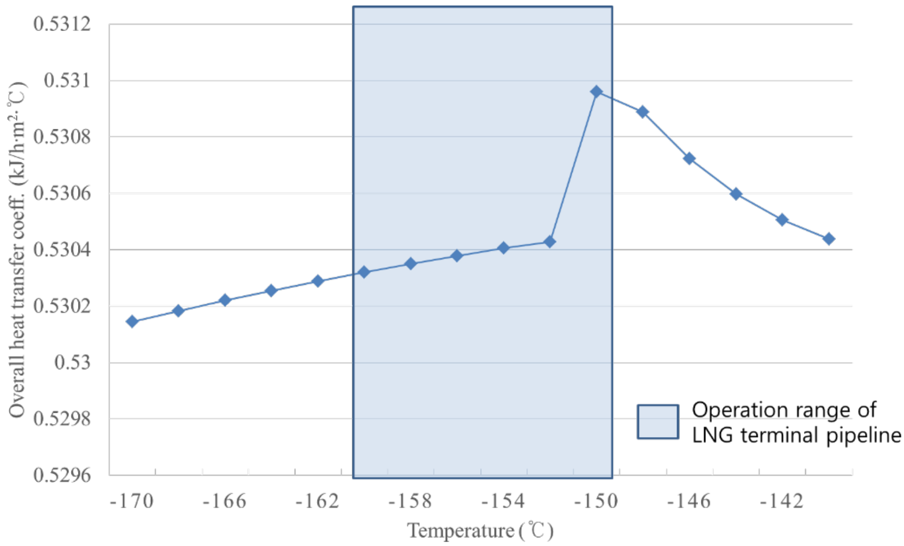

Figure 4-4. Overall heat-transfer coefficient change as a function of the LNG temperature.

4.3.3. Degree of freedom calculation for the LNG pipeline

The degrees of freedom for a single pipe are calculated as shown below.

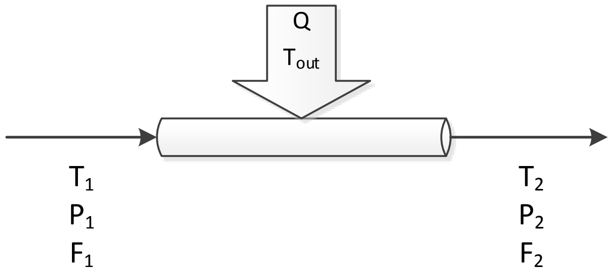

Figure 4-5. A single pipe case for degree of freedom calculation

$$F_1 = F_2$$

$$Q = F_1 \cdot C_p \cdot (T_2 - T_1)$$

$$Q = h \cdot (T_{out} - T_{in})$$

$$T_{in} = \frac{T_2 - T_1}{2}$$

$$P_2 - P_1 = f_D \cdot \frac{L}{D} \cdot \frac{\rho V^2}{2}$$

$$C_p = f(T_1, P_1)$$

Number of variables: 16

Number of equations: 6

Predefined specifications: $f_D, L, D, \rho, V, T_{out}$: 6

Degrees of freedom = 16 – 6 – 6 = 4

If there is a branch line attached to a pipeline, the degrees of freedom are as seen below.

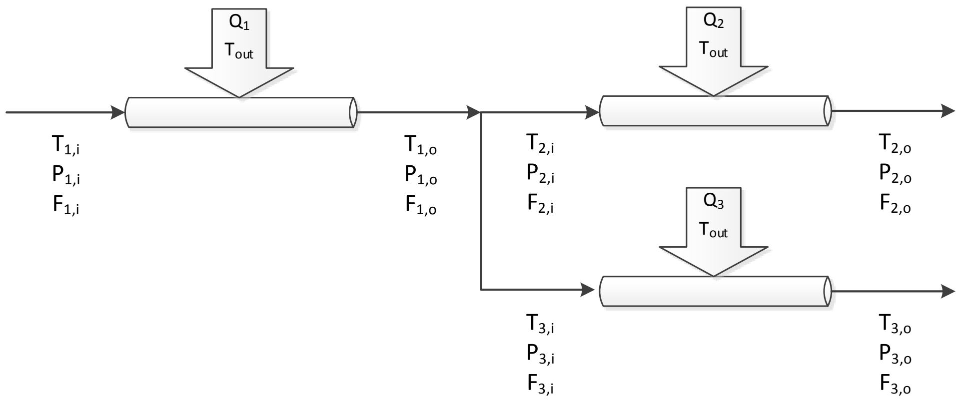

Figure 4-6. A multiple pipe case for degree of freedom calculation

$$F_{1,i} = F_{1,o}$$

$$F_{2,i} = F_{2,o}$$

$$F_{3,i} = F_{3,o}$$

$$F_{1,o} = F_{2,i} + F_{3,i}$$

$$T_{1,o} = T_{2,i} = T_{3,i}$$

$$P_{1,o} = P_{2,i} = P_{3,i}$$

$$Q_1 = F_1 \cdot C_p \cdot \left(T_{1,o} - T_{1,i}\right) = h_1 \cdot \left(T_{out} - \frac{T_{1,o} - T_{1,i}}{2}\right)$$

$$Q_2 = F_2 \cdot C_p \cdot \left(T_{2,o} - T_{2,i}\right) = h_2 \cdot \left(T_{out} - \frac{T_{2,o} - T_{2,i}}{2}\right)$$

$$Q_3 = F_3 \cdot C_p \cdot \left(T_{3,o} - T_{3,i}\right) = h_3 \cdot \left(T_{out} - \frac{T_{3,o} - T_{3,i}}{2}\right)$$

$$\mathrm{P}_{1,o} - P_{1,i} = f\left(f_D, \frac{L}{D}, \frac{\rho V^2}{2}\right)$$

$$\mathrm{P}_{2,o} - P_{2,i} = f\left(f_D, \frac{L}{D}, \frac{\rho V^2}{2}\right)$$

$$P_{3,o} - P_{3,i} = f\left(f_D, \frac{L}{D}, \frac{\rho V^2}{2}\right)$$

$$C_p = f(T, P)$$

Adding the first assumption in methodology,

$$h_1 = h_2 = h_3$$

Number of variables: 29

Number of equations: 20

Predefined specifications: $f_D, \frac{L}{D}, \frac{\rho V^2}{2}, T_{out}$: 4

Degrees of freedom: 29 – 20 – 4 = 5

When the branch line is attached to the pipeline, the degrees of freedom increase by one.

4.3.4. Simulation of the target model with minimizing error

Following Stage 2, the simulation for the determined modeling boundary is made using the information in the BOM such as the number, properties, and location of the pipeline. At the beginning of this stage, the base model for simulation is built automatically. The model building process is different depending on the process simulation software, e.g., Aspen plus, HYSYS, or Pro/II, and in the case of HYSYS, the conceptual process is illustrated in **Figure 4-7**.

After defining the model for the target LNG pipeline, the process simulation software calculates a stream result of the target. The simulation procedure consists of inlet flow determination by recursive flow condition change, as seen in **Figure 4-8.** This procedure can be defined as an optimization problem as shown below.

$$\min \sum_{i=1}^{n} (x_{i,measured} - x_{i,simulated})^2$$

Subject to

$$\mathrm{f}(\mathrm{x}_{\mathrm{i,simulated}}) = 0$$

n: number of measured data

$\mathrm{x}_{\mathrm{i,measured}}$: measured data

$\mathrm{x}_{\mathrm{i,simulated}}$: simulation result at the measuring position

The determination of an object function is quite similar to a casual data reconciliation problem whose constraints are heat and mass balance equation sets, and these constraints are substituted with process simulation software, as in this research.[82],[83] The constraint equation "$\mathrm{f}(\mathrm{x}_{\mathrm{i,simulated}}) = 0$" means the simulation model is converged. The process simulation software is composed of various and complex equation sets so that the model building workload can be decreased.

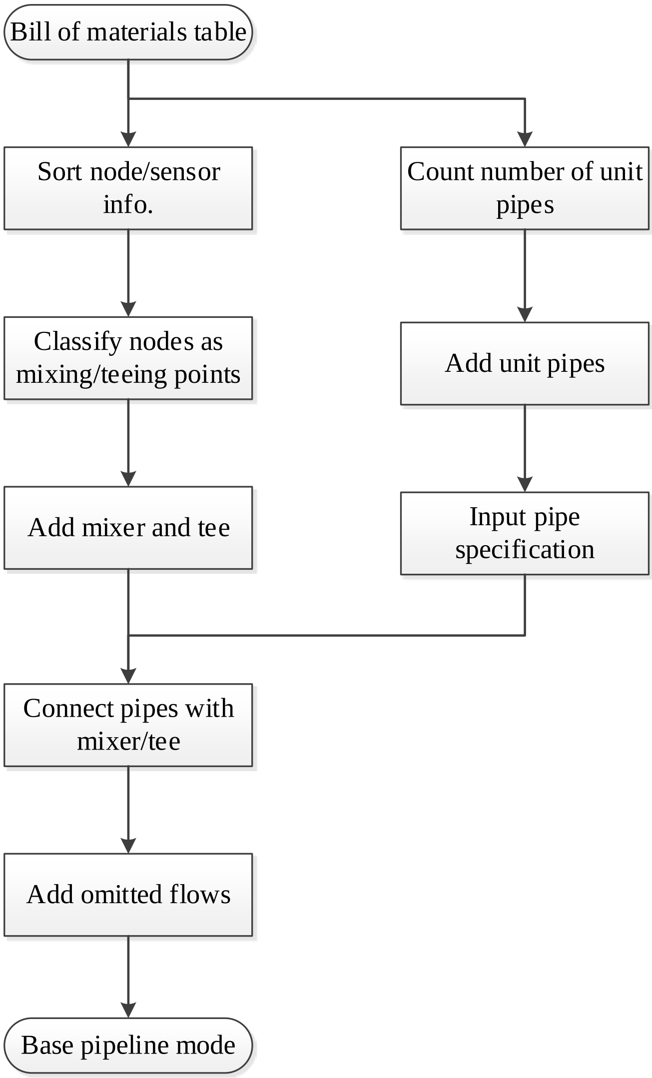

Figure 4-7. Flowchart of model-building process

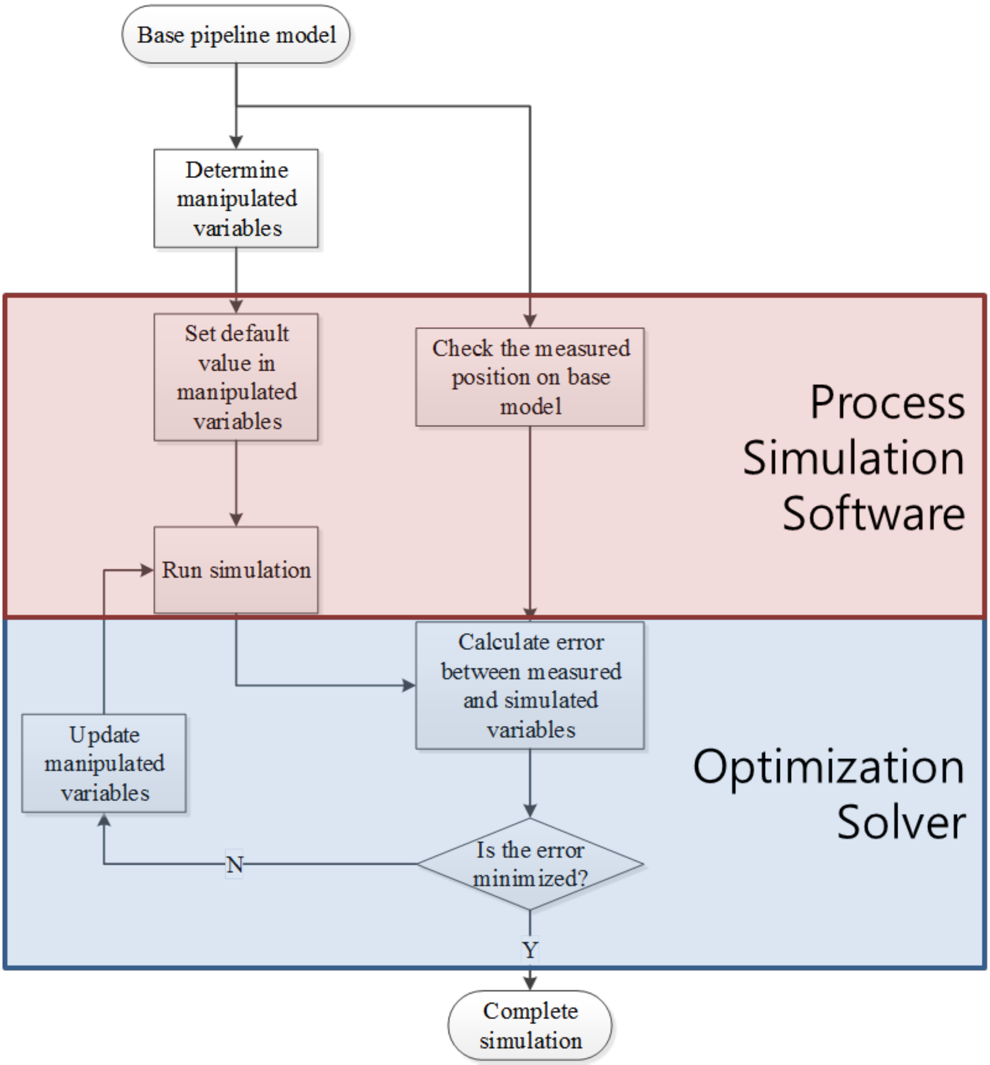

Figure 4-8. Algorithm of process simulation for a specified boundary

Although the optimization function can be solved by many programs, MATLAB is chosen because it can easily connect to various process simulation software. The MATLAB software recursively changes the input variables of process simulation to find a solution that minimizes the error between the simulation results and the measured data.

These input variables, which refer to manipulated variables, are the same as the measured variables when the process simulation software is of the equation-oriented type, as is gPROMS; however, there is some difficulty using these programs directly on a sequential modular process simulator. For the sequential modular process simulator, the calculation process starts from the input flow definition, so when the input condition is not fixed, but only the values in the other position are given, the simulation speed and problem consistency will decrease. Nevertheless, the sequential modular approach is necessary for AMS because many LNG terminals use HYSYS as a process simulator; it is widespread in the LNG industry, and this is the reason why the determination of manipulated variables is required in AMS.

1) The manipulated variables of the pipeline model are as follows:
2) input flow conditions (temperature, pressure, and flow rate)
3) overall heat transfer coefficient
4) flow rate of teeing point

Through cooperation of the process simulation and optimization solver, the result is available with minimum differences between the measured variable and the simulation result. The extraction of the target's information, the process for automatic model-based soft sensor is over, and finally the information is presented to the operator on the GUI.

4.4. Case study

For verification of the developed methodology, case studies of an unloading pipeline of the LNG receiving terminal were made. Before the case studies, the surrounding conditions should be determined in advance. As in a typical LNG receiving terminal, the unloading pipeline is composed of a main line that transfers LNG from ship to terminal and branch lines that bring LNG to each storage tank (**Figure 4-9**). This unloading pipeline is installed in a vast plane so that there is no elevation in the main line, while some branch lines have a sloping area because in this case study, it is assumed that there are both aboveground and underground storage tanks.

The number, type, and location of the installed sensors are determined in reference to P&ID of an LNG terminal in South Korea and the sensor installation guidelines of a typical LNG-receiving terminal.[40], [107] There are three sensors measuring temperature, pressure, and flow rate in the ship input and recirculation input flow, and two sensors measuring temperature and pressure for each tank inlet flow. The pressures of the branch lines are monitored in each tank, so these values are used to estimate the LNG pressure inside the branch lines. The temperatures for the entire pipeline are estimated by distributed temperature sensors (DTSs), which provide information about the temperature of the LNG inside the pipe at intervals of several meters, but only data at 400-m intervals are used to maximize the efficiency.

With these assumptions, a BOM table and the simulation results at the sensor position are available. The BOM table covers the general information about the specification of pipe, inlet/outlet position, and geometry data such as length and elevation changes. The process simulation software for the case study is HYSYS because of its popularity in the LNG industry and its sufficient performance. Using HYSYS, the pipeline simulation model, which represents the target LNG receiving terminal pipeline, is built as seen in **Figure 4-10**, and the extracted results at the sensor position are utilized for the case study.

To validate and explain the proposed methodology, two different case studies are performed. The first case determines the accuracy of the AMS methodology by reverse calculation of eliminated raw data. The second case study evaluates the performance of the methodology, particularly in calculating various types of data such as vapor fraction or actual volume flow rate, which are difficult to measure but important for judging the safety of the terminal pipeline.

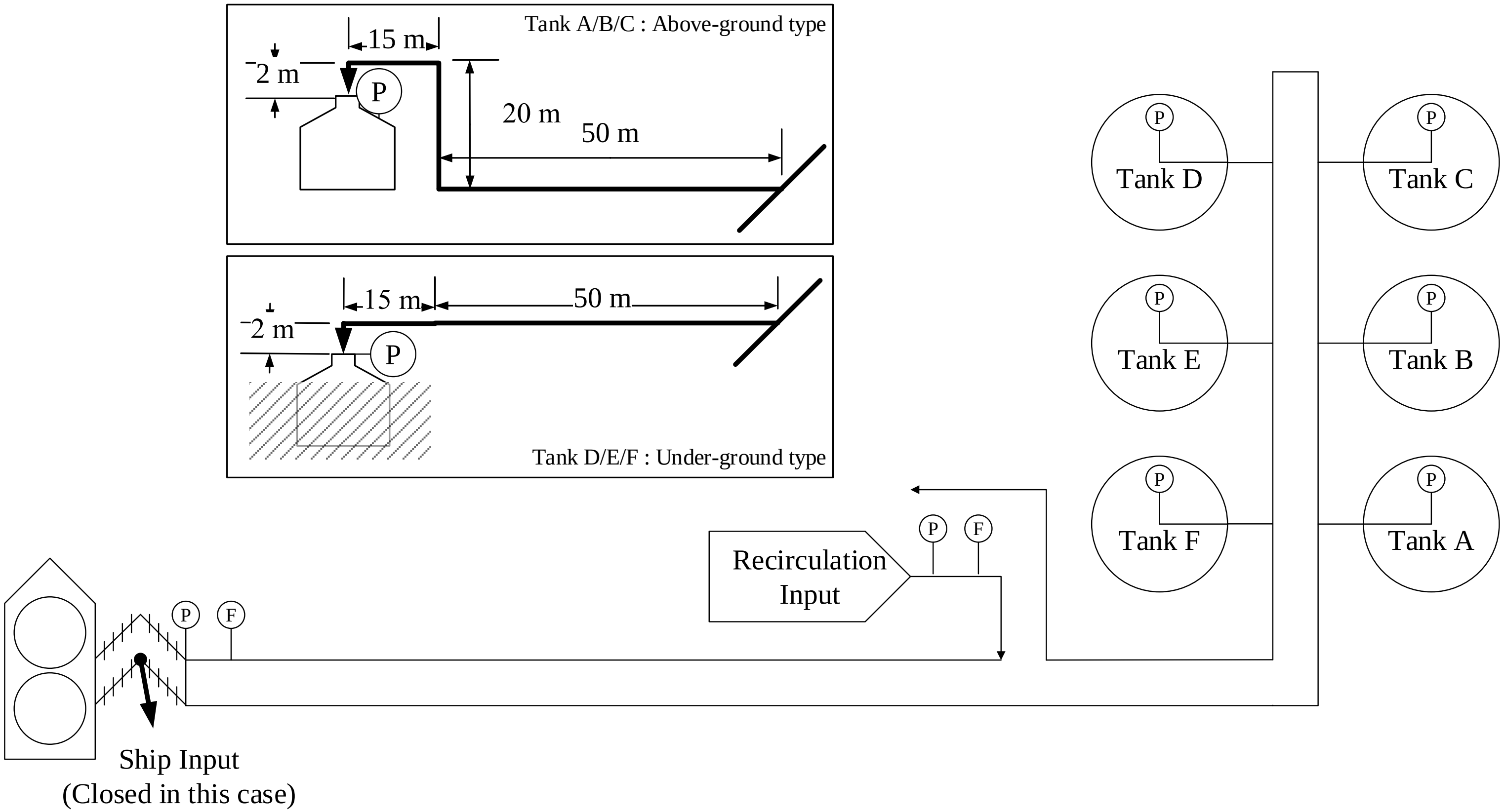

Figure 4-9. LNG terminal unloading pipeline example with three targets in case study 1.

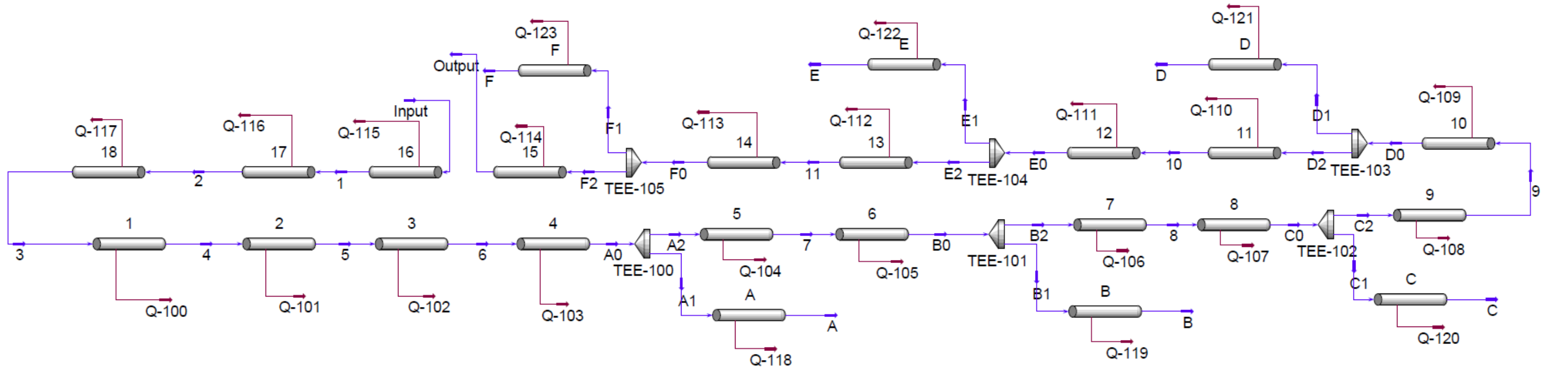

Figure 4-10. A HYSYS model of an entire LNG unloading pipeline for the case studies

4.4.1. Case study 1

For the first case study, some raw temperature data are assumed to be unmeasured, and then the deleted temperatures are inversely calculated by the AMS methodology. The target positions are chosen to consider various examples of pipeline modeling cases; therefore, the three positions shown in **Figure 4-9** are specified.

In the beginning of the methodology, when a position is selected by the operator, the target location information is reflected in the BOM in **Table 4-1**, and the selected position is regarded as a new sensor. Based on the new BOM table, the model boundary for the target positions is formulated automatically. Position A has more than four measured data available in a single pipe, and the types of data are various enough not to eliminate any because of redundancy, so the model boundary is simple, as seen in **Figure 4-11**. For positions B and C, there are insufficient number of data in target stream, thus, the modeling boundaries are expanded until the algorithm loop finds the DOF is zero as seen in **Figures 4-12** and **4-13**.

At the simulation stage, a simulation model of the LNG pipeline is built with ASPEN HYSYS using the boundary information determined above. The model-building process is automated by the algorithm shown in **Figure 4-8**, which is embodied with Macro Editor in HYSYS.[78] Because of the automated model building process, the simulation model for each case is specified as in **Figure 4-14**. After the model about the target is fixed, an optimization process to calculate the stream result for the selected target is assigned by MATLAB because of its wide compatibility with HYSYS. Changing the variables indicated in **Figure 4-14**, such as pressure, temperature, mass flow rates of the pipe inlet flows, other mass flow rates for the branch line flows, and the heat transfer coefficient of the pipes, as those are explained in the Methodology section, the optimization process is executed with the “fmincon” function in MATLAB as an optimization solver. The objective function for the optimization is formulated shown in **Figure 4-15**. The result for each case is available when the simulation is complete, having minimized the error between the measured data and the simulation result. Finally, the stream result for the selected target is extracted to the GUI, and the methodology is completed.

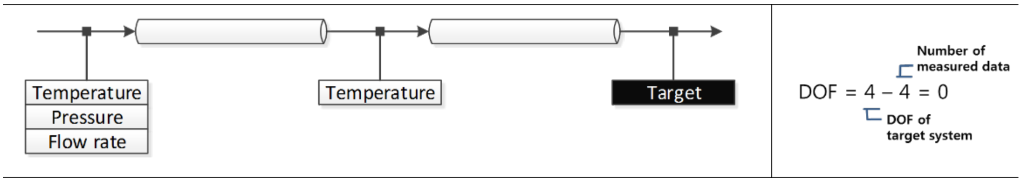

Figure 4-11. Specified model boundary for position A

Table 4-1. Bill of materials table for a terminal unloading pipeline

PIPE_#	INPUT (Sensor type)	OUTPUT (Sensor type)	DESCRIPTION	LENGTH	DIA_IN	DIA_OUT
1	Input(T/P/F)	Tag-1(T)	Main line	400	0.8128	0.828
	Tag-1(T)	Tag-2(T)	Main line	400	0.8128	0.828
	Tag-2(T)	Tag-3(T/P/F)	Main line	400	0.8128	0.828
	Tag-3(T/P/F)	Tag-4(T)	Main line	400	0.8128	0.828
	Tag-4(T)	Tag-5(T)	Main line	400	0.8128	0.828
	Tag-5(T)	Tag-6(T)	Main line	400	0.8128	0.828
	Tag-6(T)	Node A	Main line	200	0.8128	0.828
2	Node A	Tag-7(T)	Main line	200	0.8128	0.828
	Tag-7(T)	Node B	Main line	200	0.8128	0.828
3	Node B	Tag-8(T)	Main line	200	0.8128	0.828
	Tag-8(T)	Node C	Main line	200	0.8128	0.828
4	Node C	Tag-9(T)	Main line	200	0.8128	0.828
	Tag-9(T)	Node D	Main line	200	0.8128	0.828

5	Node D	Tag-10(T)	Main line	200	0.8128	0.828
	Tag-10(T)	Node E	Main line	200	0.8128	0.828
6	Node E	Tag-11(T)	Main line	200	0.8128	0.828
	Tag-11(T)	Node F	Main line	200	0.8128	0.828
7	Node F	Output	Main line	200	0.8128	0.828
8	Node A	Tank A(T/P)	Branch line	87	0.8128	0.828
9	Node B	Tank B(T/P)	Branch line	87	0.8128	0.828
10	Node C	Tank C(T/P)	Branch line	87	0.8128	0.828
11	Node D	Tank D(T/P)	Branch line	57	0.8128	0.828
12	Node E	Tank E(T/P)	Branch line	57	0.8128	0.828
13	Node F	Tank F(T/P)	Branch line	57	0.8128	0.828

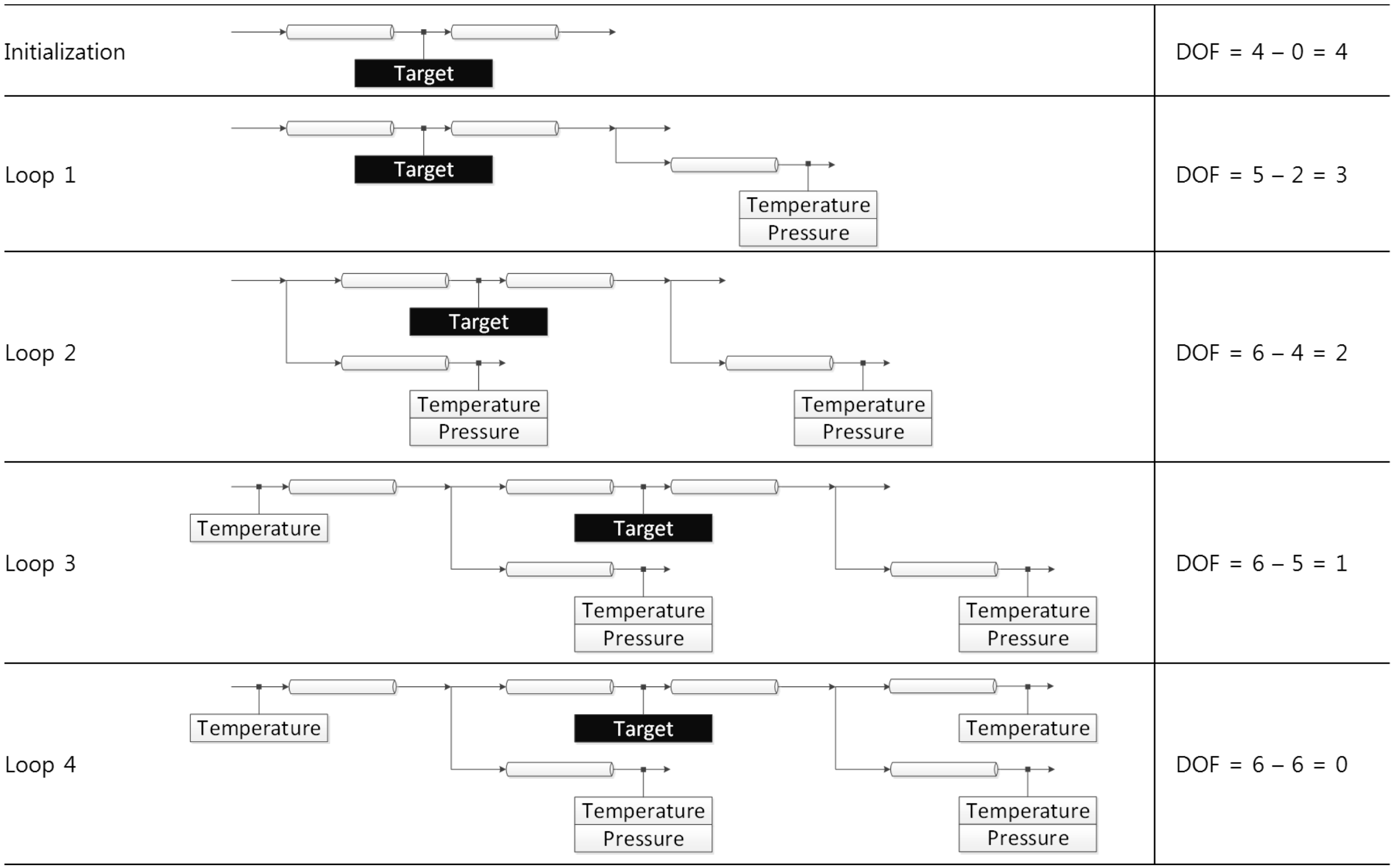

Figure 4-12. Model boundary-selection procedure for position B

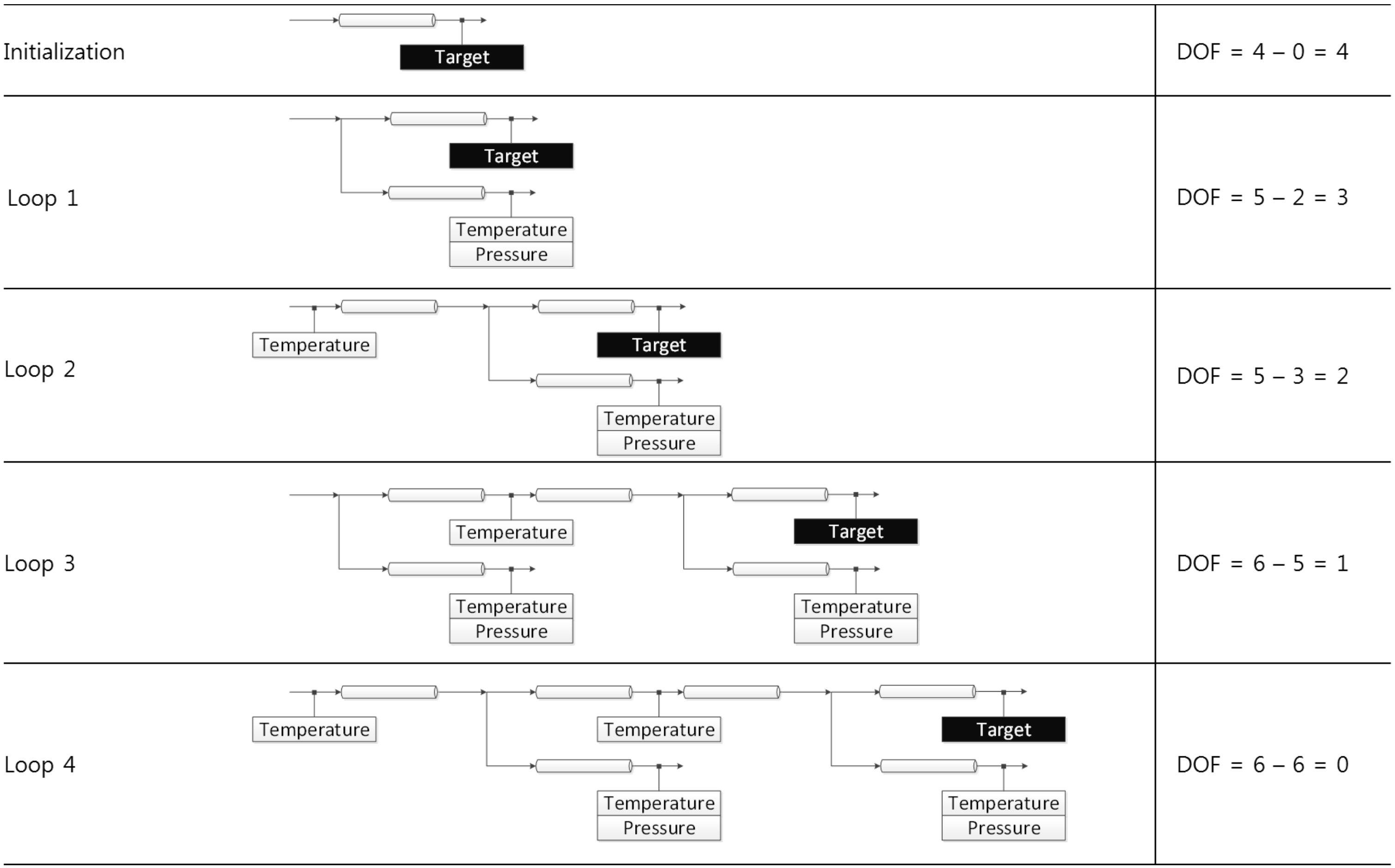

Figure 4-13. Model boundary-selection procedure for position C

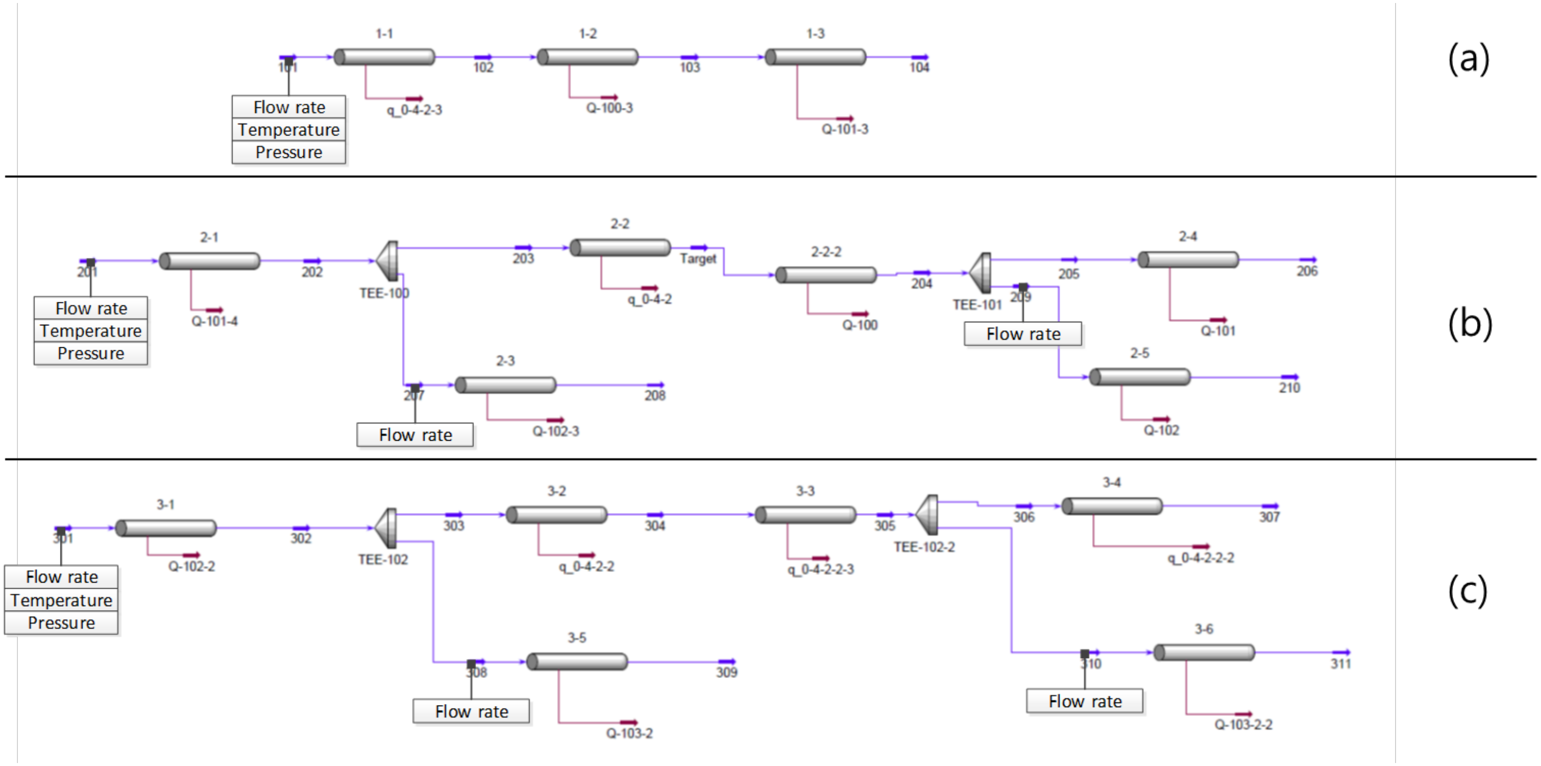

Figure 4-14. Specified simulation models for case study 1: (a) position A; (b) position B; (c) position C

```
function Error = Casestudy_1_1(x)

    % Launching HYSYS
    hysys = actxserver ('HYSYS.Application');
    hyCase = hysys.ActiveDocument;

    % reference data
    Temp_ref =              [
                            -155.2986454;   % input
                            -153.769355429552;          % 4
                            -151.152287290427;          % 6
                            ];
    Press_ref =  [
                            199.996273775955;           % input
                            ];
    Mass_ref =  [
                            5.55555555555556;           % input
                            ];

    % insert manipulated variable
    hyCase.Flowsheet.Operations.Item('1-1').OverallHTCValue = x(1);                   % Overall heat transfer coefficient
    hyCase.Flowsheet.Operations.Item('1-2').OverallHTCValue = x(1);                   % Overall heat transfer coefficient
    hyCase.Flowsheet.Operations.Item('1-3').OverallHTCValue = x(1);                   % Overall heat transfer coefficient
    hyCase.Flowsheet.MaterialStreams.Item('101').TemperatureValue = x(2);     % Input temperature
    hyCase.Flowsheet.MaterialStreams.Item('101').PressureValue = x(3);                % Input pressure
    hyCase.Flowsheet.MaterialStreams.Item('101').MassFlowValue = x(4);                % Input flow rate

    % extract simulation result for measured position
    Temp_sim = empty(3,1);
    Press_sim = empty(1);
    Mass_sim = empty(1);
    Temp_sim(1) = hyCase.Flowsheet.MaterialStreams.Item('101').TemperatureValue;
    Temp_sim(2) = hyCase.Flowsheet.MaterialStreams.Item('102').TemperatureValue;
    Temp_sim(3) = hyCase.Flowsheet.MaterialStreams.Item('104').TemperatureValue;
    Press_sim(1) = hyCase.Flowsheet.MaterialStreams.Item('101').PressureValue;
    Mass_sim(1) = hyCase.Flowsheet.MaterialStreams.Item('101').MassFlowValue;

    % Estimating the error between model and data
    Md =   Mass_sim - Mass_ref;
    Pd =   Press_sim - Press_ref;
    Td =   Temp_ref - Temp_sim;

    Error = transpose(Pd) * Pd + transpose(Td) * Td + transpose(Md) * Md;
end
```

Figure 4-15. Objective function for case study 1, position A

4.4.2. Case study 2

The same procedure is performed with another case study that represents the availability of various types of properties. As mentioned above, BOG formation is a huge risk to the LNG terminal's safety and it must be monitored quite closely. In case study 2, the vapor fraction and actual volume flow rates at the end of the branch lines, which indicate the BOG formation and are also important variables for the safety of the LNG storage tank, are calculated with the AMS.

The overall process for this case study is the same as in case study 1 above, but the target locations are changed, and the model boundaries should be different. There are only two sensors installed at the target position, so many other measurement variables are necessary to verify the simulation result. The boundary selection stage is applied to build new modeling perimeters for branch line simulations, and the extended model boundaries were specified, as **Figure 4-16**.

Each branch pipeline has different geometry conditions, but the sensor installation environments are similar so that the structure of the pipeline model for each simulation is the same. **Figure 4-17** represents the specified base HYSYS model through Stage 2, which presents the boundary for each branch pipe with different measurement locations.

The procedure for the simulation stage in case study 2 is the same as in case study 1. The specified boundaries are utilized to make the simulation model for HYSYS, and the input variables of the pipe flows are specified with a minimized difference between the measured data and the simulated result. The "fmincon" function in MATLAB is applied to solve the optimization problem. Consequently, the volumetric flow rate and vapor fraction, which cannot be measured physically in real-time, are calculated through AMS for each branch line.

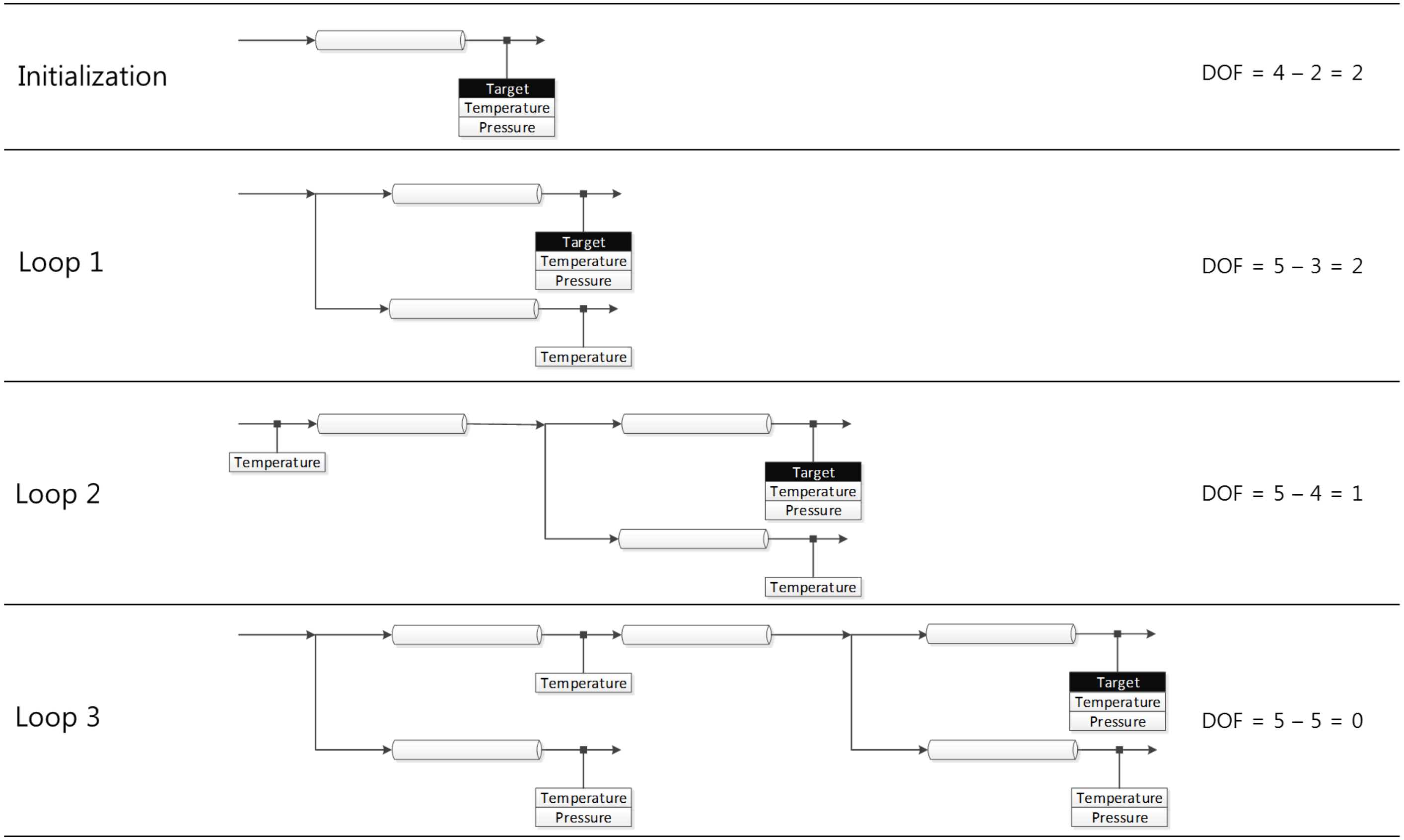

Figure 4-16. Model boundary-selection procedure for case study 2

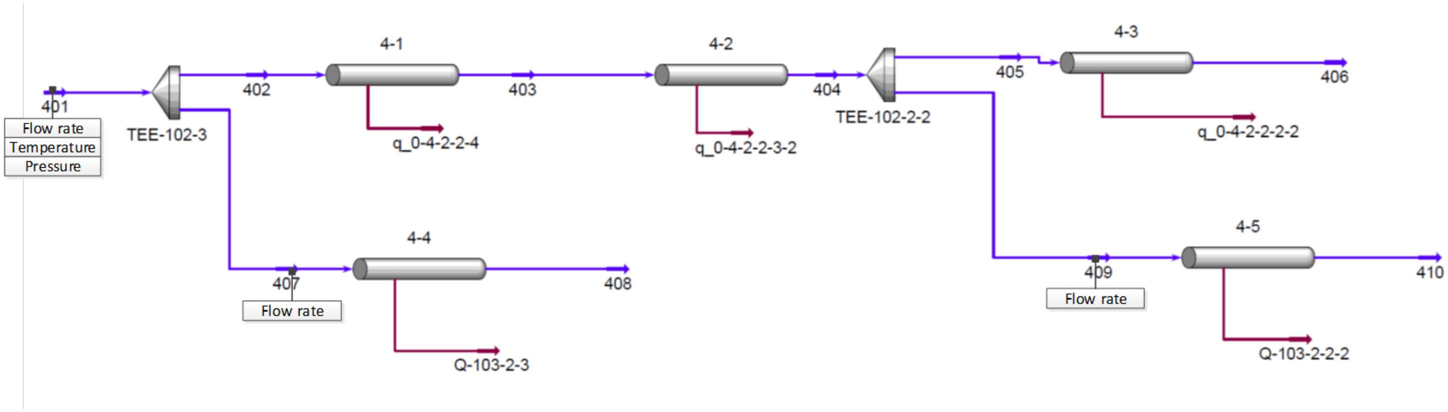

Figure 4-17. Specified simulation models for case study 2

4.5. Result and discussion

We performed two case studies to characterize the performance and advantages of the developed AMS methodology. In the first case, the temperature data at several positions are deleted and regarded as unmeasured; the estimated values by AMS are then compared with the deleted raw values. First, the model boundaries for each of the three positions are built well. Although the location and neighboring sensors are diverse for each case, the selected boundaries offered a good base for the subsequent process simulation through the boundary selection algorithm. In position A, a single pipeline with several sensors is composed through the algorithm, and with that simple structure, the stream result can be calculated quickly. Positions B and C do not have flow rate sensors nearby, resulting in more complex structures for these positions. Nonetheless, the determined model boundaries have simpler structures than the original pipeline simulation model that covers the entire area (**Figure 4-10**). That is, the proposed boundary selection algorithm generates the optimum structures for the target variable calculation in a shorter time and with sufficient accuracy as presented in **Table 4-2**.

Table 4-2. A comparison of calculation time between overall pipeline model and AMS model

<table>
<tr><th></th><th>Overall pipe</th><th>Case 2-1</th><th>Case 2-2</th><th>Case 2-3</th><th>Case 2-4</th><th>Case 2-5</th><th>Case 2-6</th></tr>
<tr><td rowspan="2">Calculation time (s)</td><td rowspan="2">442</td><td>44</td><td>50</td><td>30</td><td>33</td><td>24</td><td>24</td></tr>
<tr><td colspan="6">34.2</td></tr>
</table>

To estimate the accuracy of the AMS method, the simulated temperatures for three target positions are analyzed (**Table 4-3**). The AMS methodology estimated the temperature for each target with almost negligible errors. The result at position B demonstrates the best performance with the smallest error, but the amount of error in other positions is not significantly different.

Table 4-3. Temperature estimation results for case study 1

	Position A		**Position B**		**Position C**	
	Sim. result	Raw data	Sim. result	Raw data	Sim. result	Raw data
Temp. (°C)	-152.26	-152.26	-151.11	-151.09	-150.99	-151.09
Error (%)	0.027		0.012		0.069	

In the second case study, the actual volumetric flow rate and vapor fraction at the end of the branch pipeline were calculated using AMS. The selected target in case study 2 is each tank inlet flow; thus, the simulation results for those branch streams must be specified by AMS. In the boundary selection stage, all targets in case study 2 have equal simulation models because every targeted branch line has similar nearby sensors, and this is the reason why the same boundaries are built for these targets. There are insufficient sensors to see the boundary structure in detail, and the boundaries extend only to the main line. However, even with six nearby measurement data being used to build a simulation model for the branch line, the result is much smaller than the entire unloading pipeline simulation model.

Through the process simulation and error-minimizing algorithm in AMS for each target, the results are available in **Table 4-4**, which also includes a comparison of the simulated results to the raw data. The amount of error between them is less than 1.13% for the volumetric flow rate and 1.55% for the vapor fraction. These errors come from the first assumption regarding the heat-transfer coefficient in the model boundary selection stage. The conditions of the unloading pipeline in this case study were harsher than in real terminal operations; therefore, the simulation of every pipeline overestimated the BOG inside.

Despite the errors included in the results, the supposed methodology is meaningful, as the error is not large. Moreover, these types of data such as volumetric flow rate and vapor fraction, which are essential for plant risk assessment, are not immediately available without physical sensors; when the process simulation is not accessible because of such difficulties, this methodology can be used to propose various data with reasonable errors to process operators and effectively help them to operate the chemical process in a safer manner.

In conclusion, LNG-FSRU has strong demands for various and precise data, and many studies have been performed to estimate the unmeasured or immeasurable data. However, almost all such research has been designed to estimate the data from a predefined sensor location. To determine the data from any position in the chemical process, the target should be modeled as a soft sensor with model-based or data-based soft sensor methods. However, the process of making a soft sensor is not easy for many field operators, who are the first consumers of this technique, and this is an obstacle in the utilization of soft sensor techniques. In this paper, we presented an automation algorithm for building a soft sensor on the operator's demand and verified our methodology with the help of case studies of an LNG pipeline, which has a large demand for determining unmeasured data at any position. Because the case studies showed the reliability of the model, which faced only a small error, and the availability of various types of data, this developed methodology can help to safely manage chemical processes. This methodology also shows advantages over other soft sensor technology, as shown in **Table 4-5**.

Table 4-4. Differences between the measured data and simulation results for case study 2

		Tank A	Tank B	Tank C	Tank D	Tank E	Tank F
Actual volume flow rate	Raw data	84.42	64.21	42.99	54.64	50.14	36.19
	Simulated	85.03	64.95	43.42	55.12	50.80	36.42
	Error	0.72	1.13	1.00	0.86	1.29	0.62
Vapor fraction	Raw data	0.064	0.078	0.11	0.06	0.08	0.13
	Simulated	0.064	0.079	0.11	0.06	0.09	0.13
	Error	0.64	1.55	1.14	1.07	1.35	0.68

Table 4-5. Score table for a comparison of data-based, model-based, and automated model-based soft sensors

	DBS	MBS	AMS
Appropriate for new target	3	2	1
Various data type	3	1	1
Soft sensor building time	2	3	1
Dynamic situation	1	1	3

CHAPTER 5 : CONCLUSION AND FUTURE WORKS

5.1. Conclusion

This thesis has addressed the design of LNG-FSRU topside process. The improvements on each result are validated with official information and reference data.

At first, the topside process flowsheet of LNG-FSRU is designed for considering the offshore features. These factors are ship motion, small footprint, and equipment weight and the design of LNG-FSRU topside is implemented with consideration of these factors. As a result of consideration, all the process equipment on the LNG-FSRU topside is guaranteed for offshore condition and the vaporizer type is selected to shell and tube vaporizer which is smaller, lighter and safe in offshore motion effect.

Secondly, the dynamic model of LNG-FSRU is built with a novel dynamic modeling methodology for BOG recondenser. BOG recondenser is a core process unit in LNG receiving terminal process and this research dealt with the exact estimation of BOG recondenser. The performance of the developed methodology was superior to other researches before and with more modification, the methodology will give perfect accuracy.

Lastly, we presented an automation algorithm for building a soft sensor of LNG-FSRU pipeline on the operator's demand and it was verified with the case studies of an LNG pipeline, which has a large demand for determining unmeasured data at any positions. Because the case studies showed the reliability of the model, which faced only a small error, and the availability of various types of data, this developed methodology can help to safely manage chemical processes.

5.2. Future works

Future studies about the offshore plant such as LNG-FPSO (Floating Production, Storage and Offloading) or GTL-FPSO (Gas to Liquid FPSO) can be considerable using the methodology presented in this thesis. Especially these offshore plants have heavier topside processes and more motion-sensitive equipment that considering these offshore condition should be strongly required. The layout optimization based on the weight reduction result is also recommended as future research because the change of layout will bring enhancement of safety and dynamic stability for each process unit. About the modeling about BOG recondenser, more data about the bottom of the unit will guarantee the accuracy of simulation model. And finally the automatic soft sensor building methodology will become powerful when it turns to a software package. Furthermore, the methodology is focusing on the pipeline only but if the model building algorithm is expanded to other process facilities, the process operator can get nearly every process variable about LNG terminal.

References

[1] International Gas Union, “World LNG Report - 2014 Edition,” 2014.

[2] ExxonMobil, “2012 The Outlook for Energy : A View to 2040 Contents,” 2012.

[3] R. R. Bowen, M. R. Miller, J. L. Planteen, O. W. Tredennick, G. M. Norman, C. M. Duke, and M. N. Greer, “LNG Technology Advances and Challenges,” in *International Petroleum Technology Conference*, 2008, vol. 1990, no. c, pp. 1–9.

[4] B. Ertl, M. W. K. Limited, C. Durr, D. Coyle, I. Mohammed, and S. Huang, “New LNG Receiving Terminal Concepts,” *18th World Petroleum Congress*, Jan. 2005.

[5] Y. Sohn, Y. Yang, I. Yoon, S. Choi, and G. Choi, “Expansion of Pyeongtaek LNG Receiving Terminal of Korea Gas Corporation,” in *Proceedings of The Fifteenth International Offshore and Polar Engineering Conference*, 2005, vol. 8, pp. 304–308.

[6] A. Kaplan and C. Yang, “Design Considerations for an LNG Receiving Terminal,” in *SPE Annual Technical Conference and Exhibition*, 2003.

[7] W. R. Shu and C. W. H. Anderson, “Design, Siting and Marine Operation of an Offshore LNG Receiving Terminal,” in *Gastech 2000*, 2000.

[8] Y. Sohn, S. Kim, and I. Yoon, “Conceptual Design of LNG FSRU Topside Regasification Plant,” *The Twenty-second International Offshore and Polar Engineering Conference*, vol. 4, pp. 917–920, Jan. 2012.

[9] J. I. Lee, W. J. Choi, and G. R. Lim, “Development of 270k Cbm LNG-FSRU Operator Training System,” *The Twenty-second International Offshore and Polar Engineering Conference*, vol. 4, pp. 889–894, Jan. 2012.

[10] P. M. Wingate, J. W. Hasz, M. D. McGee, and P. Wingage, “TOPSIDE FACILITIES DESIGN FOR HUTTON TLP,” in *Proceedings of Offshore Europe*, 1983.

[11] X. Wang, J. H. Hwang, H. Sun, H. N. Patel, and P. Liao, “Challenges on the Safety of Floating Liquefied Gas Terminals - Hull, Topside and Interface,” in *Proceedings of Offshore Technology Conference*, 2012.

[12] N. G. Boyd and W. Offshore, “OTC 5257 Topsides Weight Reduction Offshore Platforms Design Techniques for,” 1986.

[13] R. Mikkelsen, F. M. C. Technologies, and D. Melo, “OTC 24429 Development of a Compact Topside Processing Facility,” no. October, pp. 29–31, 2013.

[14] R. Mikkelsen, P. Verbeek, M. R. Akdim, F. M. C. Technologies, and S. Innovation, “SPE 166363 Development of a Compact Topside Processing Plant,” 2013.

[15] W. B. Cook, W. M. Prindible, I. Sumantri, and A. Richfield, “Design Requirements For A Major Offshore Processing Facility,” in *Proceedings of Offshore Technology Conference*, 1976.

[16] Y. Sohn, D. Kim, S. Choi, and Y. Yang, “Design Development of BOG Handling System In LNG-FSRU,” *The Twentieth International Offshore and Polar Engineering Conference*, vol. 7, pp. 33–36, Jan. 2010.

[17] E. MELAAEN, “FUEL GAS HANDLING SYSTEM AND BOG RELIQUEFACTION FOR LNG CARRIER,” 2013. .

[18] B. M. Beladjine, A. Ouadha, and L. Adjlout, “Performance Analysis of Oxygen Refrigerant in an LNG BOG Re-liquefaction Plant,” *Procedia Computer Science*, vol. 19, no. Seit, pp. 762–769, Jan. 2013.

[19] Y. Li and X. Chen, “Dynamic Simulation for Improving the Performance of Boil-Off Gas Recondensation System At Lng Receiving Terminals,” *Chemical Engineering Communications*, vol. 199, no. 10, pp. 1251–1262, Oct. 2012.

[20] Y. Li, X. Chen, and M.-H. Chein, “Flexible and cost-effective optimization of BOG (boil-off gas) recondensation process at LNG receiving terminals,” *Chemical Engineering Research and Design*, vol. 90, no. 10, pp. 1500–1505, Oct. 2012.

[21] M. A. Westhoff, “Using Operating Data at Natural Gas Pipelines.”

[22] M. J. Bagajewicz and E. Cabrera, “Data Reconciliation in Gas Pipeline Systems,” *Industrial & Engineering Chemistry Research*, vol. 42, no. 22, pp. 5596–5606, Oct. 2003.

[23] D. Sliškovic, R. Grbic, and Ž. Hocenski, “Methods for Plant Data-Based Process Modeling in Soft-Sensor Development,” *AUTOMATIKA*, vol. 52, no. 4, pp. 306–318, 2011.

[24] 성홍근, “해양플랜트산업 발전을 위한 제언,” *Machinery Industry*, vol. 9, pp. 41–48, 2014.

[25] L. T. Biegler, I. E. Grossmann, and A. W. Westerberg, *Systematic Methods of Chemical Process Design*. Prentice Hall PTR, 1997, p. 796.

[26] J. Hwang, K. Lee, J. Cha, S. Ham, B. Kim, and M. Roh, “Establishment of Offshore Process FEED (Front End Engineering Design) Method for Oil FPSO Topsides Systems,” *The Nineteenth International Offshore and Polar Engineering Conference*, vol. 1, pp. 144–150, Jan. 2009.

[27] D. C. SEN, “Process Design for Offshore Oil and Gas Production in - Cold Ocean Environment,” *THE CANADIAN JOURNAL OF CHEMICAL ENGINEERING*, vol. 66, 1988.

[28] R. Smith, *Chemical Process Design and Integration*. .

[29] R. E. E. Allen, W. O. Engineers, S. Crane, T. Lift, and D. Plowden, “Will Very Large Modules Reduce the Cost of Offshore Platforms?,” in *Proceedings of European Petroleum Conference*, 1986.

[30] J. Hwang, “Selection of Optimal Liquefaction Process System considering Offshore Module Layout for LNG FPSO at FEED stage,” Seoul National University, 2013.

[31] W. V. Wijngaarden and S. B. Moorings, “OTC 16077 Offshore LNG Terminals : Sunk or Floating ?,” 2004.

[32] G. Gourdet, C. Toderan, B. Veritas, and M. Division, “New Classification Rules for Offshore Floating Gas Terminals,” in *Proceedings of SPE International Conference on Health, Safety and Environment in Oil and Gas Exploration and Production*, 2010, no. April, pp. 12–14.

[33] H. N. Patel, P. Rynn, X. Wang, B. Das, M. Pham, and A. Bureau, “Safety and Regulatory Perspective for Floating LNG plant Offshore (FLNG),” in *Proceedings of OTC Brasil*, 2011.

[34] American Petroleum Institute, “Recommended Practice for Planning , Designing and Constructing Fixed Offshore Platforms — Working Stress Design,” API Publishing Services, 2006.

[35] J. Westover, A. Hoadley, C. Engineering, and A. E. S. Dyson, “Weight reduction of off-shore natural gas liquids processing facilities,” in *Proceedings of SPE Asia Pacific Oil and Gas Conference and Exhibition*, 2002, no. figure 2.

[36] J. Hwang, J. Min, Y. Ahn, H. H. Kim, M. Roh, and K. Lee, “Optimized Methodology to Build an Integrated Solution to Offshore Topside Process Engineering,” *The Eighteenth International Offshore and Polar Engineering Conference*, vol. 8, pp. 233–240, Jan. 2008.

[37] American Petroleum Institute, “Recommended Practice for Planning, Designing, and Constructing Floating Production Systems,” no. March, 2001.

[38] J. T. Cullinane, N. Yeh, and E. Grave, “SPE 143766 Effects of Tower Motion on Packing Efficiency,” no. June, pp. 14–17, 2011.

[39] The Millennium Challenge Corporation, “GHANA LIQUID NATURAL GAS STUDIES AND DESIGN SCREENING REPORT,” Englewood, 2014.

[40] A. Thesis and G. W. Yun, "BAYESIAN-LOPA METHODOLOGY FOR RISK ASSESSMENT OF AN LNG IMPORTATION TERMINAL BAYESIAN-LOPA METHODOLOGY FOR RISK ASSESSMENT OF AN LNG IMPORTATION TERMINAL," no. December, 2007.

[41] C. Park, C.-J. Lee, Y. Lim, S. Lee, and C. Han, "Optimization of recirculation operating in liquefied natural gas receiving terminal," *Journal of the Taiwan Institute of Chemical Engineers*, vol. 41, no. 4, pp. 482–491, Jul. 2010.

[42] W. D. Seider, J. D. Seader, and D. R. Lewin, *Product & Process Design Principles - Synthesis, Analysis & Evaluation*, 2nd editio. John Wiliey and Sons, Inc.

[43] J. M. Douglas, *Conceptual Design of Chemical Processes*. McGraw-Hill, 1988.

[44] H. Silla, *CHEMICAL PROCESS ENGINEERING : Design and Economics*. Taylor & Francis Group LLC, 2003.

[45] H. Devold, *Oil and gas production handbook : An introduction to oil and gas production*, 2nd editio. ABB Oil and Gas, 2009.

[46] Y. Lee, T. Cho, J. Lee, O. Kwon, D. Shipbuilding, and M. E. Co, "OTC 19339 Trends and Technologies in LNG Carriers and Offshore LNG Facilities," no. May, pp. 5–8, 2008.

[47] DET NORSKE VERITAS, "DNV-OSS-102 Rules for Classification of Floating Production , Storage and Loading Units," 2014.

[48] DET NORSKE VERITAS, "Floating Liquefied Gas Terminals : Offshore Technical Guidance OTG-02," 2011.

[49] E. Aronsson, "FLNG compared to LNG carriers Requirements and recommendations for LNG production facilities and," Chalmers University of Technology, 2012.

[50] "CURACAO CNG-LNG TERMINAL FEASIBILITY STUDY." Shaw Concultants International, Inc., Houston, 2012.

[51] S. Lee and D. Division, "OPERATING INFORMATION SYSTEM FOR LNG FACILITIES."

[52] Y. Sohn, Y. Yang, I. Yoon, S. Choi, G. Choi, and K. G. Corporation, "BASIC DESIGN OF PYEONGTAEK LNG RECEIVING TERMINAL-II OF KOREA GAS CORPORATION LA CONCEPTION DE BASE DU TERMINAL METHANIER PYEONGTAEK-II," no. 1, pp. 1–7.

[53] H. S. Lee, H. C. Lee, S. H. Kim, and M. K. Ha, "Consequence Analysis of Major Hazards for Concept Design of LNG-FSRU," pp. 4–7, 2010.

[54] S. Levitus, J. I. Antonov, O. K. Baranova, T. P. Boyer, C. L. Coleman, H. E. Garcia, A. I. Grodsky, D. R. Johnson, R. A. Locarnini, A. V. Mishonov, J. R. Reagan, C. L. Sazama, D. Seidov, I. Smolyar, E. S. Yarosh, and M. M. Zweng, "The World Ocean Database," *Data Science Journal*, vol. 12, pp. WDS229–WDS234, May 2013.

[55] P. D. Jones and C. Harpham, "Estimation of the absolute surface air temperature of the Earth," *Journal of Geophysical Research: Atmospheres*, vol. 118, no. 8, pp. 3213–3217, Apr. 2013.

[56] R. A. Locarnini, A. V. Mishonov, J. I. Antonov, T. P. Boyer, H. E. Garcia, O. K. Baranova, M. M. Zweng, C. R. Paver, J. R. Reagan, D. R. Johnson, M. Hamilton, and D. Seidov, "WORLD OCEAN ATLAS 2013 Volume 1 : Temperature," 2013.

[57] L. Spittael, M. Zalar, P. Laspalles, and L. Brosset, "METHODOLOGY FOR LIQUID MOTIONS ANALYSIS," in *Gastech 2000*, 2000.

[58] H. D. Cueva and F. Faria, "ROLL MORIONS OF FPSOs."

[59] P. J. M. Lapidaire, J. D. Leeuw, and S. Protech, "OTC 8075 The Effect of Ship Motions on FPSO Topsides Design."

[60] S. Cho, H. Sung, and S. Hong, "Study on the Dynamics of Turret Moored FSRU in Waves," pp. 27–33, 2010.

[61] S. K. Chakrabarti, *Handbook of Offshore Engineering*, vol. I. Elsevier, 2005.

[62] "Höegh LNG – The Floating LNG Service Provider." Höegh LNG, 2014.

[63] M. Zolfkhani, "Optimize LNG boil-off gas systems for regasification terminals," *Hydrocarbon Processing*, vol. 92, 2013.

[64] M. W. Shin, D. Shin, S. H. Choi, E. S. Yoon, and C. Han, "Optimization of the Operation of Boil-Off Gas Compressors at a Liquified Natural Gas Gasification Plant," *Ind. Eng. Chem. Res.*, vol. 46, pp. 6540–6545, 2007.

[65] J. Kwan and H. Chang, "Introduction of LNG Regasification Vessel," *대우엔지니어링기술보*, vol. 24, no. 1, pp. 80–89, 2008.

[66] "Pressure-relieving and Depressuring Systems - ANSI/API STANDARD 521." API Publishing Services, Washington, 2007.

[67] P. Helge, S. Madsen, D. Karsten, R. Strande, H. Gas, and S. As, "OTC 20809 Intermediate Fluid Vaporizers for LNG Re-gasification Vessels , SRV ' s and FSRU ' s," pp. 1–14, 2010.

[68] D. A. Franklin, "LNG Vaporizers : An Overview of LNG Vaporizer Technologies," 2006, no. March.

[69] S. Egashira, “LNG Vaporizer for LNG Re-gasification Terminal,” *KOBELCO TECHNOLOGY REVIEW*, no. 32, pp. 64–69, 2013.

[70] D. Patel, J. Mak, D. Rivera, and J. Angtuaco, “LNG vaporizer selection based on site ambient conditions.” .

[71] H. Kelle, Y. J. Wong, and J. Schlatt, “Floating Regasification Terminals - Selection & Marinisation of Regasification Equipment for Offshore Use,” *Proceedings of Offshore Technology Conference*, May 2011.

[72] T. Dendy and R. Nanda, “Utilization of Atmospheric Heat Exchangers in LNG Vaporization Processes :,” 2008.

[73] B. Boundy, S. W. Diegel, L. Wright, and S. C. Davis, “BIOMASS ENERGY DATA BOOK : EDITION 4,” 2011.

[74] M. Endo, “Overview of ORV and IFV characteristics and operation in LNG receiving terminals in Japan and worldwide Who are we ?”

[75] Đ. Dobrota, B. Lalić, and I. Komar, “Problem of Boil - off in LNG Supply Chain,” *Transactions on Maritime Science*, vol. 02, no. 02, pp. 91–100, Oct. 2013.

[76] Gerald E. Engdahl, “SYSTEM AND APPARATUS FOR CONDENSING BOIL-OFF VAPOR FROM A LIQUIFIED NATURAL GAS CONTAINER,” U.S. Patent US 6,470,706 B12002.

[77] J. K. Jones, “RELIQUEFACTION OF BOIL OFF GAS,” U.S. Patent 3,857,2451974.

[78] R. Brannock, W. H. Isalski, and P. V. den Bossche, “Recondensers in LNG Import Terminals,” *Gastech 2009*, 2009. [Online]. Available: http://www.tge-gas.com/sites/cms/tge/WebFiles/Recondensers in LNG Import Terminals.pdf. [Accessed: 01-Jun-2004].

[79] J. W. Sudduth and W. A. Carpenter, “BOIL-OFF GAS REMOVAL SYSTEM,” U.S. Patent US 2006/0032239 A12006.

[80] D. Kim, J. M. Ha, Y. Park, I. K. Yoon, and Y. S. Baek, “Study on the improvement of BOG recondensation process at LNG receiving terminal,” *KIGAS*, vol. 5, no. 3, 2001.

[81] C. Park, K. Song, S. Lee, Y. Lim, and C. Han, “Retrofit design of a boil-off gas handling process in liquefied natural gas receiving terminals,” *Energy*, vol. 44, no. 1, pp. 69–78, Aug. 2012.

[82] C. Liu, J. Zhang, Q. Xu, and J. L. Gossage, “Thermodynamic-Analysis-Based Design and Operation for Boil-Off Gas Flare Minimization at LNG Receiving

Terminals," *Industrial & Engineering Chemistry Research*, vol. 49, no. 16, pp. 7412–7420, Aug. 2010.

[83] "Aspen HYSYS : Tutorials and Applications." Aspen Technology, Inc., 2006.

[84] M. Satuluri, "Development of Effective & Accessible Approach to Analyze Unsteady State Plant Performance," University of Kansas, 2011.

[85] R. W. Serth and B. Srikanth, "Gross Error Detection and Stage Efficiency," *AIChE Journal*, vol. 39, no. 10, pp. 1726–1731, 1993.

[86] G. E. P. Box, G. M. Jenkins, and G. C. Reinsel, *Time Series Analysis: Forecasting and Control*. 2013.

[87] N. Jang, M. W. Shin, S. H. Choi, and E. S. Yoon, "Dynamic simulation and optimization of the operation of boil-off gas compressors in a liquefied natural gas gasification plant," *Korean Journal of Chemical Engineering*, vol. 28, no. 5, pp. 1166–1171, Apr. 2011.

[88] "Aspen HYSYS customization guide," Aspen Technology, Inc., 2010.

[89] P. Kadlec, B. Gabrys, and S. Strandt, "Data-driven Soft Sensors in the process industry," *Computers & Chemical Engineering*, vol. 33, no. 4, pp. 795–814, Apr. 2009.

[90] B. Lin, B. Recke, J. K. H. Knudsen, and S. B. Jørgensen, "A systematic approach for soft sensor development," *Computers & Chemical Engineering*, vol. 31, no. 5–6, pp. 419–425, May 2007.

[91] S. Park and C. Han, "A nonlinear soft sensor based on multivariate smoothing procedure for quality estimation in distillation columns," *Computers & Chemical Engineering*, vol. 24, pp. 871–877, 2000.

[92] M. L. Thompson and M. a. Kramer, "Modeling chemical processes using prior knowledge and neural networks," *AIChE Journal*, vol. 40, no. 8, pp. 1328–1340, Aug. 1994.

[93] M. Fellner, a Delgado, and T. Becker, "Functional nodes in dynamic neural networks for bioprocess modelling.," *Bioprocess and biosystems engineering*, vol. 25, no. 5, pp. 263–70, Mar. 2003.

[94] C. C. Pantelides and J. G. Renfro, "The online use of first-principles models in process operations: Review, current status and future needs," *Computers & Chemical Engineering*, vol. 51, pp. 136–148, Apr. 2013.

[95] S. Papastratos, C. Hart, K. Speaks, and P. Hayot, "STATE ESTIMATION FOR ON-LINE FIRST PRINCIPLE MODELS," *2nd European Congress of Chemical Engineering*, 1999.

[96] D. C. Psichogios and L. H. Ungar, "A hybrid neural network-first principles approach to process modeling," *AIChE Journal*, vol. 38, no. 10, pp. 1499–1511, Oct. 1992.

[97] W. MARQUARDT, "TRENDS IN COMPUTER-AIDED PROCESS MODELING," *Computers & Chemical Engineering*, vol. 20, no. 6, pp. 591–609, 1996.

[98] V. M. Dozortsev and E. Y. Kreidlin, "State-of-the-art automated process simulation systems," *Automation and Remote Control*, vol. 71, no. 9, pp. 1955–1963, Sep. 2010.

[99] R. Bogusch, B. Lohmann, and W. Marquardt, "Computer-aided process modeling with MODKIT," vol. 25, pp. 963–995, 2001.

[100] M. Barth and A. Fay, "Automated generation of simulation models for control code tests," *Control Engineering Practice*, vol. 21, no. 2, pp. 218–230, Feb. 2013.

[101] M. Barth, M. Strube, A. Fay, P. Weber, and J. Greifeneder, "Object-oriented engineering data exchange as a base for automatic generation of simulation models," *2009 35th Annual Conference of IEEE Industrial Electronics*, pp. 2465–2470, Nov. 2009.

[102] S. Middleman, *An Introduction to Mass and Heat Transfer: Principles of Analysis and Design*. Wiley, 1998, p. 672.

[103] C. O. Bennett and J. E. Myers, *Momentum, Heat, and Mass Transfer*. McGraw-Hill International, 1988, p. 832.

[104] J. Welty, G. L. Rorrer, and D. G. Foster, *Fundamentals of Momentum, Heat and Mass Transfer, 6th Edition*. Wiley, 2014, p. 768.

[105] G. R. Stephenson and C. F. Shewchuk, "Reconciliation of process data with process simulation," *AIChE Journal*, vol. 32, no. 2, pp. 247–254, Feb. 1986.

[106] R. S. Mah, G. M. Stanley, and D. M. Downing, "Reconciliation and Rectification of Process Flow and Inventory Data," vol. 15, no. 1, pp. 175–183, 1976.

[107] British Standards, *Installation and equipment for liquefied natural gas — Design of onshore installations*, vol. 3. 2007.